# Chapter 2
# Reactions Involving Maleic Anhydride

**Michael A. Tallon**

## 2.1 Introduction

### *2.1.1 Physical Properties of Maleic Anhydride and Its Derivatives*

The rich chemistry that maleic anhydride can participate in makes it the quintessential building block for a variety of small and polymeric molecules that are in use today. This is derived from the electron-deficient conjugated double bond and the cyclic anhydride functionality present. This activated double bond allows it to take part in Michael reactions, electrophilic addition, formation of Diels–Alder adducts, alkylation and acylation reactions, sulfonation, halogenations, reduction, photodimerization, hydroformylation, or free-radical polymerization reactions to generate poly-anhydride copolymers.

Likewise, the reactive anhydride functionality permits a whole host of organic reactions like esterification, amidation, imidation, hydrolysis, decarboxylation, and metal chelation to name a few. This chapter begins with the basic chemistry of maleic anhydride due to its molecular structure and the types of reactions it can participate in, as well as its physical and chemical properties. For instance, the bond angles and bond lengths for maleic anhydride are depicted in Fig. 2.1, and this results in a very compact and particularly planar structure [1].

Even though the double bond in maleic anhydride is quite electron deficient and would be expected to be slightly shorter than 1.1 Å for the C–H and 1.3 Å for the C=C bond length, they are still comparable to a typical alkene like ethylene that corresponds to 1.08 Å and 1.33 Å, respectively. The anhydride bond lengths are typical of anhydrides like acetic anhydride. However, the bond angles are significantly

M.A. Tallon (✉)
Ashland Inc., 1005 Route 202/206, Bridgewater, NJ 08807, USA
e-mail: mtallon@ashland.com



O.M. Musa (ed.), *Handbook of Maleic Anhydride Based Materials*,
DOI 10.1007/978-3-319-29454-4_2

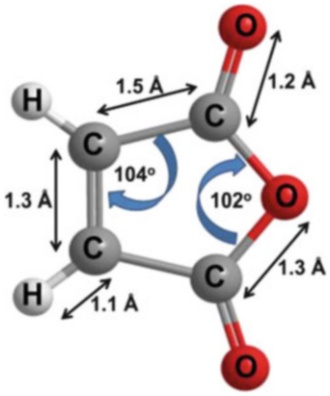


**Fig. 2.1** Bond angles and bond lengths for maleic anhydride

different from 120° reflecting the internal ring strain of the cyclopentane ring structure. With the exception of the C–O–C bond angle of 102°, the remaining four carbon–carbon bond angles are all 104°, Fig. 2.1. The cumulative effect of all these factors forces all the atoms within the maleic anhydride molecule to lie in one plane.

The true nature of this extreme planarity and compact nature for the maleic anhydride molecule can be depicted by the ball–stick and space-filling models illustrated in Fig. 2.2, where the oxygen's lone pairs are depicted in pink [2]. This molecular structure also allows for efficient packing of the molecules into its crystal lattice resulting in a relatively high density value of 1.48 g/cc.

The olefinic double bond within maleic anhydride is quite electron deficient and can be better portrayed by its resonance structures shown in Fig. 2.3a, which results in its potent electron-acceptor behavior. This electron deficiency is particularly important in free-radical polymerization reactions and is responsible for the creation of a charge-transfer complex between an electron-rich comonomer and an electron-poor monomer like maleic anhydride. This charge-transfer complex results in activating maleic anhydride to participate in free-radical copolymerization thereby resulting in an alternating copolymer. In contrast, homopolymerization of maleic anhydride is not particularly favored so that only low molecular weight oligomers are generated.

The electron-density map of maleic anhydride is depicted by the electropositive (red) nature of the conjugated double bond and by the electronegative (blue) anhydride functionality in Fig. 2.3b. The maleic anhydride molecule exhibits a very strong dipole moment of 3.96 debye and strong coulombic attractions between maleic anhydride molecules. This results in its high melting (53 °C) and boiling (202 °C) points than expected by its neutral structure alone [1, 3, 4].

Maleic anhydride crystallizes as orthorhombic needlelike crystals, while maleic acid and fumaric acid form monoclinic crystals. The crystal structure for maleic anhydride was first deduced by Marsh and coworkers in 1962 [2]. They found that it forms an orthorhombic crystal structure, with a $P2_12_12_1$ unit cell that contains four

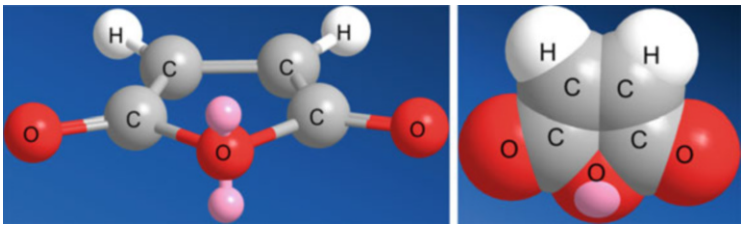


**Fig. 2.2** Ball–stick (**a**) and space-filling (**b**) models for maleic anhydride

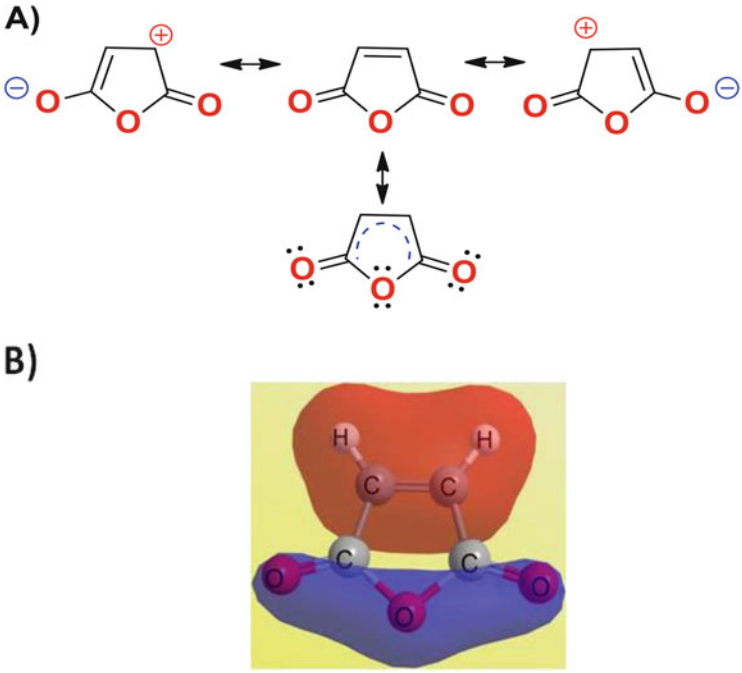


**Fig. 2.3** Resonance structures (**a**) and electron density were partially positive (*red*) and partially negative (*blue*) for maleic anhydride (**b**)

molecules of maleic anhydride. This is schematically depicted in Fig. 2.4, in the ball–stick (2.4a) and space-filling (2.4b) models.

It should be noted that the electrophilic double bonds align themselves in close spatial proximity to the electron-rich anhydride atoms of adjacent molecules thereby giving rise to the strong coulombic attraction between maleic anhydride molecules thereby increasing its melting point. These interactions are denoted by the yellow arrows in Fig. 2.4a.

The corresponding dimensions of each unit cell, as defined by axes a, b, and c, the number of maleic molecules within each unit cell (Z), and its corresponding volume are summarized in Table 2.1. The numbering system used for individual

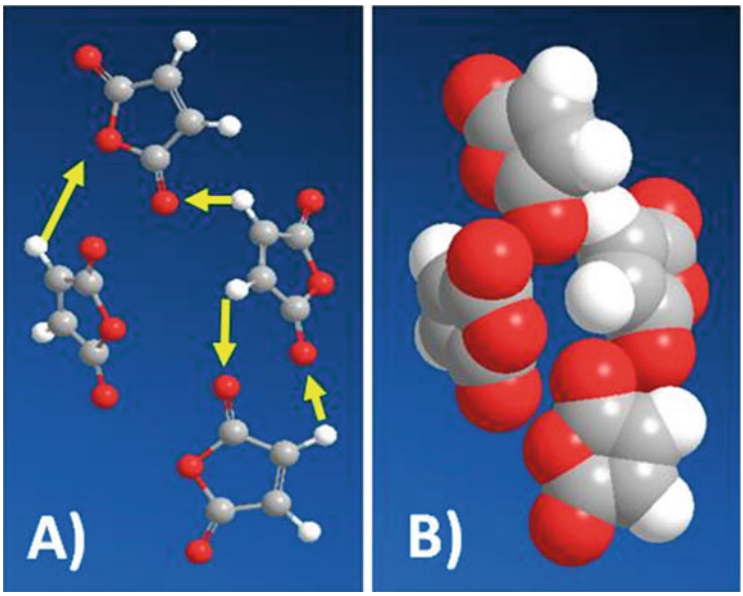


**Fig. 2.4** Maleic anhydride's $P2_12_12_1$ unit-cell crystal structure, (**a**) ball–stick and (**b**) space-filling models

**Table 2.1** Crystallographic data for maleic anhydride at 295°K

| Lattice | Orthorhombic | Numbering system |
|---|---|---|
| Space Group | $P2_12_12_1$ | 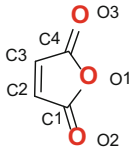 |
| a | 7.18 Å | |
| b | 11.23 Å | |
| c | 5.39 Å | |
| Unit-cell Volume | 434.60 Å$^3$ | |
| Density | 1.505 g/ml | |
| Z | 4 molecules | |



Molecule volume 108.65 Å$^3$, Actual density=1.48g/cc

atoms, bond lengths, and bond angles of the maleic molecule are reported in Table 2.2.

This molecular structure further results in some practical consequences toward its physical properties, as summarized in Table 2.3 [3, 4]. For instance, this planar structure with conjugated double bond, along with its compact electron cloud, makes it a very *efficient mirror* with visible light thereby resulting in a very high refractive index value of 1.55 [1, 3, 4].

The dipolar nature of the maleic anhydride molecule not only affects the physical properties of the molecule, but this electron-deficient double bond is activated to reactions with nucleophilic reagents, thereby enabling it to participate in Michael-type reactions. Similarly, maleic anhydride is a potent dienophile in Diels–Alder reactions.

**Table 2.2** Bond angles/distances for maleic anhydride crystal structure

| Bonds | Angle (°) | Bond | Distance (Angstrom) |
|---|---|---|---|
| C2–C1–O1 | 107.9 | C2–C3–H3 | 130 |
| C2–C1–O2 | 131.2 | C4–C3–H3 | 121 |
| O1–C1–O2 | 120.9 | C1–O1 | 1.396 |
| C1–C2–C3 | 108.4 | C1–C2 | 1.476 |
| C2–C3–C4 | 108.5 | C2–C3 | 1.317 |
| C1–C2–H2 | 119 | C1–O2 | 1.200 |
| C3–C2–H2 | 133 | C2–H2 | 1.085 |
| C3–C4–O1 | 107.8 | C3–C4 | 1.480 |
| C3–C4–O3 | 131.6 | C4–O1 | 1.389 |
| O1–C4–O3 | 120.6 | C4–O3 | 1.203 |
| C1–O1–C4 | 107.4 | C3–H3 | 1.01 |

**Table 2.3** Select physical and toxicological properties of maleic anhydride, maleic acid, and fumaric acid

| Property | Maleic anhydride | Maleic acid | Fumaric acid |
|---|---|---|---|
| Chemical formula | $C_4H_2O_3$ | $C_4H_4O_4$ | $C_4H_4O_4$ |
| Molecular weight (g/Mole) | 98.06 | 116.07 | 116.07 |
| [a]Physical form | White solid | White solid | White solid |
| Refractive index | 1.55 | 1.35 | 1.34 |
| [a]Melting point | 52.9 °C | 138–139 °C | 287 °C |
| [a]Boiling Point | 202 °C | 138(dec) | 290 °C |
| Density, g/cc 20 °C | 1.48 | 1.59 | 1.64 |
| Dipole moment, Debye | 3.96 | 3.18 | 2.45 |
| Crystalline form | Orthorhombic | Monoclinic | Monoclinic |
| Solubility in $H_2O$@ 25 °C | Hydrolyzes | 30.6 % | 0.7 % |
| Acidity p$K_a$ @ 25 °C | NA | p$K_{a1}$= 1.5<br>p$K_{a2}$= 6.5 | p$K_{a1}$= 3.0<br>p$K_{a2}$= 4.5 |
| Acid number (mg KOH/g) | Hydrolyzes | 966 | 966 |
| Flash point<br>Open cup | 110 °C | Decomposes @ 135 °C | 282 °C |
| Closed cup | 102 °C | ND | 230 °C |
| Viscosity centipoises @ 70 °C | 1.5 | ND | ND |
| Oral rat $LD_{50}$ mg/Kg | 400 | 708 | 10,700 |
| Skin rabbit $LD_{50}$ mg/Kg | 2620 | 1560 | 20,000 |
| Intraperitoneal rat<br>$LD_{50}$ mg/Kg | 97 | ND | 587 |
| Subcutaneous rat<br>$LD_{50}$ mg/Kg | 1220 | ND | ND |

[a]At 25 °C and 760 torr, *NA* not applicable, *ND* not determined

Films of maleic anhydride and its copolymers, or its derivatives, tend to exhibit very high gloss or shine. Hydrolysis of maleic anhydride yields maleic acid, which can be isomerized to its sister-isomer, fumaric acid. Table 2.3 presents the comparative properties between maleic anhydride, maleic acid, and fumaric acid. All three molecules are hygroscopic solids at room temperature.

Maleic anhydride slowly sublimes around 40–50 °C and exhibits a relatively high vapor pressure that is partially responsible for its acrid odor. Maleic anhydride slowly hydrolyzes into maleic acid by absorption of moisture and therefore exhibits a slight deliquescence behavior. Molten maleic anhydride exhibits an absolute viscosity of 1.5 centipoise at 70 °C.

OSHA's threshold for inhalation is 0.25 ppm (1 mg/$M^3$), while dermal limits to prevent contact dermatitis are approximately around 100–500 ppm depending on the global regulatory body involved [3, 5]. In summation, the chemical reactivity of maleic anhydride is best described by its electrophilic conjugated *cis*-double bond and its reactive anhydride functionality in a compact five-membered planar ring structure. These attributes are the foundation for its versatility in organic syntheses.

The thermodynamic properties for maleic anhydride are listed in Table 2.4. The two most practical properties in manufacturing are the heat of hydrolysis and heat of neutralization. These values are needed to determine if the reactor size has the correct cooling capacity to handle the heat generated by hydrolyzing, reacting the anhydride ring, and/or neutralization. Process engineers use this data by converting these values to British thermal units (BTU) and comparing them to the cooling capacity rate of the chiller in the reactor.

For instance, 1 kJ (kilojoule) is equal to 0.9478 BTU, meaning that neutralizing 5000 Kg of maleic acid to disodium maleate will generate 3.7 million BTUs of heat. That will raise the temperature of a 50 % aqueous solution by 95 °C. Therefore, even if you started at room temperature, say about 25 °C, the neutralization would result in a temperature increase of the solution to roughly 120 °C, well above the boiling point of water.

Maleic acid begins to decompose at 120 °C by decarboxylation into $CO_2$ gas. Significant formation of gas can ultimately result in a substantial explosive potential. Such a large energy release from the enthalpy of neutralization requires dilute solutions of maleic acid to be used for neutralization coupled to a slow rate of addition of neutralizer. In addition, a low temperature glycol chiller must be used for safety and practical reasons.

Since maleic anhydride is a solid at room temperature, a solvent is often used to dissolve it prior to any syntheses operations. Table 2.5 summarizes maleic anhydride, maleic acid, and fumaric acid solubilities in different solvents. Interestingly, maleic anhydride is not readily soluble in water even though it exhibits a strong dipole moment, but instead it slowly hydrolyzes to form maleic acid at room temperature, which is readily soluble in water.

Usually mild heating is applied ≈ 60–70 °C to accelerate hydrolysis and prevent off-gassing by decarboxylation. This will be discussed more fully in the following hydrolysis section. Maleic anhydride is extremely soluble in polar aprotic solvents

**Table 2.4** Thermodynamic properties of maleic anhydride, maleic acid, and fumaric acid

| Property | Maleic anhydride | Maleic acid | Fumaric acid |
|---|---|---|---|
| Heat of formation kJ/Mol | −470.41 | −790.57 | −811.03 |
| Heat of combustion kJ/Mol | −1389.5 | −1355.2 | −1334.7 |
| Specific heat (solid) kJ/Mol °K | −0.1199 | −0.1356 | −0.1418 |
| Heat of evaporation kJ/Mol | 54.8 | NA | NA |
| Heat of fusion kJ/Mol | 13.55 | NA | NA |
| Heat of hydrolysis kJ/Mol | −34.9 | NA | NA |
| Heat of neutralization kJ/Mol | −126.9 | −92 | −92 |
| Heat of sublimation kJ/Mol | 71.5 | 105.4 | 123.6 |

*NA* not applicable

**Table 2.5** Solubilities of maleic anhydride, maleic acid, and fumaric acid

| Solvent | Maleic anhydride wt% | Maleic acid wt% | Fumaric acid wt% |
|---|---|---|---|
| Acetone @ 20 °C | >69 | 27.8 | ND |
| Acetone @ 29.7 °C | >70 | 20.8 | 1.66 |
| Benzene 25 °C | 50 | 0.02 | 0.003 |
| Chloroform 25 °C | 34.4 | 0.10 | 0.02 |
| Ethanol 22.5 °C | Esterifies | 34.4 | ND |
| Ethyl acetate 25 °C | 52.8 | ND | ND |
| Kerosene 25 °C | 0.25 | ND | ND |
| Methanol 22.5 °C | Esterifies | 29.1 | ND |
| 1-Propanol 22.5 °C | | 24.3 | ND |
| Water @ 25 °C | Hydrolyzes into maleic acid | 30.6 | 0.7 |
| 40 °C | | 34.6 | 1.04 |
| 60 °C | | 37.1 | 2.28 |
| 97.5 °C | | 44.4 | ND |
| 100 °C | | ND | 8.19 |
| Toluene 25 °C | 19 | ND | ND |
| *o*-Xylene 25 °C | 16 | ND | ND |

*ND* not determined

like acetone, methyl ethyl ketone, and ethyl acetate (Table 2.5). It is also moderately soluble in apolar solvents like benzene, xylene, and toluene.

Solubility parameters in protic solvents like alcohols are meaningless since maleic anhydride will slowly react with them to form half esters. This results in a new composition with different solubility characteristics. Therefore, its Log *P* coefficient is a somewhat misleading value in octanol, since it is capable of reacting with the alcoholic component. In contrast, maleic acid is practically insoluble in apolar solvents like benzene and toluene and only moderately soluble in acetone and in water.

### 2.1.2 *Spectroscopic Properties of Maleic Anhydride*

The spectroscopic profiles for maleic anhydride are illustrated in Figs. 2.5, 2.6, 2.7, and 2.8. The UV trace (see Fig. 2.5) depicts the UV absorption of the conjugated double bond and carbonyl group spanning 220–250 nm region.

The FT-IR profile of maleic anhydride is shown in Fig. 2.6. Typical absorption bands at 3130 $cm^{-1}$ for the olefinic =C–H stretch, the antisymmetrical and symmetrical C=O stretches at 1856 and 1774 $cm^{-1}$, C=C stretch at 1630 $cm^{-1}$, C–O

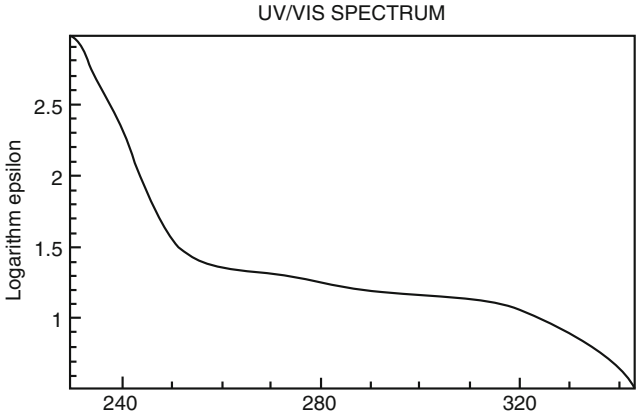


**Fig. 2.5** UV profile for maleic anhydride

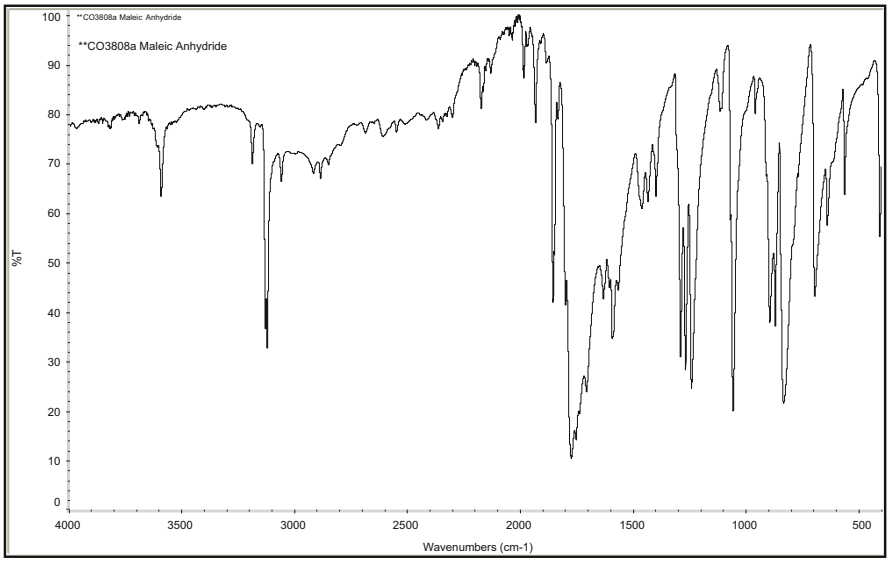


**Fig. 2.6** FT-IR profile for maleic anhydride

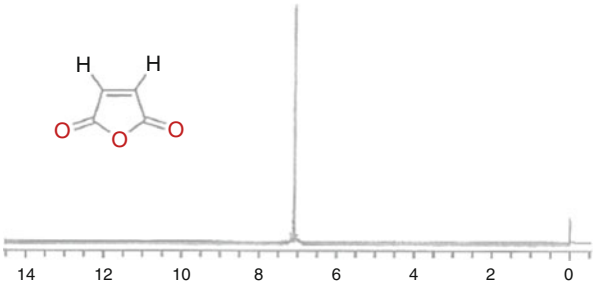


**Fig. 2.7** Proton-NMR profile for maleic anhydride

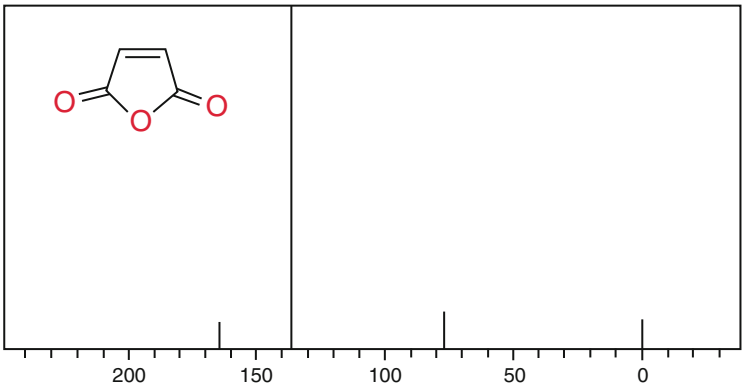


**Fig. 2.8** Carbon-NMR profile for maleic anhydride

stretch at 1030 $cm^{-1}$, and the *cis*-C=C wag band 700 $cm^{-1}$, all characteristic of the maleic anhydride structure.

The proton-NMR profile for maleic anhydride is depicted in Fig. 2.7. The sharp singlet at 7.1 ppm is consistent with the olefinic =C–H proton signal, while the absence of a broad carboxylic acid signal at 12–10 ppm indicates the anhydride functionality in the aprotic $CDCl_3$ solvent.

The carbon-NMR profile for maleic anhydride is portrayed in Fig. 2.8. The sharp singlet at 136 ppm is consistent with the olefinic =C–H proton signal, while the carboxylic anhydride signals O–C=O at 165 ppm are both consistent with the maleic anhydride structure in $CDCl_3$ solvent. The carbon signal at 77 ppm is deuterochloroform, while the carbon peak at 0 ppm is attributable to tetramethylsilane as an internal reference standard.

## 2.2 Reactions of the Anhydride Functionality

### *2.2.1 Hydrolysis and Acidity*

Maleic anhydride will slowly hydrolyze to maleic acid at room temperature at a rate slower than typical anhydrides like acetic anhydride, which generally occurs very rapidly when mixed with water. This effect is due in part to the strong intermolecular columbic attraction between maleic anhydride molecules. However, once hydrolyzed to maleic acid, it exhibits some rather unique stability and acidity characteristics [6].

Note the double-sided equilibrium arrows in Scheme 2.1. The hydrolysis reaction of maleic anhydride into maleic acid and the dehydration reaction of maleic acid into maleic anhydride are in equilibrium and can be interconverted under rather mild conditions. For example, the forward reaction will occur in water at 60 °C to form maleic acid; however, the reverse reaction in vacuum occurs at 55 °C to generate maleic anhydride up to 50–60 % by weight. This is due to the *cis*-double bond *locking in* the diacid groups in close special proximity as depicted in Fig. 2.9.

The close spatial proximity of the diacid group, resulting from the *cis*-double bond, has another consequence with regard to acidity. The acidity of maleic acid is roughly thirty times stronger than its *trans*-counterpart fumaric acid, for the first proton dissociation step (Scheme 2.2a), notably due to the anionic charge stabilization by the neighboring acid proton that can transfer back and forth between the two *cis*-carboxyl groups, denoted by structures 1–3 in Scheme 2.2a.

Therefore, resonance structures 1–4 actually delocalize the proton from the first dissociation across six atoms. This extreme resonance stabilization results in very acidic $pK_{a1} = 1.5$ value (Table 2.1).

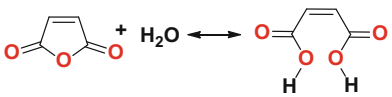


**Scheme 2.1** Aqueous hydrolysis of maleic anhydride to form maleic acid

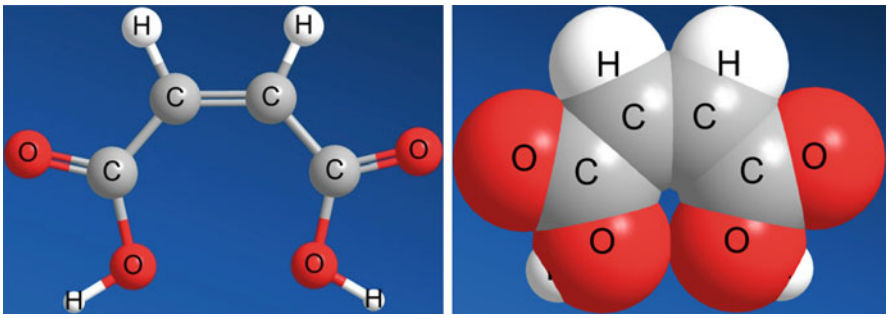

**Fig. 2.9** Ball–stick (**a**) and space-filling (**b**) models for maleic acid

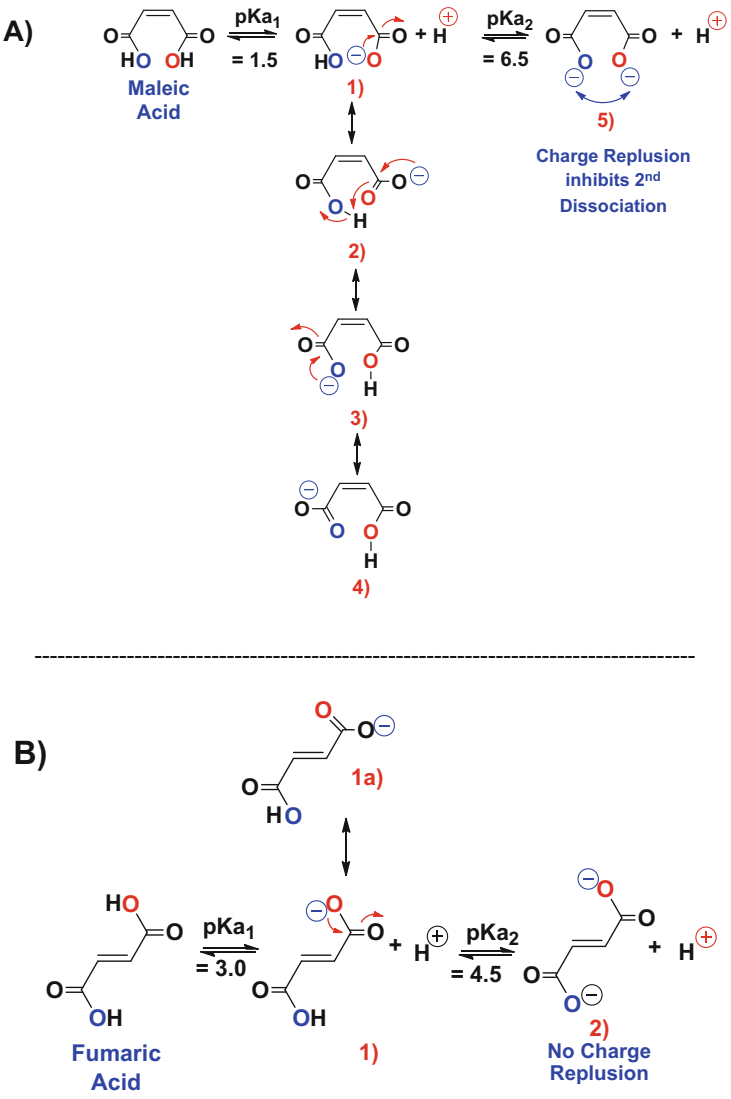


**Scheme 2.2** Acidity of maleic acid (**a**) versus fumaric acid (**b**)

In contrast, the *trans*-configuration of fumaric acid positions these two carboxyl groups further apart. This increased separation suggests the second neighboring carboxyl group is less capable of stabilizing the first dissociated proton. As a result there is less resonance stabilization (Scheme 2.2b structures 1-1a) which generates an increase in the p$K_a$ value for fumaric acid, to that more typical of an organic acid, p$K_{a1} = 3.0$ (Table 2.1).

Fumaric acid (p$K_{a2} = 4.5$) is a hundred times stronger acid for the second ionization step than maleic acid (p$K_{a2} = 6.5$). This effect arises from the charge repulsion of the *cis*-di-anion that is formed in maleic acid. The second dissociation

is inhibited by the first proton dissociation, because the two anionic charges are in close spatial proximity to each other and they are *locked in* by the *cis*-double bond. This effect is illustrated in Scheme 2.2a structure 5. Conversely, the *trans*-configuration of fumaric acid places these two carboxyl groups far apart so that the di-anion formed is not destabilized by charge repulsion (Scheme 2.2b structure 2), and occurs at much lower pH values.

An additional consequence of the *cis*- versus *trans*-configuration for the diacid group is manifested in their respective melting and boiling points. Experimentally fumaric acid exhibits a melting point (287 °C) versus maleic acid (138–139 °C) (Table 2.1). (This arises because each fumaric acid molecule can hydrogen bond to multiple partners within the crystal lattice and therefore requires more energy to break them apart for the melting point transition to occur.)

This becomes apparent when looking at the crystal structure of maleic acid versus fumaric acid, Fig. 2.10a, b. The *cis*-diacid group of maleic acid enables strong hydrogen bonding corresponding to one intramolecular H-bond per molecule and either two or three intermolecular H-bonds. In contrast, fumaric acid's *trans*-configuration permits only strong intermolecular hydrogen bonding corresponding up to eight potential H-bonds per molecule. (One would expect a higher melting point for fumaric as compared to maleic.)

In addition, better packing due to the *trans*-configuration results in a slightly higher solid density than maleic acid (1.64 vs. 1.59 g/mole). The enhanced packing also permits for more efficient intermolecular hydrogen bonding across multiple fumaric molecules, as depicted in Figs. 2.10, 2.11, and 2.12. Hence, fumaric acid can H-bond in all three dimensions across multiple "chains" as depicted in Fig. 2.10b, while maleic acid can only hydrogen bond mostly in two dimensions, Fig. 2.10a. Therefore, less energy is required to fracture the interactions between maleic acid molecules for its melting transition to occur. This notion is further corroborated by the ball and stick and space-filling models for maleic acid versus fumaric acid illustrated in Figs. 2.11 and 2.12, respectively. The dotted lines represent H-bonding between atoms in Figs. 2.11a and 2.12a.

Besides H-bonding, additional factors involved for the increase in melting arises from the columbic attraction of the partial positive charge related to the olefinic methine group, to the partial negative charge ascribed to the carbonyl functionality, denoted in red and blue, respectively. For fumaric acid, the symmetry of the *trans*-configuration allows for better packing and better overlap between these partial charges across multiple fumaric molecules. In contrast, maleic acid is much less efficient in overlapping these partial charges because of the anisotropy exhibited where only one side of the molecule is partially positive (*cis*-olefinic methines) and the opposing side attributable to the *cis*-carbonyl groups is partially negative.

Therefore, the spatial group of the crystal structure caused by the atomic coordinates of the atoms prevents maximum overlap between the partial charges within the maleic acid crystal lattice, while for fumaric acid the symmetry of the *trans*-configuration does allow for better packing and overlap within its crystal lattice. This notion is illustrated by the number and orientation of blue and red partial charges depicted in Fig. 2.10a versus 2.10b for a pair of neighboring chains,

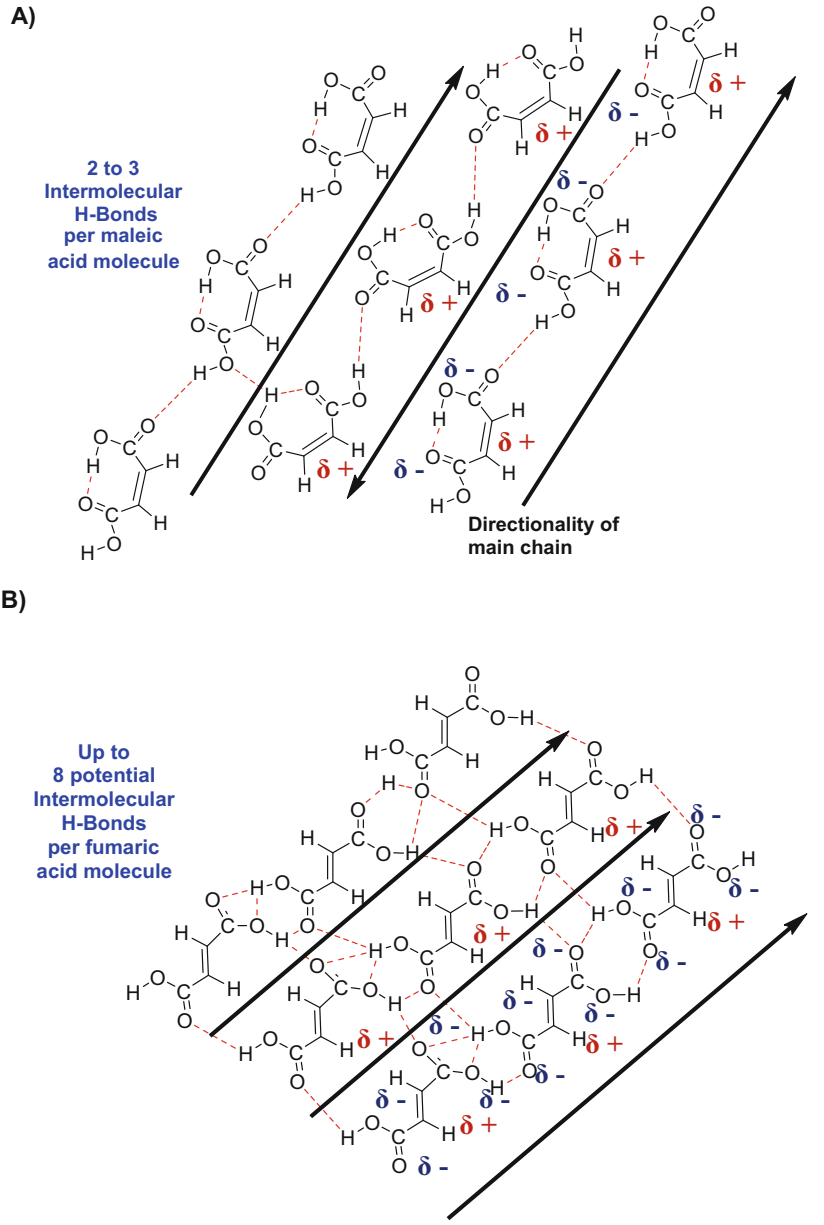


**Fig. 2.10** Hydrogen bonding and coulombic attraction of partial charges for (**a**) maleic acid versus (**b**) fumaric acid in their crystal lattice (Adapted from [7])

as well as the H-bonding network generated for maleic acid in Fig. 2.11a versus fumaric acid in Fig. 2.12a.

With regard to the crystal structures of maleic and fumaric acid, both individual molecules exhibit multiple crystal forms known as polymorphs. Polymorphism is

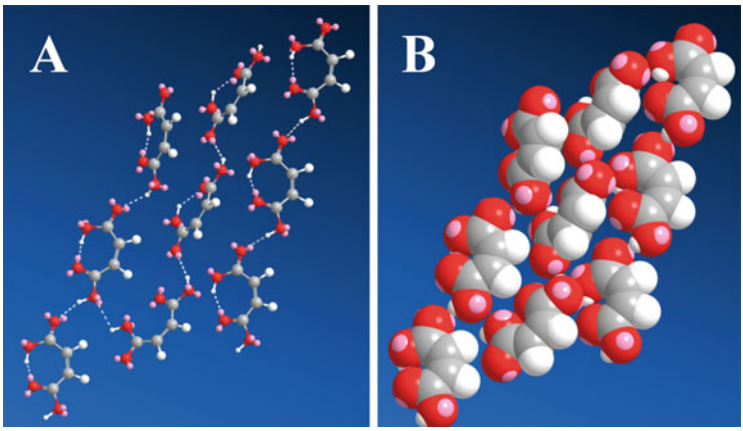


**Fig. 2.11** Maleic acid $P2_1/c$ unit-cell crystal structure, (**a**) ball–stick and (**b**) space-filling models

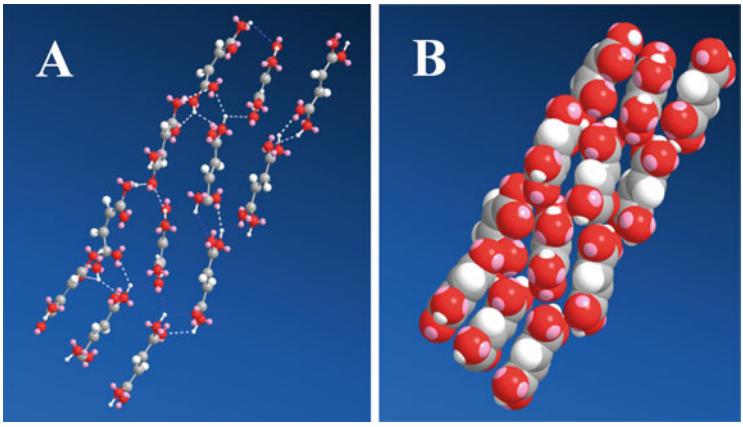


**Fig. 2.12** Fumaric acid $P2_1/c$ unit-cell crystal structure, (**a**) ball–stick and (**b**) space-filling models

the ability of a single chemical substance to adopt more than one crystal structure. Maleic acid is an example of one such compound that exhibits polymorphism. Both the pure substance itself and as a conjugate salt with pharmaceutical actives are capable of forming polymorphs. As far back as 1881, interest in maleic acid prompted the analysis of its crystal structure, which was first reported by Bodewig [8]. X-ray analysis followed to define its space group [9], while additional analyses confirmed the crystal structure for the monoclinic crystal form-I [10, 11]. 125 years later a second polymorphic monoclinic form-II was reported [12, 13].

The polymorphic forms of maleic acid are built up from molecular sheets or planes wherein molecules interact with each other via OH···O=C hydrogen bonds, thereby forming 1D chains that alternate in directionality within one plane. As these chains oscillate in direction back and forth as depicted by the black arrows in Fig. 2.10a, they also H-bond through close special contacts between the antiparallel aligned chains through their hydroxyl groups. The α-form-I forms sheets or planes

**Table 2.6** Crystallographic data for maleic acid at 295°K

| Lattice | Monoclinic α-Form-I | Monoclinic β-Form-II |
|---|---|---|
| Space Group | $P2_1/c$ | $Pc$ |
| a | 7.47 Å | 3.69 Å |
| b | 10.15 Å | 7.48 Å |
| c | 7.65 Å | 8.49 Å |
| Unit-cell volume | 580.02 $Å^3$ | 234.33 $Å^3$ |
| Density | 1.59 g/ml | 1.55 g/ml |
| Z | 4 molecules | 2 molecules |
| Molecule volume | 145.01 $Å^3$ | 117.17 $Å^3$ |

that alternate in directionality from plane to adjacent plane, such as ABAB, while the β-form-II forms sheets that are all in the same directionality, AAAA.

Form-I is the most prevalent structure reported for maleic acid in the literature today. The crystallographic data for each polymorphic form can be summarized by Tables 2.6 and 2.7, with the corresponding dimensions of each unit cell as defined by axes a, b, and c, as well as the number of maleic molecules within each unit cell (Z), and its corresponding molecular volume per maleic anhydride molecule is listed. Since Z exhibits 2–4 molecules per unit cell depending on the polymorph type, the molecular volume per molecule was listed so that a direct comparison to the density of each type can be made.

Similarly, fumaric acid also exhibits polymorphism. In general, fumaric acid crystals in their α-form contain six molecules per unit cell, while β-form contains only one molecule per unit cell [7]. Like maleic acid, sheets or planes are formed for both polymorphic forms of fumaric, but both are unidirectional with respect to the 1D chain orientation, as well as the polarity of the planes, such as AAAA. The crystallographic data for both forms are summarized in Table 2.7.

Table 2.8 summarizes the crystallographic bond lengths found for the different polymorphic forms of fumaric acid and maleic acid. Maleic acid is basically planar and exhibits compact intramolecular hydrogen bonds (2.46 Å). Additionally, both polymorphic forms of maleic acid exhibit very similar bond lengths for both the single- and double-bond carbon–carbon backbone thereby reflecting more pseudo-aromatic character within these molecules. In contrast, both the α- and β-forms of fumaric acid, the "single" and "double" carbon–carbon bond lengths, are more typical for an alkylene system (Table 2.8).

### *2.2.2 Isomerization and Stability*

At this point it should be noted that the solubility of fumaric acid in water at 25 °C is 0.7 % while maleic acid is 30.6 weight% (Table 2.3). This provides a means to manufacture fumaric acid from maleic anhydride. Specifically, maleic anhydride is manufactured by oxidation of butane as outlined in Chap. 1 and then hydrolyzed to maleic acid in water (Scheme 2.3). Then an 80 weight% aqueous solution of maleic

**Table 2.7** Crystallographic data for fumaric acid at 295°K

| Lattice | Monoclinic α-Form-I | Triclinic β-Form-II |
|---|---|---|
| Space group | $P2_1/c$ | $P\,\bar{1}$ |
| a | 7.60 Å | 5.26 Å |
| b | 15.11 Å | 7.62 Å |
| c | 6.61 Å | 4.49 Å |
| Unit-cell volume | 759.06 $Å^3$ | 179.97 $Å^3$ |
| Density | 1.63 g/ml | 1.62 g/ml |
| Z | 6 molecules | 1 molecules |
| Molecule volume | 126.51 $Å^3$ | 179.97 $Å^3$ |

**Table 2.8** Bond distances for fumaric acid versus maleic acid crystal structures

| Bond | Bond length α-Fumaric acid in angstroms | Bond length β-Fumaric acid in angstroms | Bond length α-Maleic acid in angstroms |
|---|---|---|---|
| –C–C– | 1.46 | 1.49 | 1.44 |
| –C=C– | 1.34 | 1.32 | 1.43 |
| C–OH | 1.29 | 1.29 | 1.28 |
| C=O | 1.23 | 1.23 | 1.20 |
| O···HO | 2.68 | 2.67 | 2.46, 2.75 |

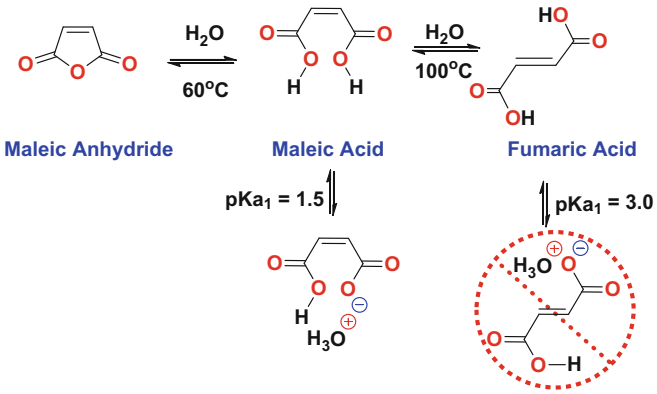


**Scheme 2.3** Isomerization of maleic acid into fumaric acid by hydrolysis of maleic anhydride

acid is refluxed in water for several hours upon which fumaric acid begins to crystallize out of solution. The resulting solution is then cooled and filtered to obtain fumaric acid crude that is subsequently washed with water and dried as pure monoclinic crystals. The process washes are combined with the mother liquor and the process can be repeated over again. This simple procedure is even practiced in undergraduate organic chemistry labs today.

This procedure works so well because the *cis*-double bond of maleic acid can be isomerized into the more thermodynamically stable *trans*-double bond of fumaric

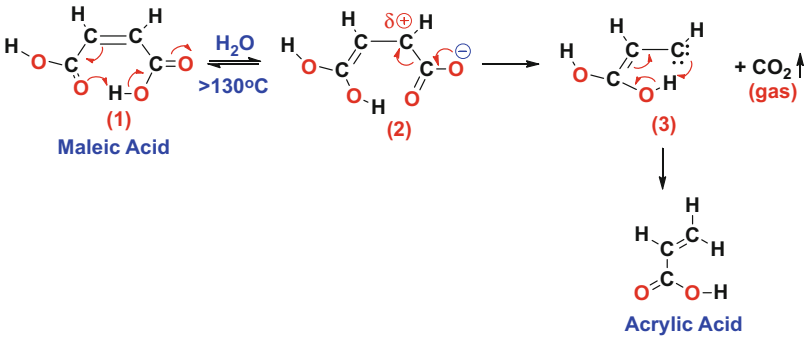


**Scheme 2.4** Decarboxylation of maleic acid due to excess heat

acid by moderate heating (Scheme 2.3). The fumaric acid so formed then crystallizes out of the aqueous solution to drive the reaction further to the right. This difference in solubility between maleic acid and fumaric acid arises because of their difference in acidity. Maleic acid having a $pK_{a1} = 1.5$ would be partially ionized (≈30 %) and hydrated in its hydronium maleate salt form at a pH around 1–2. In contrast, fumaric acid would only be ≈0.1 % ionized at the same pH. So as maleic acid is isomerized into fumaric acid, which is not readily soluble in water because of its weaker ionization potential, fumaric acid therefore crystallizes out of the solution.

Both maleic anhydride and maleic acid are unstable at high temperatures. Exposure to elevated temperature should be avoided because of the potential for decarboxylation side reactions that *off-gas* these materials. This effect is analogous to beta-keto-esters or malonic acid decarboxylation, whereby the formation of an enolate-transition state results in carbon–carbon bond fission. This degradation can occur in excess of 130 °C under highly acidic conditions, as depicted in Scheme 2.4.

For maleic anhydride, decarboxylation usually originates from the adsorption of moisture enabling the formation of some maleic acid to provide the prerequisite acidic catalyst. Because of maleic acid extreme acidity, it is easy to protonate the neighboring *cis*-carboxyl group at high temperatures. In doing so, an enolate is formed due to electronic rearrangement, as depicted in Scheme 2.4 structure 2. Carbon–carbon bond fission follows to release $CO_2$, along with proton transfer to the intermediate carbene that is formed (Scheme 2.4 structure 3) with the net result to convert maleic acid into acrylic acid with the release of $CO_2$. It should also be noted that in Scheme 2.4 structure 2 can isomerize to interconvert into fumaric acid for the arrangement of the transitional double bond, as depicted by the bold blue oxygen atom for clarity in Scheme 2.4. However, the outcome is the same regardless of the orientation, and both routes still form acrylic acid once the enolate-transition state is formed.

Fumaric acid can also undergo decarboxylation, but because it's a much weaker acid ($pK_{a1} = 3.0$) than maleic acid ($pK_{a1} = 1.5$), the formation of the enolate-transition state requires a much higher temperature in excess of 240 °C as compared to 130 °C for maleic acid. The temperature at which decarboxylation occurs can be significantly lowered to 100 °C by the presence of a weak tertiary base such as pyridine or dioctyl-methylamine, but this is generally accompanied by

polymerization to yield an intractable resinous mass. Likewise, maleate/fumarate half esters form alkyl acrylates and/or dialkyl maleate esters and free maleic acid, the latter of which transforms into acrylic acid as outlined above [3, 14].

### 2.2.3 Peroxidation

The peroxidation of linear anhydrides with concentrated hydrogen peroxide has been well known since the late 1950s [9]. However, it was not until 1962 that White and Emmons demonstrated the formation of maleic peracid from maleic anhydride and hydrogen peroxide, as shown in Scheme 2.5 [15, 16].

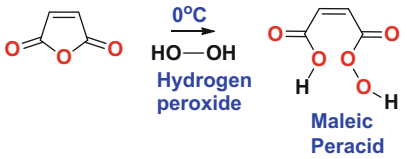


**Scheme 2.5** Peroxidation of maleic anhydride into maleic peracid

The synthesis of maleic peracid was carried out in methylene chloride at 0 °C by means of an ice bath as depicted in Scheme 2.5. Other inert solvents for this reaction include benzene, dioxane, DMF, and formamide. At 0 °C, the peroxidation reaction predominates and little to no epoxide is formed with the double-bond functionality. However, Saotome et al. [17, 18] demonstrated that at 70 °C, aqueous solutions of maleic acid can be epoxidized. Therefore, the peroxidation reaction is extremely sensitive to temperature, and the heat released upon treatment with aqueous hydrogen peroxide must be maintained as low as possible. This can be achieved by controlling the addition rate of the peroxide to maleic anhydride to keep the overall reaction temperature well below 30 °C to prevent this side reaction.

In 1967, Rohm and Haas patented the use of maleic peracid as an excellent oxidizing agent for conversion of monoketones to their esters by the Baeyer–Villiger reaction, such as the conversion of benzophenone into phenyl benzoate in near-quantitative yield in 2 h [16, 19]. Maleic peracid is also an excellent oxidizer of primary amino compounds into their nitro-derivatives, as well as conversion of olefins into their epoxide end product [15, 20].

It was demonstrated that the maleic peracid was not as potent as trifluoroperacetic acid, but was stronger than all other organic peracids, such as performic, peracetic, and perphthalic acids, and was reasonably stable in methylene chloride where it decomposes approximately 5 % in 6 h at room temperature. An additional benefit in performing the synthesis of maleic peracid in methylene chloride was the ease of removal for the unwanted maleic acid that precipitates out from the reaction medium because of its insolubility in this solvent.

It was postulated by White and Emmons that the strength of maleic peracid in the Baeyer–Villiger oxidation could be attributed to its lower basicity and higher stability of the maleic peracid monoanion intermediate, as the second acid group

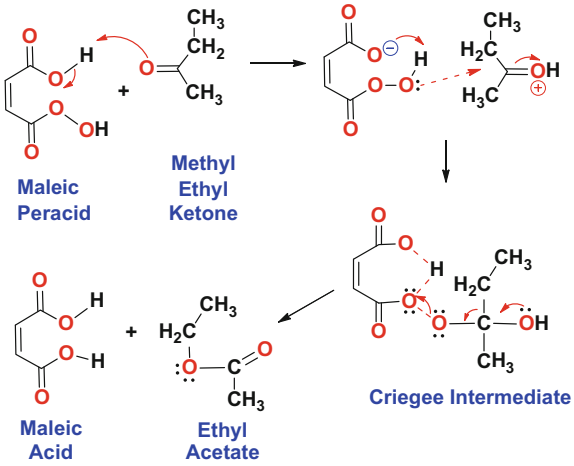


**Scheme 2.6** Baeyer–Villiger oxidation of a ketone by maleic peracid in its transition state and conversion from ketone to an ester

protonates the adjoining peroxide oxygen as depicted in Scheme 2.6. This is analogous to the acidity of maleic acid previously described by its resonance structures distributing the anionic charge across both carbonyl groups.

A carbon rearrangement ensues to transfer one of the alkyl groups onto the geminal oxygen atom as an electronic rearrangement completes the ester transformation. When different alkyl groups are attached to the keto-functionality, then the more substituted group proceeds to migrate onto the oxygen atom thereby producing the more substituted ester due to the stabilization of the transition-state intermediate.

### *2.2.4 Friedel–Crafts Acylation*

Over 130 years ago, Von Pechmann can be credited for first observing that in the presence of Lewis acid catalysts like $AlCl_3$, maleic anhydride can be used to acylate aromatic compounds under anhydrous conditions, as outlined in Scheme 2.7 [21]. If an excess of $AlCl_3$ is present, addition of another molecule of aromatic functionality can occur, but this time to the double bond of maleic anhydride to form α-aryl-*β-aroylacrylic* acids. In the case of substituted-benzene derivatives, acylation takes place at the *para*-position to generate *β-aroylacrylic* acids in very good yields, ranging from 70 to 90 % [22, 23]. Furthermore, the *trans*-isomer predominates as the acylation end product instead of the *cis-isomer*.

In many cases, the aromatic reactant is also the solvent that is used in excess to drive the reaction to these 70–90 % yields and that the *trans-isomers* are inclined to be yellow in color, while the minor *cis-isomers* are usually white. However, chlorinated solvents such as 1,2-dichloroethane tend to give the best yields for this type of reaction.

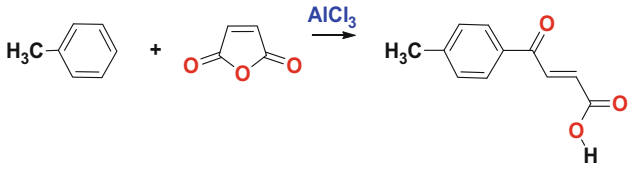


**Scheme 2.7** Friedel–Crafts acylation with maleic anhydride

Similarly, modification of pendant side chains of aromatic monomers [24], or of aromatic polymers [25], can be achieved by this approach, and carboxylic acid/salt functionality can be tailored onto the molecule, so that the physical and chemical properties are further enhanced to either reactivity, solubility, or other potential derivatives to specifically design the desired properties onto the resultant polymer. Hence, as summarized in Scheme 2.8, there are at least three ways to incorporate the maleoyl functionality onto a polymer. The first is to simply copolymerize the maleic anhydride into the polymeric backbone with an aromatic comonomer such as styrene (Scheme 2.8a) [24]. A second approach is to synthesize a *β-aroylacrylic* acid monomer and then polymerize it (Scheme 2.8b) [21, 25]. Thirdly, it can hang off as a pendant group on the polymer (Scheme 2.8c) [26]. Therefore, this simple acylation reaction summarized in Scheme 2.8b,c is quite powerful in the versatility of molecules and polymers that can be made.

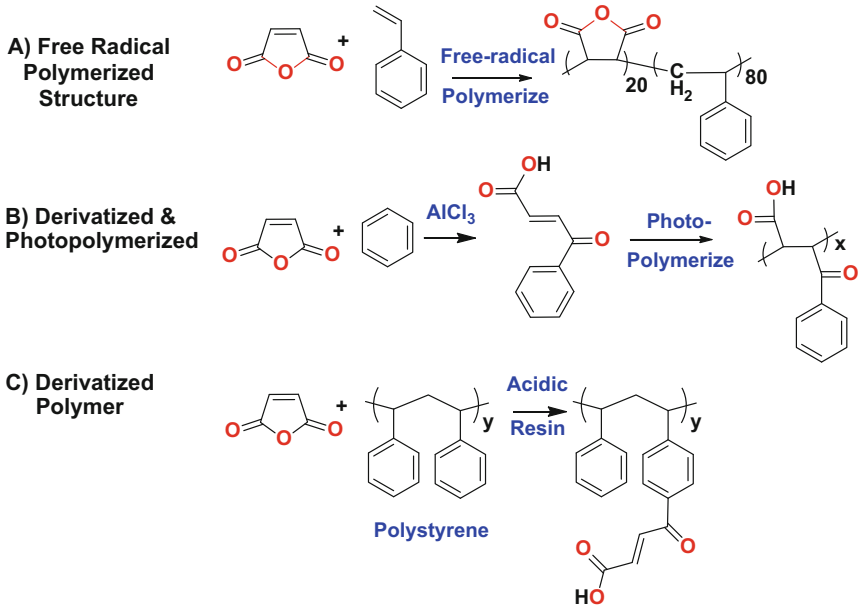


**Scheme 2.8** Formation of polymeric derivatives of maleic anhydride by copolymerization (**a**) or by Friedel–Crafts acylation (**b**, **c**) reactions

### 2.2.5 *Acid Halide Formation*

The formation of monoacid halides from maleic anhydride or from maleic acid is not readily obtained. This is primarily due to the preference of such compounds to regenerate maleic anhydride instead. Treatment of maleic anhydride with reagents

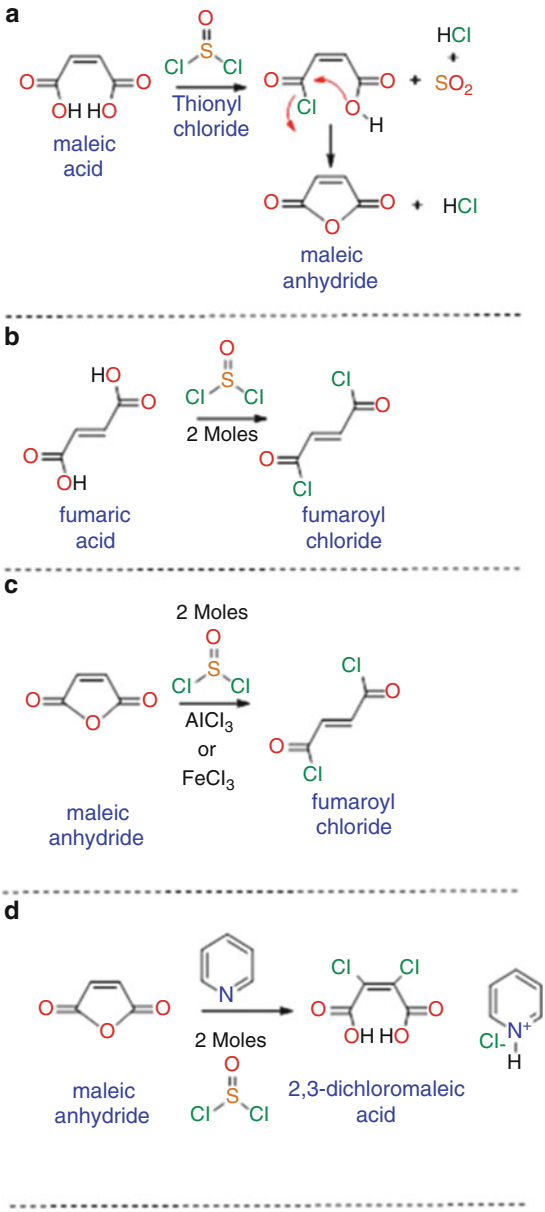


**Scheme 2.9** Formation of maleate derivatives from maleic anhydride and acid-chloride reagents

such as phthaloyl chloride, thionyl chloride, or $PCl_5$ also converts maleic anhydride into a number of different entities depending on the catalyst used in conjunction with these reagents, as outlined in Scheme 2.9. Likewise, acid dichlorides and maleoyl chlorides do not form either, but the acid dichlorides from fumaric acid, fumaroyl chloride, are achievable in high yields.

The reason for the lack of mono- and diacid-chloride formation from maleic acid is quite simple. Once the first acid chloride is formed on the maleic molecule, its neighboring sister acid spontaneously intramolecularly ring-closes to reform maleic anhydride (Scheme 2.9a). This process cannot occur for fumaric acid as it is in the *trans*-configuration, so the carbonyl groups are too far apart to react intramolecularly (Scheme 2.9b). Therefore, fumaroyl dichloride is readily formed upon treatment with thionyl chloride with fumaric acid.

With regard to the actual reaction between maleic anhydride and thionyl chloride, there appear to be some discrepancy and inconsistencies in the literature. For example, Kyrides claimed the synthesis of fumaroyl chloride from maleic anhydride–$SOCl_2$ in the presence of ZnCl and heat [27, 28], while a Union Carbide patent by Brotherton made fumaroyl chloride using $AlCl_3$ or $FeCl_3$ (Scheme 2.9c) [29].

In contrast, Trivedi and Culbertson and others claimed a structure that is highly unstable for maleoyl chloride [1, 3, 30]. US Patent 3,810,913 from General Electric claims the 2,3-dichloromaleic acid is formed in the presence of pyridine catalyst (Scheme 2.9d) [29].

The reaction pathway to the product appears to be dictated by the promoter/catalyst used in conjunction with maleic anhydride–$SOCl_2$ pair. Simply put, maleic acid dichlorides do not readily exist. But fumaroyl chloride can be made from maleic anhydride [27, 30], as well as 2,3-dichloromaleic acid [31], while 2,3-dichloromaleic dichloride can be obtained by thermal decomposition of ethyl perchlorocrotanate [32].

### 2.2.6 *Alkali Metal Salt Formation, Organic Neutralizer, and Metal Chelation*

Hydrolysis of maleic anhydride followed by neutralization with an alkali metal hydroxide provides the simplest reactions outlined in this chapter, as depicted in Scheme 2.10a. Since maleic acid is a diacid, it can neutralize and complex multivalent metals too, but this can occur both intramolecularly and intermolecularly as shown in Scheme 2.10b,c. Simple hydrolysis and neutralization really is an oversimplification of the true complexity that exists.

Maleic acid itself can also be used to neutralize pharmaceuticals and other basic compounds to increase their stability and solubility in water or blood plasma for

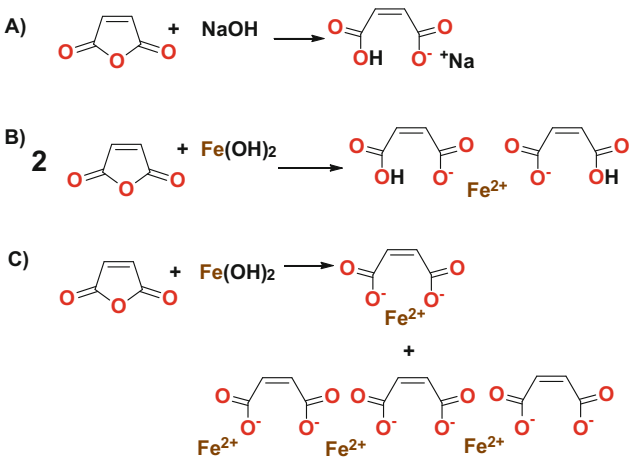


**Scheme 2.10** Maleate salt formation by neutralization

gastrointestinal adsorption. Maleic acid can be used for making maleate salts of bulk drugs like pheniramine maleate, fluvoxamine maleate, timolol maleate, chlorpheniramine maleate, enalapril maleate, and others [33]. The monosodium maleate salt can also be used as a buffer in the pH range 5.2–6.8 [34]. Zirconium and other esoteric salts can also be made by entropic factors with the use of ion-exchange resins.

Note that this scheme is a two-dimensional representation. In particular, maleic and fumarate mono- and dibasic salts are very important representatives of the β-dicarboxylic acid class for their complexation or chelating ability to metal ions. When two electron-rich carbonyl groups are conjugated to the electron-deficient double bond, the electron-acceptor character of the olefinic C=C particularly increases [35]. Maleic anhydride has the best acceptor properties among derivatives of the α,β-unsaturated dicarboxylic acids in part due to their ionization potential of their respective p$K_a$s, as previously described in Sect. 2.1.

Stable metal chelates form with maleic salts. This is particularly evident for divalent and multivalent metal ions chelating with the planar mono- and dibasic salts of maleic acid. In doing so, the interaction between the 3D orbital of the metal cation with the anionic maleic carboxylate group is optimized geometrically resulting in stabilization of the ionic salt as a whole. This stabilization is not just a consequence of the local environment around the individual metal atom, but it extends to the whole complex formed as a unit cell in the crystal structure [35].

For example, monobasic maleates with cobalt, iron, zinc, nickel, manganese, and magnesium having the general formula of (mono-metal-maleate)$_2$•tetrahydrate are typical representatives of this group of molecules. In this centrosymmetrical complex, the metal atom is linked to two monodentate maleic molecules, where, for instance, the Fe•••O distance is 2.157 Å and the octahedron structure being completed by the four water molecules, as depicted in Fig. 2.13.

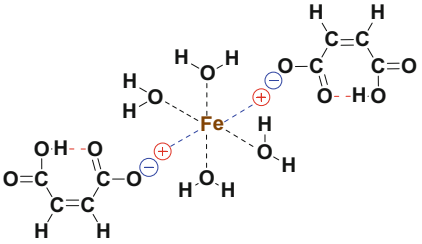


**Fig. 2.13** Structure of iron(II)-hydrogen maleate tetrahydrate salt/chelate, where *red dashes* are hydrogen bonds, *black dashes* are columbic attractions, and *blue dashes* are ionic attractions

The planar structure of the maleate ligand in these complexes is further stabilized by an intramolecular hydrogen bond of the maleate carboxyl groups as illustrated in Fig. 2.13. In fact, the Fe-maleate hydrogen bond depicted in red is H ••O = 1.87 Å, while the O•••O distances within the maleate moiety are within the range of 2.39–2.44 Å. The symmetry of these hydrogen bonds presented in Fig. 2.13 can vary significantly, from perfectly symmetrical to completely asymmetric.

In contrast, the dianionic form of maleic can play a dual role in the Fe(III) complex. First, there is an axial ligand binding the metal atom with the monodentate carboxyl group, while the other carboxyl group acts as a counterion, as illustrated in Fig. 2.14. Furthermore, the presence of a broad net of intramolecular columbic forces and ionic attractions occurs around the individual iron atom, in addition to these same interactions bridging neighboring Fe atoms to form the stabilized network structure depicted as the result [36]. The potassium iron(III)-tri-maleate hydrate also has the same overall structure, in addition to hydrogen bonding by water inside the crystal lattice as in Fig. 2.14.

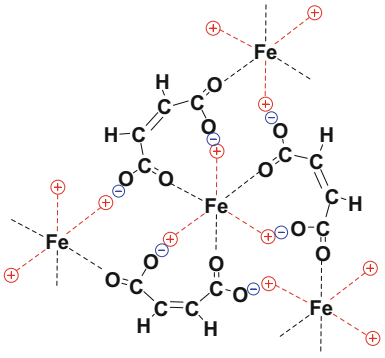


**Fig. 2.14** Structure of iron(III)-tri-maleate salt/chelate, where *blue* anions indicate bridging carboxylate group, *black dashes* are columbic attractions, and *red dashes* are ionic attractions

The two maleate salts or chelates just described demonstrate that formation of maleate salts is not as simple as one would expect. There is a higher-order structuring of the metal cation with the maleate anion that forms an anisotropic system both intramolecularly and intermolecularly. These attractive forces form an associative network of columbic and ionic interactions, sometimes further stabilized by hydrogen bonding from water, and as a whole stabilize the overall structure derived.

For iron, an octahedron array is generated, while for copper, a pyramidal–square–planar array is formed, thereby generating a whole host of structural or geometric arrays of interaction between the particular metal cations used and the mono- or dibasic maleate anions that resultantly form these higher ordered structures.

Not only do these polymorphs have different solubilities and melting points, but they are also recognized as different structural entities from an intellectual property point of view.

The polymeric analog for the maleate salts in copolymers of maleic anhydride also exhibits similar interactions and has effect to its physical properties too. While many polymers are amorphous, the incorporation of metallic cations can induce higher-order structuring.

### 2.2.7 *Esterification*

Reactions involving the reactive anhydride functionality allow for a diverse group of compounds that can be made out of maleic anhydride. Maleic anhydride esterification with alcohols proceeds readily at moderate temperatures, approximately 80–90 °C for 6 h, to generate monoalkyl esters (Scheme 2.11). The acidity of monoalkyl maleate esters are significantly lower than the diacid form of maleic acid as there is no delocalization of the anionic charge across both carbonyl groups, and therefore the p$K_a$ approaches that of typical monoalkyl esters around 5.5.

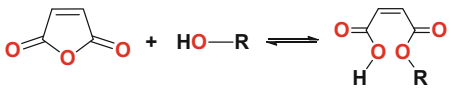


**Scheme 2.11** Esterification of maleic anhydride to form monoalkyl esters

As expected, the highest reactivity occurs with primary alcohols, followed by secondary, and lastly tertiary alcohols due largely to steric factors. Note the double-sided arrows in Scheme 2.11, as this is an equilibrium reaction and is reversible depending on the conditions.

Primary alcohols react the quickest at lower temperatures. But they are also the least stable to hydrolysis or transesterification, transforming at temperatures of 20–40 °C over the course of several months. This result is due to the anhydride functionality reforming under acidic condition liberating free alcohol at moderate

temperatures slowly. These processes can proceed over several hours when temperatures are in excess of 80–90 °C.

Alpha-branched alcohols such as 2-ethyl-hexanol, 2-methyl-1-propanol, and *sec*-butanol are slower to react. But they are more stable, inhibiting reformation of anhydride functionality by ring closure. Other secondary alcohols like menthol and cyclohexanol behave similarly.

Esterification by tertiary alcohols is the most difficult and requires even higher temperatures, in excess of 100–120 °C. These reactions are rarely quantitative unless a large excess of alcohol, usually 4–5 stoichiometric equivalents over that of the anhydride. Catalysts are sometimes used to lower the temperature of the esterifications, speed up the rate of the reaction, and improve yields.

A number of catalysts can be used. Acidic catalysts (such as *p*-toluene sulfonic acid, methane-sulfonic acid, or trifluoroacetic acid), inorganic acids like sulfuric or phosphoric acid, and metal catalysts (copper based or tin oxalate or dibutyl-tin) can be used to accelerate this reaction. The most common catalysts are sulfuric and hydrochloric acids, boron trifluoride, organo-tin, zinc salts, and aluminum halides.

In commercial practice *p*-toluene sulfonic acid, or methane-sulfonic acid, is preferred because it tends to be less corrosive to the reactor. Sometimes phosphoric acid is used but this leads to slower reaction rates. Soluble metal salts or their insoluble counterparts minimize side reactions, but require higher temperatures [37–41].

The use of acid-regenerated cation-exchange resins have grown in popularity over the years. They are easily removed by simple filtration and can be regenerated over again [42, 43]. These are typically based on styrene, ethylvinylbenzene, and divinylbenzene copolymers that are sulfonated and cross-linked to provide the macroporous nature of these types of catalysts.

These catalysts provide rapid reaction rates for esterification because of their high surface area of highly acidic sulfonic acid groups [44]. Typical resins such as Amberlite IR-116 and Amberlite IR-120B are used because despite their higher cost compared to inorganic acids, they provide better selectivity and can be used in continuous bed reactors or stir tanks, increasing throughput compared to batch reactors [45–48].

Typically, dialkyl maleate esters can be produced from maleic anhydride with alcohols, such as methanol with sulfuric acid acting as acid catalyst. The reaction proceeds via a nucleophilic acyl substitution to synthesize the monomethyl ester. This is followed by a Fischer esterification reaction for generation of the dimethyl ester. Both reactions are well known.

However, dialkyl maleate esters can also be formed from monoalkyl maleate esters as well. This requires high temperature usually >100 °C. Primarily because one of the two molecules of monoalkyl ester is capable of reverting back into maleic anhydride and free alcohol (Scheme 2.12a) followed by the attack of the second molecule of monoalkyl maleate to form an acyclic anhydride (Scheme 2.12b), then the free alcohol can attack this acyclic mixed anhydride to form the diester and maleic acid, as illustrated in Scheme 2.12c [49].

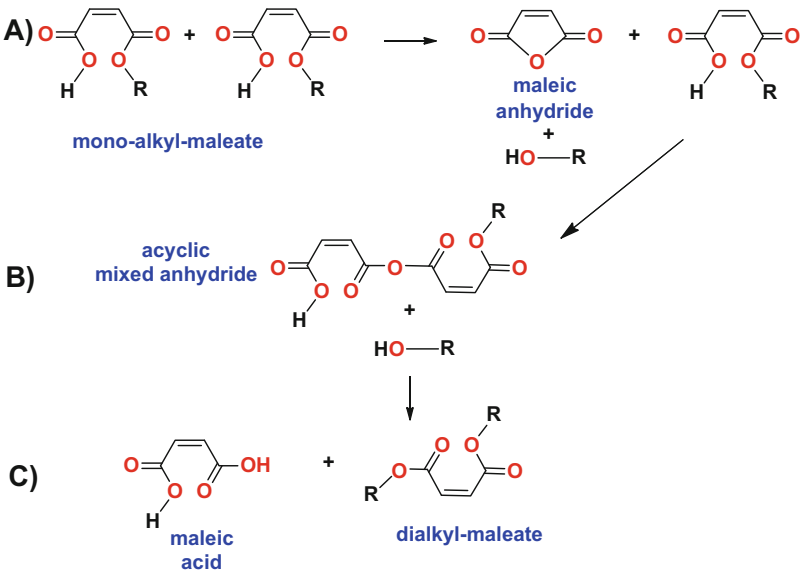


**Scheme 2.12** Formation of dialkyl esters of maleic anhydride during esterification reaction or distillation

Care needs to be exercised during distillation or purification procedures of the half esters to prevent such side reactions from occurring. Another side reaction observed at high temperatures is the unwanted isomerization of the maleate into its sister-isomer fumarate. Usually temperatures below 100 °C are employed to prevent this from happening.

The synthesis of diesters utilizing the reaction of carboxylic acids with dialkylcarbonates in the presence of weak Lewis acids such as $MgCl_2$ and optionally with the corresponding alcohol as solvent is depicted in Scheme 2.13 [50]. This approach is effective for more energy-intensive synthetic processes as described in Scheme 2.12.

The mechanism generally thought to arise from a double addition of the carboxylic acid to the alkyldicarboxylate resulting in the formation of a mixed carboxylic/carbonic anhydride and $CO_2$, as presented in Scheme 2.13. The first step is activation by $Mg^{2+}$ ion with the dialkylcarbonate. In the second step, maleic acid (A) reacts with the activated carbonate to form the mixed anhydride (B), $CO_2$, and alcohol. In the third step, the released alcohol attacks the mixed anhydride to form monoalkyl maleate (C), $CO_2$, and another molecule of free alcohol. Fourth, another molecule of activated dicarbonate reacts with the monoalkyl maleate to regenerate the mixed anhydride (D). In the fifth and final step, another molecule of free alcohol reacts with the mixed anhydride (D) to form the dialkyl maleate (E). Esterification of the carboxylic acid with the correct choice of alkyl group on the dialkyl dicarbonate results in esters with only $CO_2$ as process by-product.

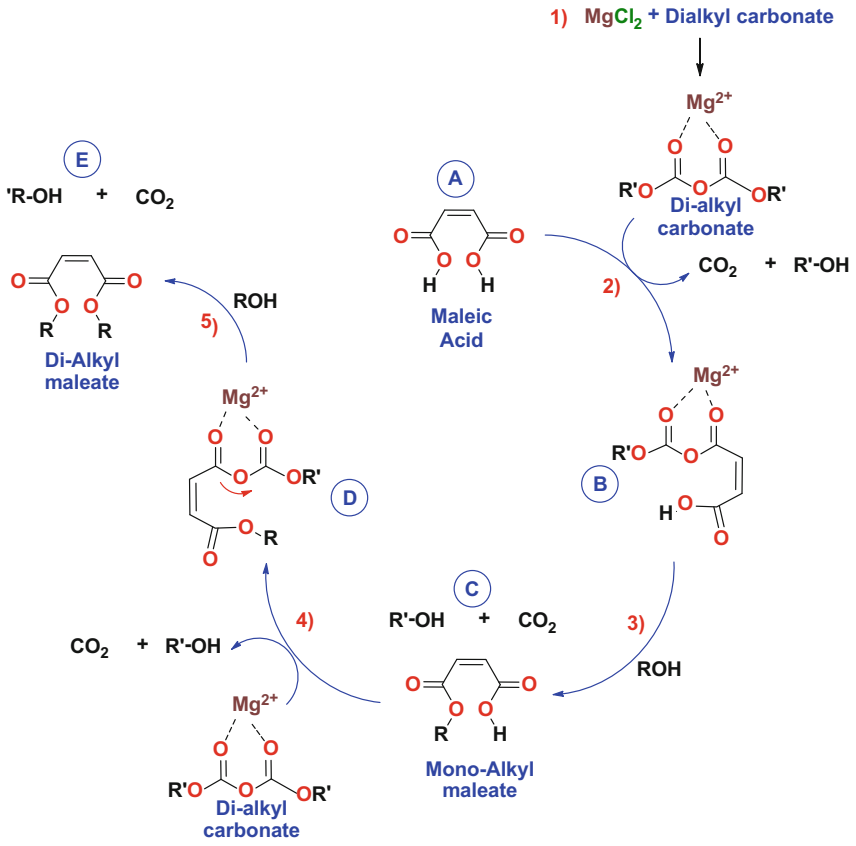


**Scheme 2.13** Maleic acid conversion to a diester with dialkyl dicarbonate and $MgCl_2$

The reaction of maleic anhydride with epoxides deserves special mention here and will be discussed in more detail in Chap. 5. These reactions lead to the synthesis of polyesters [51, 52]. In general, the reaction can be carried out at ~45 °C, with little to no side reactions. While ether formation or cross-linking is possible, the majority of product is an alternating polyester of maleic/glycol comonomer units ranging in molecular weight around 15–20 kDa, with a low polydispersity around 1–2 [53]. If a catalytic amount of organic base is added, some of the maleate units can isomerize to a fumarate/maleate polyester. Such isomerizations lead to increasing the $T_g$ by roughly 10 °C. A general reaction scheme is presented in Scheme 2.14.

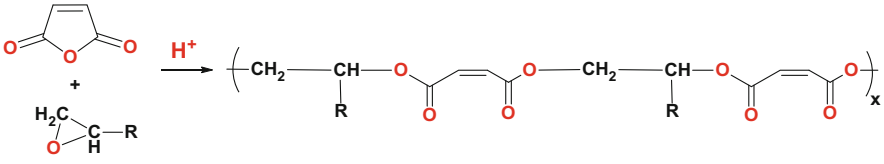


**Scheme 2.14** Polyester formation from the reaction of maleic anhydride with epoxides

### 2.2.8 *Stabilization of Maleate Monoesters*

To increase the stability of newly formed monoalkyl maleate esters, quick neutralization of the half acid immediately after the esterification reaction can inhibit anhydride reformation by ring closure. In this way, the formed alkoxy anion will rapidly reopen the transient anhydride to reform the monoester. This process is depicted in Scheme 2.15. A unique feature of regenerating the anhydride functionality is the *cis*-carbonyl structure of maleic acid and monoesters. This *cis*-configuration only inhibits the anhydride from forming and does not prevent it. Under dilute concentrations in water or another alcohol, hydrolysis or transesterification still proceeds but only at a slower rate.

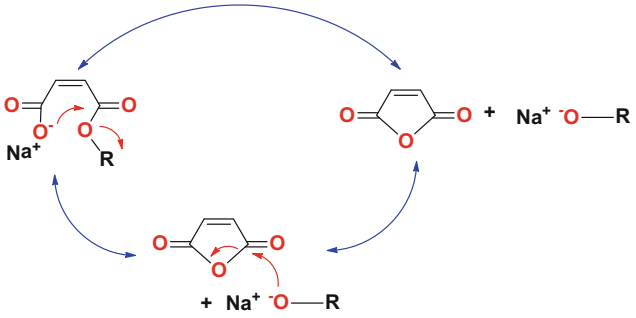


**Scheme 2.15** Stabilization of monoalkyl esters of maleic anhydride by neutralization

Esterification reactions can also be achieved indirectly. For example, maleic acid at temperatures in excess of 90–100 °C enables ring closure of the diacid to form the anhydride functionality, which then can proceed to esterification as previously described. However, removal of water is essential for this reaction to achieve any quantitative result.

The use of azeotropes is often employed to remove water during the esterification of maleic acid. With the exception of methanol, many smaller chain-length aliphatic alcohols with chain lengths up to C20 alcohols form binary azeotropes with water. The removal of these higher alcohols drives the equilibrium in favor of the ester product [54]. Under certain conditions, gases are entrained to facilitate the removal of water, like bubbling air into the liquid solutions [55].

Use of desiccants and other chemical means to dehydrate the reaction has also been employed. Typically, these strategies are utilized toward the end of the reaction process to drive it to completion. In one example, the reaction solution is continually pumped through a drying bed of calcium carbide/chloride and then back into the reactor by means of a recirculating loop over the course of the reaction [56, 57].

### 2.2.9 *Thioester Formation*

The procedures just described for simple esters can also be applied for the synthesis of simple alkyl mono-thioesters from maleic anhydride. Addition of an aliphatic thiol to maleic anhydride proceeds more rapidly than alcohols due to the polarizable electron-rich sulfur moiety. As a result, thio-esterification can occur at much lower temperatures.

However, the reaction mechanisms are much more complicated due to the presence of the activated double bond in the maleate functionality. This activated double bond is very susceptible to nucleophilic reagents, capable of participating in Michael-type reactions. Hence, attack at the anhydride is often accompanied by addition to the double bond as well, resulting in a myriad of side products as illustrated in Scheme 2.16. Nevertheless, given the labile thioester group present in intermediate-A, it is possible to drive the reaction to the thermodynamically stable alkyl-thio-succinate as the major product [58, 59].

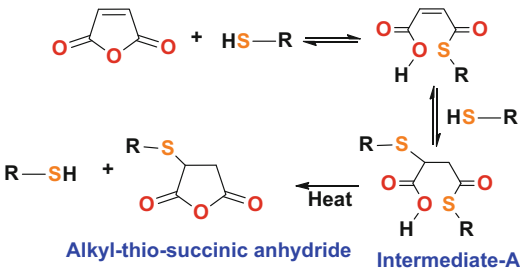


**Scheme 2.16** Thioester and S-alkylation formation of maleic anhydride with an alkyl thiol

One special case worth mentioning is the use of mercaptoethanol with maleic anhydride. The kinetic product is the thioester and not the oxy-ester. This thioester is not thermodynamically stable and spontaneously rearranges to the oxy-ester. One can obtain a free thiol esterified by its alcoholic group to the maleic functionality as depicted in Scheme 2.17. But this reaction is not yet completed, as demonstrated by addition of the free thiol to the activated double bond in Scheme 2.17. Allowed to proceed, a poly-(ester-thioether) copolymer is formed, as outlined in Scheme 2.17 [60]. It is noteworthy to note that the offensive stench from these thio-based products has prevented their widespread use.

The esterifications described so far have been under acidic conditions. Basic catalysis is not practical with maleic anhydride or its acid derivatives for a number of reasons. They tend to require more expensive catalysts and their selectivity is not very good. In addition, the presence of the activated double bond makes it very susceptible to nucleophilic reagents. In general, a multitude of by-products is observed with basic catalytic processes.

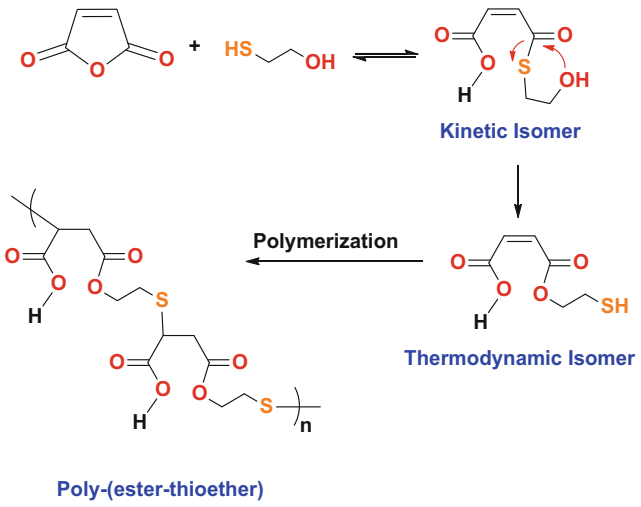


**Scheme 2.17** Esterification of maleic anhydride with mercaptoethanol

## *2.2.10 Amidation Reactions*

Addition of ammonia, primary, or secondary amines to maleic anhydride enables the formation of an amide derivatives. These amide compounds are commonly called maleamic acids, or amic acids, or half-amides. If the organic substituent is an aromatic, it is generally referred to as a maleamic acid derivative, as depicted in Scheme 2.18. Because of the presence of the activated double bond in maleic anhydride, addition across the double bond can also take place, via a Michael-type reaction. This reaction pathway lowers the overall yield of amide and generates many side products.

In general, when a Michael addition derivative is wanted, maleic diesters or its salts are used. When the half amide is desired, then maleic anhydride can be used. For this approach, temperature control is critical to the success of this reaction. In particular, if the reaction temperature is maintained at 50 °C for 5 h, 95 % yield of half amide is obtained for both aliphatic and aromatic amines [58, 59]. When temperatures exceed 50 °C, then both Michael additions and half amide formation occur simultaneously.

Hydroxylamine and hydrazine, as well as their organic counterparts such as alkyloxyamines ($NH_2OR$) and hydrazides, react in a similar fashion with maleic anhydride. The reaction of maleic anhydride with hydrazine is of considerable

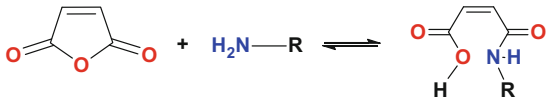


**Scheme 2.18** Amidation of maleic anhydride by amines

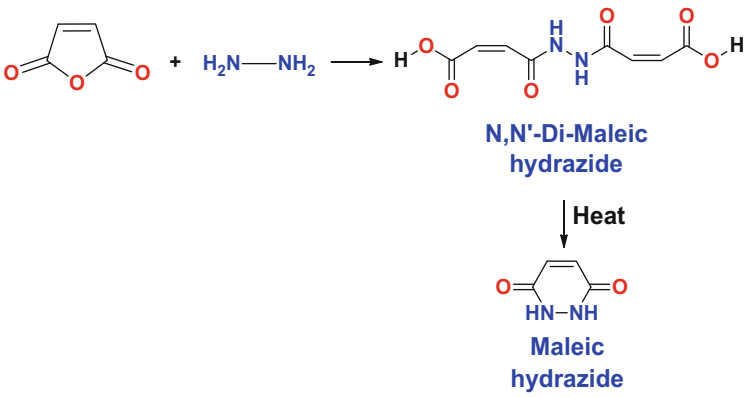


**Scheme 2.19** Reaction of maleic anhydride with hydrazine

importance synthetically and commercially. For example, Feuer and coworkers demonstrated that two reactions can occur with hydrazine depending on the conditions employed for the reaction [61]. When maleic anhydride and hydrazine in a 1:1 ratio are dissolved in acetic acid, the mono-hydrazide is not formed. But the *N*, *N*′-dimaleic hydrazide is the major product at 96 % yield. Yet, upon heating this product, it can cyclize upon itself, intramolecularly rearranging to maleic hydrazide in 83 % yield. These processes are depicted in Scheme 2.19.

Interestingly, this reaction occurs only under weakly acidic conditions, such as acetic acid or in refluxing water. Under highly acidic conditions such as in polyphosphoric acid, the cyclization reaction does not readily occur and only the intermolecular *N*,*N*′-dimaleic hydrazide is formed. A similar result is found when the maleic anhydride to hydrazine ratio is 2:1, under highly acidic condition. When a hydrazinium salt such as hydrazine hydrochloride, sulfate, or phosphate is used, then cyclization into the intramolecular hydrazide readily proceeds [62].

### *2.2.11 Maleimides and Imidation Reactions*

Maleimides can be produced by dehydration/cyclization of maleamic acids/esters (Scheme 2.20) [63]. Simple heating of maleamic acid derivatives with concomitant water removal or use of its ester offers the simplest way to produce maleimides. An acid catalyst, such as those employed for esterifications, can also be employed [64]. In particular, maleamic acids can be converted to maleimides with strongly acidic cation-exchange resins, in conjunction with vacuum or azeotropic distillation of the water. Once the reaction is complete, then the acidic resin is simply filtered off [65].

In the absence of a strongly acidic catalyst, the thermal dehydration reaction requires very high temperature, 130 °C or higher. To reduce this temperature,

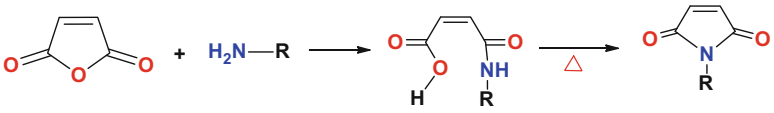

**Scheme 2.20** Maleimide formation from maleamic acids by dehydration using high temperature or an acidic catalyst

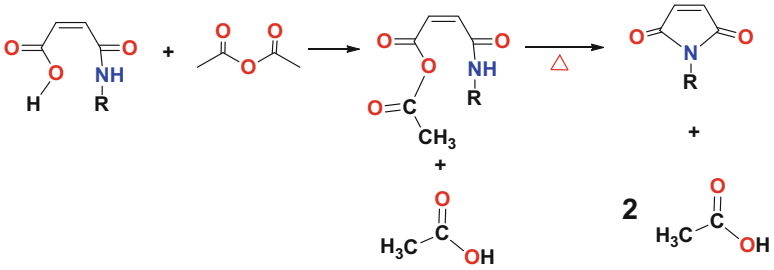

**Scheme 2.21** Maleimide formation using a mixed anhydride scheme

100 °C or less, requires removal of water by vacuum or azeotropic distillation and addition of an acidic catalyst. Other catalytic imidation methods include the addition of acetic anhydride with triethylamine to form the mixed anhydride. This approach leads to cyclization and dehydration and is presented in Scheme 2.21 [65]. In the case of very hydrophobic imides, the removal of the ammonium acetate salt can be achieved by washing the biphasic mixture with water and/or recrystallization from hydroalcoholic blends.

Commercial tactics employed often include air sparging during the reaction, or super-heated steam/nitrogen sparge, to facilitate water removal. Vapor-phase reaction of maleic anhydride with anhydrous ammonia over a dehydration catalyst like $Al_2O_3$, and zeolites, is another commercial approach.

Similarly, bis-maleimide cross-linkers can be produced from di-amines. The length of the spacer between the maleimide units can impart either rigidity or flexibility as in six or more linear methylene groups (this feature has been exploited in the manufacture of liquid-based maleimide precursors that after heat treatment polymerize into a solid adhesive for electronic circuitry boards. Mixtures of metals and the liquid maleimides have also been used to form conductive adhesives between silicon wafers in the manufacture of computer chips too), as outlined in Scheme 2.22 [66, 67].

Another indirect approach to imidation is the reaction of maleic anhydride with urea or alkylurea to obtain the *N*-carbamoylmaleic acid in the presence of acetic acid solvent up to 80 °C, as summarized in Scheme 2.23 [68]. This *N*-carbamoylmaleic acid can be ring closed to form the *N*-carbamoyl-maleimide at 100 °C or at 140 °C upon which thermolysis in DMF produces maleimide, ammonia, and isocyanate by-products, as summarized in Scheme 2.24 [69].

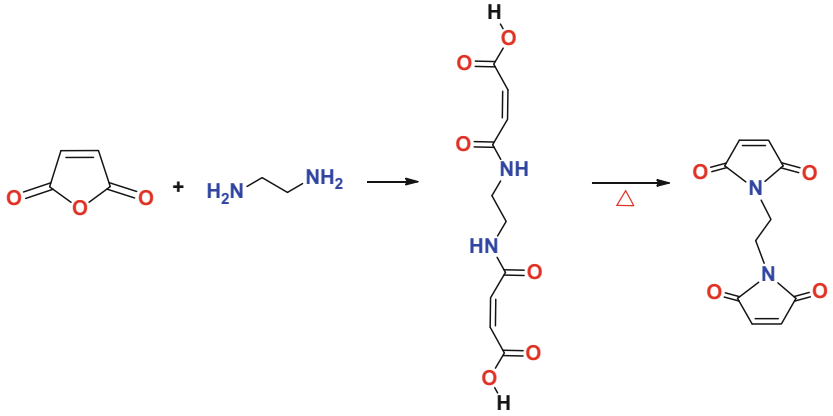

**Scheme 2.22** Bis-maleimide formation from maleamic acids by dehydration using high temperature and/or an acidic catalyst

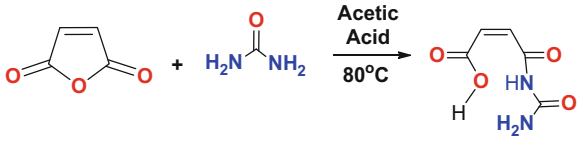


**Scheme 2.23** Reaction of maleic anhydride with ureas

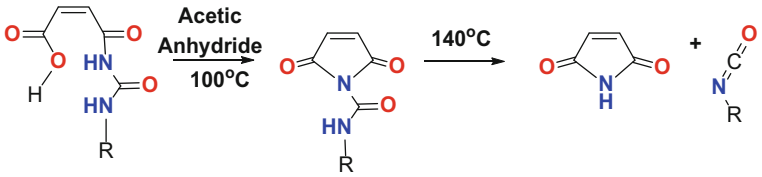


**Scheme 2.24** Maleimide formation using thermolysis of the *N*-carbamoyl-maleimide

For temperature-sensitive and/or chiral substituents, activation of the amic acid can be achieved using more sophisticated strategies. For instance, imide formation can be achieved at much lower temperature (25 °C) when using acyl halide formation on the free acid functionality with thionyl halides ($SOCl_2$) or phosphorous halides ($PCl_5$, $PBr_3$). Likewise, mixed anhydrides with the use of phosphorous pentoxide, or chloroformates, or carbodiimides can also achieve the same result. However, these reagents are more costly and impractical for most large commercial syntheses.

The synthesis of maleimido-hydrazide can be achieved by the use of a protected-hydrazide like *t*-butoxycarbonyl-hydrazide (Boc-hydrazide) with maleic anhydride followed by thermal dehydration/cyclization. Subsequent deprotection with an acid enables the generation of gaseous $CO_2$ and isobutylene. This reaction is outlined in Scheme 2.25 [70].

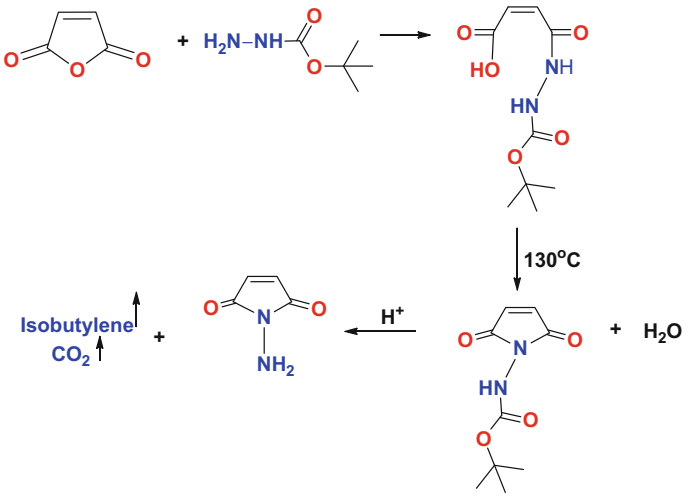


**Scheme 2.25** Maleimido-hydrazide formation using thermal dehydration of BOC-hydrazide with maleic anhydride

## 2.3 Hydrogenation of the Electron-Deficient Double-Bond Functionality

### *2.3.1 Catalytic Hydrogenation of Maleic into Succinic Derivatives*

In principle, hydrogenation of maleic anhydride can be the most direct, environmentally safe, and economical route to manufacture succinic acid. Maleic anhydride is readily available and low price is the result of large production plants in use today. There are several approaches to the hydrogenation of maleic anhydride: catalytic, electrolytic, and transfer hydrogenation.

Maleic or fumaric acids or its salts, as well as their esters, or (thio)esters, amides, and its imides can be reduced to their succinate counterparts [71, 72]. A number of hydrogenation catalysts can accomplish this task. For example, disodium maleate can be reduced with Raney Nickel at 100 °C and 156 bar [73]. After acidification, the yield is nearly quantitative. Milder conditions for hydrogenation are often employed with more expensive metal catalysts like platinum or palladium. These approaches suffer from side reactions to form γ-butyrolactone (BLO) and tetrahydrofuran (THF), as depicted in Scheme 2.26 [74]. In some cases, these side reactions are desired for the production of useful downstream chemicals.

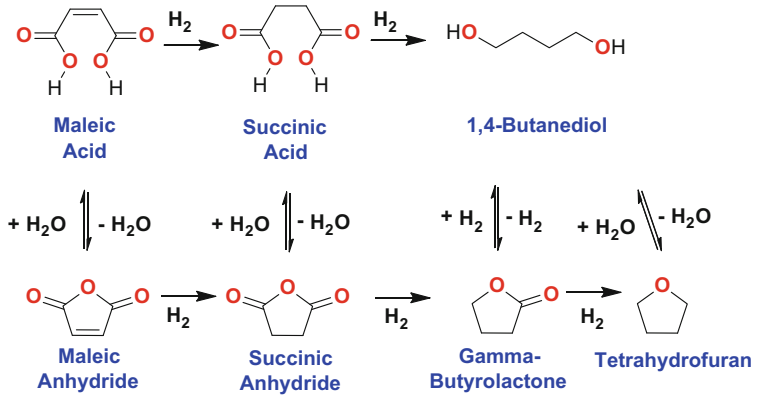


**Scheme 2.26** Hydrogenation reactions of maleic anhydride

Maleic anhydride provides a route for many industrially significant chemicals and intermediates: succinic anhydride, 1,4-butanediol, γ-butyrolactone, and THF. The production routes are depicted in Scheme 2.26 [75, 76]. These molecules are produced by both hydrogenation and hydrogenolysis reactions.

There are basically four processes to produce these industrially significant molecules: (1) the Reppe process is based on the condensation of acetylene with formaldehyde; (2) the Davy McKee process is based on hydrogenation of maleate diesters [77]; (3) the Mitsubishi-Kasei process (MKC) is based on diacetoxylation of 1,3-butadiene; (4) and the Arco process is based on isomerization of propylene oxide to allyl alcohol, followed by hydroformylation [78]. Each of these processes has shortcomings. For example, the Reppe process uses explosive acetylene as a starting reagent under rather severe temperature and pressures (140–280 bar, 250–350 °C); hence, specialized knowledge and equipment are required to follow this route [79]. Likewise, the Arco process uses explosive propylene oxide, while the Davy McKee and Mitsubishi processes use costly reagents and precursors.

Maleic anhydride hydrogenation employing different noble metal or copper-based catalysts in either the vapor phase or liquid phase has also been reported [75, 77–83]. Nickel promotes the hydrogenation reaction of maleic toward succinic anhydride, while small amounts of copper are used to prevent the side reaction of maleic anhydride to form γ-butyrolactone. But the catalysts tend to be expensive and are susceptible to deactivation. Typically, the deactivation is a result of homopolymerization of γ-butyrolactone into a viscous poly-butyrolactone polyester that deposits onto the catalyst surface. Metal/clay composites have also been studied like Pd-$Al_2O_3$, Ni/$(NO_3)_2$, or Ni$(NO_3)_2$ hexahydrate for hydrogenation of maleic anhydride into succinic anhydride. Under the most optimized conditions of 190 °C at 10 bar, it was demonstrated that these nickel-based systems are good alternatives [84].

More recent academic and patent literature explores sol–gel formation to increase the surface area of the different types of catalysts for the hydrogenation of maleic anhydride [85], as well as using different solvents [86, 87]. Various products, including 1,4-butanediol, γ-butyrolactone, THF, and butyric acid, can be obtained, depending on the catalyst choice and reaction conditions employed

[88–92]. In particular, Palladium on carbon can be used for the hydrogenation of maleic anhydride in supercritical carbon dioxide, achieving 97.3 % selectivity for gamma-butyrolactone, or 100 % conversion into maleic anhydride can be achieved at an $H_2$ pressure of 40 bar and reaction temperature of 100 °C [93].

Newer catalysts have been investigated for hydrogenation of maleic anhydride to succinic anhydride. For example, complete selectivity was achieved when employing $RhCl(PPh_3)_3$, also known as Wilkinson's catalyst, in the liquid phase during maleic anhydride hydrogenation in ethylene glycol dimethylether [85]. In another approach which avoids the high cost of removing the solvent from the reaction mixture, solvent-free hydrogenation of maleic anhydride has been carried out using metallic nickel catalyst [94].

Many catalysts have also been explored in fixed bed reactors. For example, $Ni/SiO_2$, $Co/SiO_2$, and $Cu/SiO_2$ have been used as hydrogenation catalysts with maleic anhydride [95]. However, partial deactivation occurred, primarily due to polymer deposition onto the metallic phase. Nickel–platinum catalysts are commonly employed in maleic anhydride hydrogenation, where a Pt-adjunct has been found to increase the stability of the catalyst. In one example, only a 4 % loss in activity was detected after 120 hours of use [75, 95].

One pathway for catalytic hydrogenation is summarized in Scheme 2.27 as observed for hydrogenation of ethylene. Hydrogen adsorbs onto the surface of metal catalyst followed by formation of an activated metal-hydride intermediate. This process is reversible. The maleic molecule can also adsorb onto the catalyst through π bonding with the catalyst surface. Then in a stepwise fashion, one hydrogen atom is transferred from catalyst to organic acceptor. This is followed by addition of a second hydrogen atom from catalyst to the partially hydrogenated acceptor to complete the hydrogenation reaction.

This sequential addition of hydrogen was invoked to explain the lack of stoichiometry observed when deuterium gas $D_2$ was used in the hydrogenation reaction of ethylene with Pd. In particular, it was observed that the average reaction product

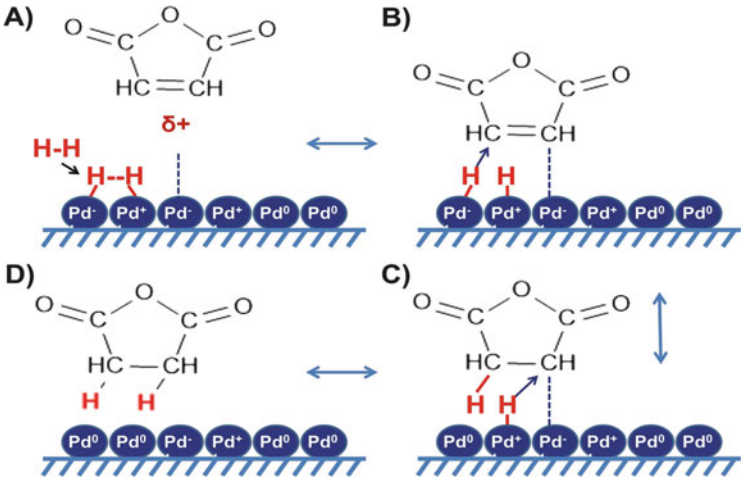


**Scheme 2.27** Catalytic hydrogenation mechanism of maleic into succinic (Adapted from [96])

was $C_2H_{2.63}D_{1.37}$ instead of the expected $C_2H_2D_2$ [96]. Therefore, the surface atoms of the catalyst can be in three different oxidation states, with a net change of −1, 0, +1. This partially explains why an electron-rich double bond would adsorb onto an electron-rich catalyst. The net +1 site on the metal exerts a columbic attraction to the electron-rich double bond of the ethylene moiety. Similarly, the electron-deficient double bond of maleic anhydride or its acid can be attracted to the net −1 site of the metal by this columbic attraction, as depicted in Scheme 2.27. Then a shuffling of electrons between the surface metal atoms acts in concert to form the transient organometallic intermediate for hydrogenation to ensue.

### 2.3.2 *Electrolytic Hydrogenation of Maleic into Succinic Derivatives*

Succinic acid can be also produced by an electrolytic reduction method using maleic acid or maleic anhydride. The production of succinic acid with electrolytic technology had been industrialized since the 1930s. After nearly 85 years of development of this technology, the mature electrolytic synthesis technology continues to accomplish higher and higher conversion ratios, yield, purity, and current efficiency in producing succinic acid. In the meantime, zero discharge of wastewater has been realized by recycling the mother liquor. Electrolytic technology has long been considered as a green chemical synthesis technology.

Electrolytic hydrogenation is another method for the conversion of maleic/fumaric derivatives. These processes generally employ less hazardous protic solvents. For instance, Takahashi and Elving reported that maleic and fumaric behaved identically in this reaction [97]. However, since pyridine (a known isomerization agent to convert maleic acid into fumaric acid) is employed as a catalyst, some have speculated that isomerization of maleic acid into fumaric acid has occurred and then hydrogenation follows to describe this behavior.

The literature presents two primary routes using electrolytic technology of succinic acid production, namely, a membrane technique or a membrane-free approach. At present, the membrane-free method is more widely adopted, as indicated by the number of increasing patent applications from 2006 onward.

As a result, the electrooxidation pathway with oxygen evolution has been adopted as the most preferred anodic reaction for production of succinic acid today [97]. Some manufactures have chosen $PbO_2$ as the preferred anode material. The disadvantage in this method is the high cell voltage, the short life of $PbO_2$ anode, and the costly initial investment of the anode. Other than the oxygen evolution reaction, it was also reported that the electrooxidation reaction of glyoxal to glyoxylic acid had been employed as the anodic reaction by one Chinese manufacture of fine chemicals. But the yields of glyoxylic acid and succinic acid were still relatively low.

US patent application 20130134047 A1 (Zhejiang University of Technology) teaches a new technology for the electrolytic synthesis of both succinic acid and sulfuric acid in the redox couple from a waste stream of $SO_2$ gas in water [98]. The process creates sulfuric acid that can be used as a beneficial chemical reagent.

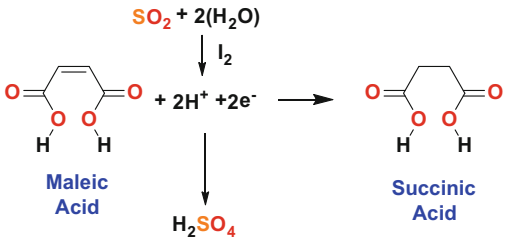


**Scheme 2.28** Electrolytic reduction of maleic acid into succinic acid

Remediation of this waste stream while generating a useful reagent is environmentally attractive. Either sulfurous or sulfuric acid formed by oxidation of $SO_2$ transfers electrons that are mediated through the redox reaction of $I_2$ (or $I_3^-$) into the anode-lyte. Iodine (or $I_3^-$) is generated through the electrooxidation reaction of iodide. Their present invention is a novel technology in producing succinic acid and sulfuric acid at the same time with this paired electrolytic technology.

Maleic acid or maleic anhydride can be used as the raw material for the cathodic reaction. In this process sulfuric acid is the cathodic reactant and the supporting electrolyte of the reaction system. The electrolyte solution in the anode and cathode compartments of the electrochemical cell is separated by a cation-exchange membrane. The resultant reaction on the cathode is described by the following redox reaction presented in Scheme 2.28.

In the anodic compartment, sulfuric acid is produced and iodide ion is regenerated through the redox coupling reaction of $I_2$ and $I_3^-$, with sulfur dioxide as the following electrooxidation reactions take place.

$$2I^- \rightarrow I_2 + 2e \text{ (or } 3I^- \rightarrow I_3^- \rightarrow 2e) \tag{2.1}$$

$$I_2 + SO_2\,(\text{gas}) + 2H_2O \rightarrow H_2SO_4 + 2HI \tag{2.2}$$

$$H_2SO_3 + I_2 + H_2O \rightarrow 4H^+ + 2I^- + SO_4^{2-} \tag{2.3}$$

$$I_3^- + SO_2 + 2H_2O \rightarrow 4H^+ + 3I^- + SO_4^{2-} \tag{2.4}$$

In the above anodic reaction, the iodide ion is regenerated through the following chemical redox reaction of $I_2$ and $I_3^-$ with $SO_2$ or $H_2SO_3$, represented by Eqs. (2.1) and (2.2). Concurrently, sulfuric acid is produced. The net reactions can be expressed as follows. In the anodic compartment, sulfur dioxide gas is fed into the anolyte where sulfurous acid is formed through the reaction of $SO_2$ and water.

Compared with the related technologies, the beneficial results of the this process include (1) reducing the energy consumption of succinic acid electrolytic synthesis significantly by adopting appropriate paired anodic and cathodic reactions; (2) decreasing the initial investment and production cost by using inexpensive anode material, overcoming the problem of short lifetime of anode; (3) providing a new wet technology to produce sulfuric acid at lower temperatures; and (4) increasing

current efficiency, recycling electrolyte, and achieving green production. The technology of this approach is suitable for industrial scale production [98].

After 10 h at constant current density, the electrolysis reaction is stopped, and the catholyte is taken out for post-processing. After posttreatment which includes cooling, crystallization, filtration, rinsing with icy deionized water, and drying, 68.4 g succinic acid is obtained finally. The cathodic current efficiency is calculated to be 95.1 %.

### 2.3.3 *Transfer Hydrogenation of Maleic into Succinic Derivatives*

Safety in an industrial plant is of paramount importance. The use of explosive hydrogen gas to hydrogenate maleic into succinic derivatives is only employed by specialized and experienced manufacturers. An alternative and safer process to hydrogenate organic molecules is the use of transfer hydrogenation where hydrogen-donor molecules are used instead of $H_2$ gas, as depicted in Scheme 2.29. Generally, these donors are special solvents which enhance the efficiency of the overall process. Some typical hydrogen donors include hydrazine, cyclohexene or its diene, isopropanol, dihydronaphthalene, dihydroanthracene, and formic acid to name a few. The commercially preferred hydrogen donors tend to be formic acid or its formates, or a combination of formic acid and organic base, hydroquinone, cyclohexene, phosphorus acid, or alcohols like isopropanol [97].

The catalysts can be a solid for heterogeneous catalysis or an organometallic for liquid homogenous catalysis. Recent advances in asymmetric transfer hydrogenation enable stereospecific addition of hydrogen in the reduction step for synthesis of chiral intermediates [99, 100].

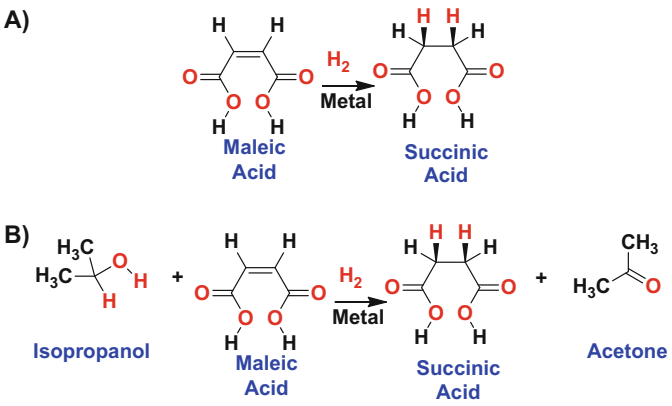


**Scheme 2.29** Catalytic hydrogenation (**a**) versus (**b**) transfer hydrogenation of maleic acid into succinic acid

Typically, solid catalysts used include Pd black; Pd/carbon, Pd or Ni on alumina, and Raney nickel. Homogenous organometallic catalysts like Ru, Rh, Ir, and Pt complexes can also be employed. Besides temperature and pressure, other variables affecting hydrogenation rates include mechanical agitation and flow rates. Commercial processes usually use Pd/carbon since only the double bond is reduced with this catalyst. These catalysts do not affect the carbonyl groups. Chemical selectivity should also be considered prior to the reduction step to obtain the desired product.

Catalytic transfer hydrogenation employing platinum group metals (pgms) Ru, Rh, and Ir has been the most successful. While other metal catalysts or organocatalysts have been employed, their rates are generally slower. Most often, the metal-catalyzed transfer hydrogenation reactions are performed in isopropanol, or in an azeotropic mixture of formic acid (HCOOH) and triethylamine ($Et_3N$) with a molar ratio 2.5:1. This admixture can act as both the solvent and the reductant. Transfer hydrogenation reactions can be carried out in water in a highly efficient manner [101]. The use of water in these processes is environmentally advantageous. These reductions are simple to perform, requiring no ligand modification or organic solvents, and often do not require an inert gas headspace. These processes use one of the most easily available and inexpensive hydrogen sources, sodium formate (HCOONa), thus providing a new viable tool for carbonyl or double-bond reduction.

It should be pointed out that catalytic transfer hydrogenation is not just a regular catalytic hydrogenation where the hydrogen donor replaces $H_2$ gas as the hydrogen source. But the process is mechanistically different. For example, Pt black and Rh/carbon are very efficient hydrogenation catalysts with $H_2$. However, they do not work with hydrogen donors under the same set of conditions. Instead, the metal activates the donor for the hydrogen transfer event in a stepwise fashion. This sequential addition of hydrogen was invoked to explain the isomerization of olefinic double bonds from *cis* to *trans* and *trans* to *cis*, as well as the positioning of the double bond via allylic isomerization along the chain during the hydrogenation of oils with Pd. Kinetically, a ternary complex of metal, donor, and acceptor is required for the transfer hydrogenation as the preformed metal hydride is the active species.

## 2.4 Oxidation Reactions of the Electron-Deficient Double Bond

### *2.4.1 Epoxidation*

Epoxidation of suitable maleate and fumarate derivatives can be performed in a variety of ways. The primary use of maleic epoxidation has been in the production of tartaric acid, where R is hydrogen, as depicted in Scheme 2.30. Since the (*d*,*d*)-isomer is the natural form, routes to produce this isomer in highest yields were sought. Synthetic tartaric acid is mainly the *meso*-(*d*,*l*)-isomer, but sometimes the (*l*,*l*)-isomer is also referenced.

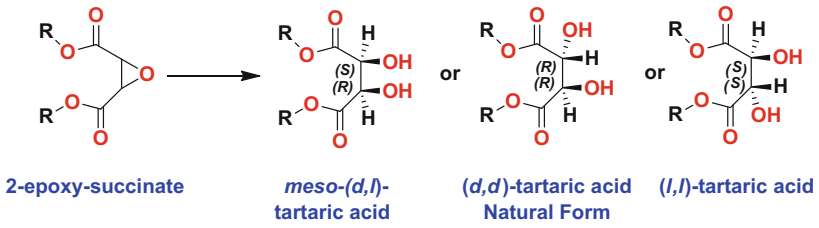


**Scheme 2.30** Conversion of 2-epoxysuccinate into tartaric acid

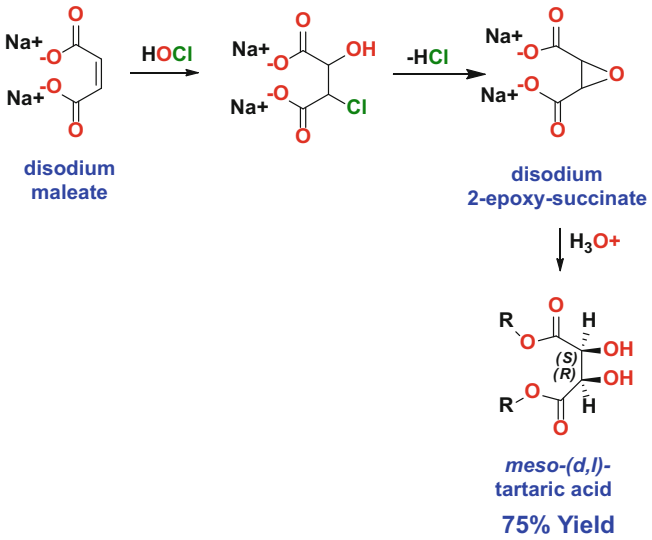


**Scheme 2.31** Hypochlorite epoxidation of maleate into *meso*-tartaric acid

Epoxidation of disodium maleate with hypochlorite followed by acidification is one route to this product that has been isolated in 75 % yield, as outlined in Scheme 2.31 [102].

There are many routes to the dihydroxylation of maleates and fumarates into dihydroxy compounds [103]. These include $OsO_4$-based routes for *cis*-hydroxylation, either directly or with a co-oxidant, such as hydrogen peroxide, or many transition-metal variants. The hazardous nature and high cost of $OsO_4$-based routes have precluded their widespread use in commercial processes.

Using hydrogen peroxide with catalysts, such as titanium, tungsten, molybdenum, vanadium, and composites with silicates and combinations of these metals, has been used more recently. Modern oxidation methods have been reported with in-depth details [103].

In 1959, Payne and Williams reported the selective epoxidation of crotonic, fumaric, and maleic acids using aqueous hydrogen peroxide with a catalytic amount of sodium tungstate (2 mol%) [104]. The control of pH (4–5.5) was essential in the reaction media. Electron-deficient substrates like maleates, fumarates, and

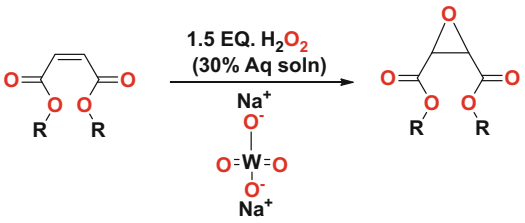


**Scheme 2.32** Sodium tungstate epoxidation of maleate

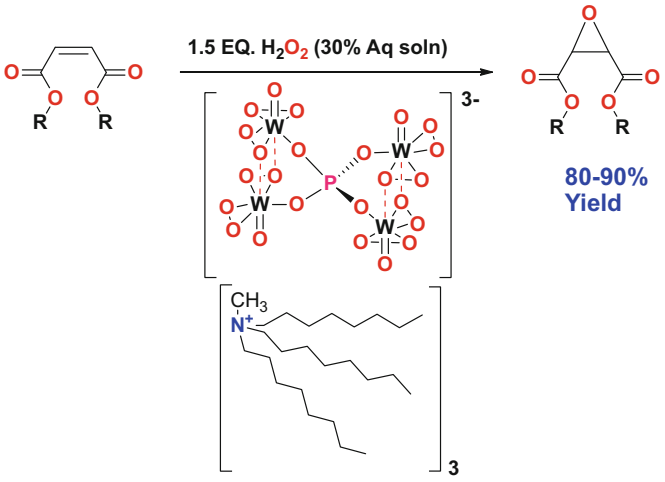


**Scheme 2.33** Tungstate complex for epoxidation of maleate

crotonates were difficult to selectively oxidize using common techniques like peroxy acids. Earlier attempts using this combination failed because of rapid hydrolysis of the newly formed epoxide (Scheme 2.32) [103].

Addition of phosphoric acid and quaternary ammonium salts substantially improved the epoxidation of maleates [105]. Active tungstate catalysts are typically produced in situ. Noyori and coworkers reported conditions for the selective epoxidation of aliphatic terminal alkenes employing toluene, or absolutely solvent-free system [106]. One shortcoming with the previous systems was the use of chlorinated solvents. Their approach provided for a *greener* process. In the media, 2 mole% sodium tungstate, aminomethylphosphonic acid, and methyltrioctylammonium bisulfate were used at 90 °C with no solvent, which resulted in high yields directly from the reaction medium. The use of these additives was essential for epoxidation, as presented in Scheme 2.33.

Replacement of aminomethylphosphonic acid with other phosphonic acids, or simply phosphoric acid itself, significantly lowered the conversion. The phase-transfer catalyst trioctyl-methyl-ammonium bisulfate ($HSO_4$) generated better results than the corresponding chloride or hydroxide salts [105, 106]. The size of the alkyl group on the ammonium quat was found to be important, since C6 or less was inferior to C8 or higher

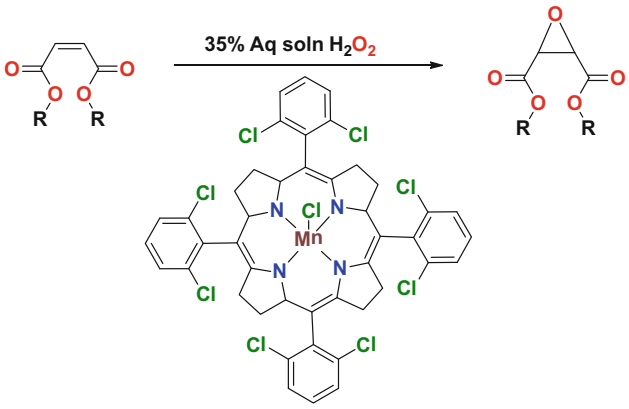


**Scheme 2.34** Manganese(III) complex for epoxidation of maleate (Adapted from [108])

chain lengths. This system was further optimized by addition of more aminomethylphosphonic acid and $Na_2WO_4$ and the pH adjusted closer to 4.2–5.5 [106].

Another highly efficient tungsten-based system for epoxidation was introduced by Mizuno and coworkers who used the tetrabutylammonium salt of a Keggin-type silicon cotungstate $[\gamma\text{-}SiW_{10}O_{34}(H_2O_2)]^{4-}$ that was found to catalyze epoxidation with aqueous hydrogen peroxide with 99 % selectivity and 99 % yield [107]. Furthermore, the catalyst could be recycled at least five times without loss in selectivity or efficiency.

Other catalysts based on manganese complexes with porphyrins have also been used (Scheme 2.34). Co-oxidants that are compatible with manganese include sodium hypochlorite, alkyl peroxides or hydroperoxides (*t*-butylhydroperoxide in *t*-butanol), N-oxides, $KHSO_5$, and molecular $O_2$. These catalysts can be used in the presence of an electron-donor source [108].

Another effective catalyst system uses rhenium with hydrogen peroxide to form a bis-peroxorhenium complex. This catalyst is intensely yellow in color and has been used to epoxidize olefinic compounds. One preferred type of oxidation catalyst comprises an alkyl trioxorhenium-based material. The size of the alky group can range from 1 to 4 carbons in length that is attached to the rhenium catalyst complex. Methyltrioxorhenium (MTO) has been found to perform the best in these types of oxidations [109]. MTO is a well-known catalyst because of its commercial availability and it stability in air.

MTO reacts with $H_2O_2$ to generate an equilibrium mixture with the formation of monoperoxo- and diperoxo-rhenium (VII) species, as presented in Scheme 2.35. The diperoxo-rhenium species structure (III) in Scheme 2.35a is the most reactive toward maleic anhydride resulting in epoxidization and hydroxylation by this process (Scheme 2.35b). Notably, the MTO/$H_2O_2$ system employs nontoxic reagents, the work-up is simple, and water is the only by-product. Moreover, MTO does not decompose $H_2O_2$, unlike other transition-metal-based catalysts [110].

Generally, the MTO/$H_2O_2$ system exhibits high acidity and can promote hydrolysis of the epoxidized products to unwanted diol side products. Addition of one or

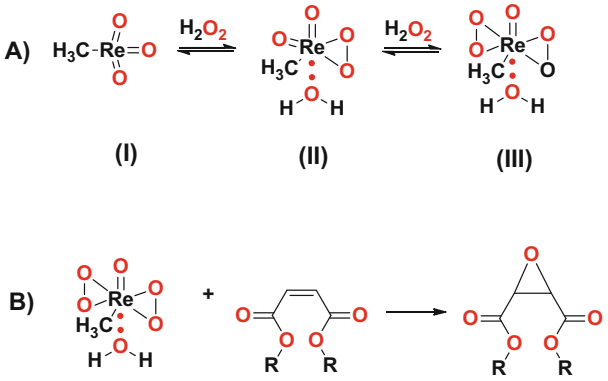


**Scheme 2.35** (**a**) Catalyst preparation of rhenium complex. (**b**) Epoxidation of maleate by this catalyst (Adapted from [109])

more basic ligands to the MTO complex reduces the acidity and improves yields. Ammonia, alkyl amines, pyridine, bipyridine, or other pyridine derivatives can all be used as the basic ligand. Typically, the level of hydrogen peroxide oxidant can range from about 1.05 to about 10 moles per equivalent of olefinic double bond, while the catalyst level used ranges from 0.001 to 0.1 mole% [111].

Ruthenium catalysts have also been employed, as depicted in Scheme 2.36. Late transition metals, such as cobalt(II) Schiff bases, have been used with molecular oxygen with reported yields up to 98 %. Additionally, nickel- and platinum(II)-based catalysts have also been used.

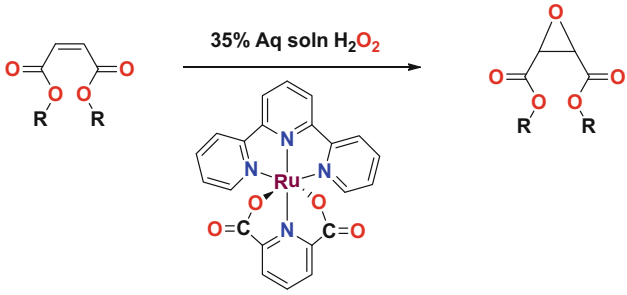


**Scheme 2.36** Ruthenium complex for epoxidation of maleate

Other factors that influence the epoxidation process have included solvents to replace methylene chloride. Solubilizing the organometal catalysts in solvents like trifluoroethanol or hexafluoro-isopropanol (HFIP) has been used but requires at least 60 % hydrogen peroxide to be efficient. Additionally, immobilization of catalysts onto a solid support for easier removal and reuse is becoming important. Also Iron salts and complexes as catalysts have also been used. For water-sensitive epoxides, the use of anhydrous hydrogen peroxide as its urea complex has been quite beneficial. Likewise, percarbonate- or persulfate-based derivatives can be used as well.

### 2.4.2 *Ozonolysis*

Ozonolysis of maleic acid was first reported by Harries in 1903 [112]. Since then, a deeper understanding of this complex chemistry has been revealed, as illustrated in Scheme 2.37. Ozone forms a five-membered tri-oxo ring structure with maleate followed by hemolytic cleavage of the tri-oxo species to generate a diradical species, pathway (A). An internal rearrangement yields glyoxylic acid as one product and the peroxy-glyoxylate diradical

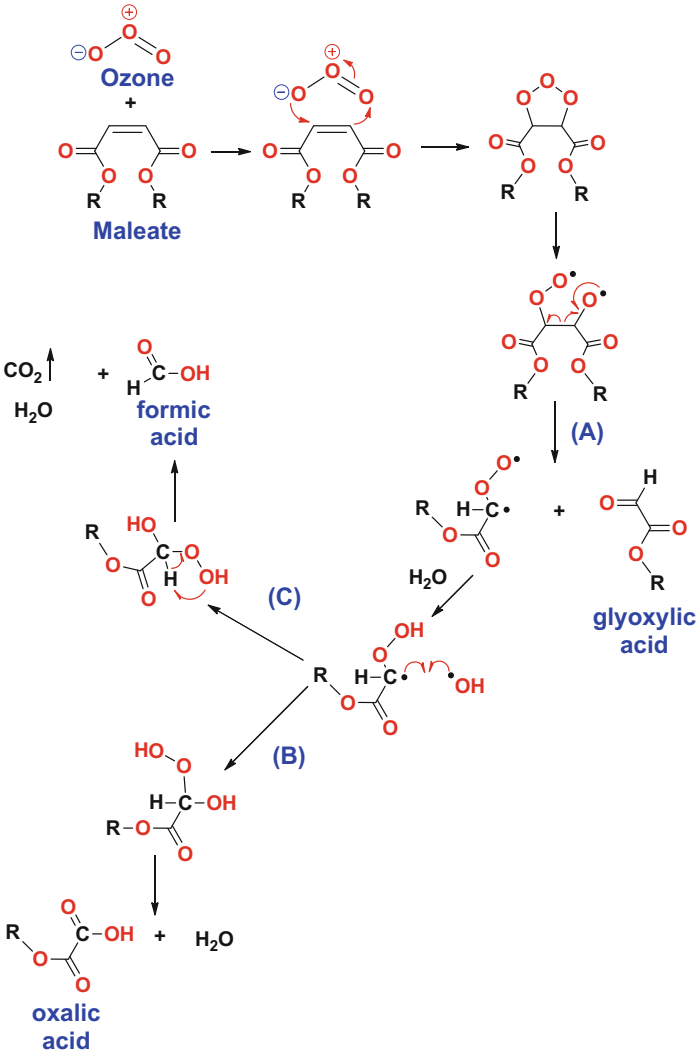


**Scheme 2.37** Ozonolysis of maleate

adduct as the other. Attack of this adduct by a hydroxyl radical can yield a variety of products. In one route, the adduct forms oxalic acid and water as depicted in pathway (B), while in the other route formic acid and $CO_2$ are formed (pathway (C)).

These two routes are not mutually exclusive. Both pathways can proceed concurrently. Only the reaction conditions dictate which predominates over the other.

## 2.5 Addition Reactions to the Electron-Deficient Double Bond

### *2.5.1 Hydroformylation Reaction*

Besides hydrogen or oxygen addition across the double bond of maleic anhydride, a number of other reactants exhibit utility. For example, diethyl fumarate generated by esterification and isomerization of maleic anhydride can be hydroformylated with carbon monoxide and $H_2$ gas employing a cobalt catalyst at 150 °C and 300 bar with a reported yield of 51 % [113]. Better yields were obtained by Umemura and Ikada using lower temperatures and pressures 70–120 °C at 115 bar or 25 °C at 150 bar in the presence of a 1:1 ratio of CO: $H_2$ using dimethyl maleate generating 83 % yield of formyl product and 17 % dimethylsuccinate, as depicted in Scheme 2.38 [114].

Other catalysts including rhodium with aryl phosphine or aryl phosphite ligands (e.g., $HRh(CO)(PPh_3)_3$) have been proposed as the active species in the hydroformylation reaction to generate aldehydic derivatives. The conditions can be exploited for whole range of olefin conversion into aldehydes as well, operating at 70–100 °C and 35 bar, with less than 5 % hydrogenation by-products [113, 114].

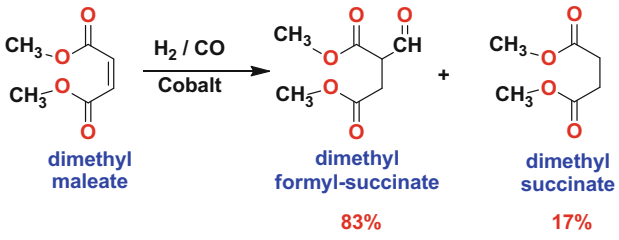


**Scheme 2.38** Hydroformylation of dimethyl maleate

### 2.5.2 Addition of Water for Conversion of Maleic into Malic Compounds

Conversion of aqueous solutions of maleic acid into malic acid is achieved by contacting with a steam sparge under pressure. Optionally, partially neutralized maleic sodium salts up to 50 mole% can be used to enhance hydration. This process is summarized in Scheme 2.39 and proceeds through a fumaric acid intermediate [113]. Note that (*l*)-malic acid is the naturally occurring form while this process yields a racemic mixture.

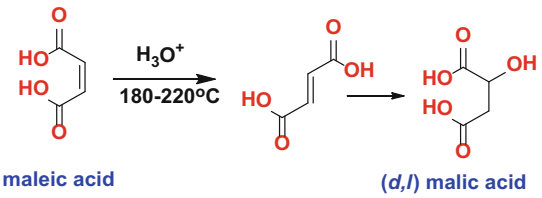


**Scheme 2.39** Conversion of maleic acid into malic acid

Another route to convert maleic acid into (*l*)-malic acid is the use of biological enzymes and/or bacteria. For instance, when the enzyme fumarase is added to an aqueous solution of calcium fumarate and the enzyme acts on water-dissolved fumarate converting a portion to calcium malate. Due to the lower solubility of the malate, it crystallizes and precipitates out from the system before the reaction has reached chemical equilibrium.

This precipitation process enables the continuous production of calcium malate. In a typical hydration reaction, maleic acid is hydrated in the presence of various catalysts including sulfuric acid. Aluminum and chromium hydroxide catalysts have been found to increase yields of malic acid in the aqueous hydration of maleic acid. Smaller amounts of fumaric acid were also found in the hydration product [114].

### 2.5.3 Addition of Halo Acids for Conversion of Maleic into Halosuccinate Compounds

Halosuccinic acid can be directly prepared by addition of HBr or HCl with maleic anhydride, or its diacid under anhydrous conditions. These processes have not found much commercial use. Similarly, fumaric acid in the presence of acetic acid saturated with HCl or HBr will also form the halosuccinate derivatives, as outlined in Scheme 2.40. Other routes are also known.

For example, chlorosuccinic acid can be obtained through the reaction of malic acid and phosphorous pentachloride at room temperature [115]. Chlorosuccinic acid can also be derived from malic acid with thionyl chloride, as well as through

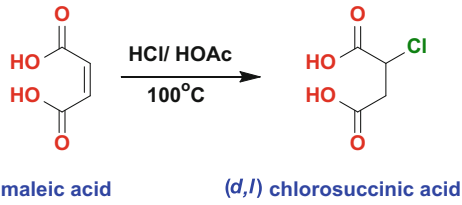


**Scheme 2.40** Conversion of maleic acid into a halosuccinic acid

the addition of hydrogen chloride to maleic acid in acetic acid at 100 °C [116]. Additionally, chlorosuccinic acid can be obtained by reduction of 2-chlorobutenedioic acid with chromium powder in perchloric acid at 25 °C [117] and from the reaction of chloroacetic acid with lithium diisopropylamide at −80 °C and then heating to 50 °C [118]. Similar reactions are expected from similar brominated derivatives, such as thionyl bromide, etc.

To achieve a stereoselective form of one enantiomer of chlorosuccinic acid, such as (S)-chlorosuccinic acid, the use of thionyl chloride with (S)-malic acid should be used for retention of configuration. To produce (R)-chlorosuccinic acid, the use of thionyl chloride with pyridine, a weak nucleophile, would be employed. Likewise, the R-isomer can be produced from (S)-malic acid using $PCl_5$, for inversion of configuration as presented in Scheme 2.41.

The mechanism by which inversion of configuration is obtained was first elucidated by Paul Walden in 1896 and was dubbed the Walden Inversion. It proceeds by an $S_N2$ reaction mechanism when using $PCl_5$ resulting in inversion of configuration, as outlined in Scheme 2.42. In contrast, the use of thionyl chloride proceeds via an $S_N1$ mechanism with retention of configuration.

Assuming complete conversion of malic acid into its cyclic anhydride form (Scheme 2.42 panel b). The alcohol of the malic anhydride in panel b attacks the $PCl_5$ to form the activated intermediate shown in panel c, and the chloride anion then attacks the opposing face of the molecule forming the chlorosuccinic compound, panel d, resulting in inversion of configuration from the (S)-enantiomer into the (R)-enantiomer. Meanwhile, rearrangement of the protonated phosphorous oxychloride, panel d, occurs to form HCl and $O{=}PCl_3$, panel d. In the last step, water opens the anhydride to generate the (−) R-chlorosuccinic acid molecule (Scheme 2.42-panel e).

Walden proposed that retention of configuration can result from a double inversion. For instance, an *l*-isomer is converted to a *d*-isomer that is an intermediate in the reaction, and then the *d*-isomer is converted back into its *l*-isomer by a second reaction as the final product.

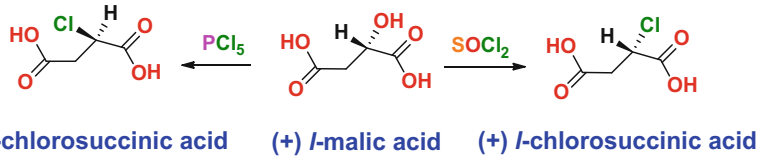


**Scheme 2.41** Conversion of malic acid into a halosuccinic acid

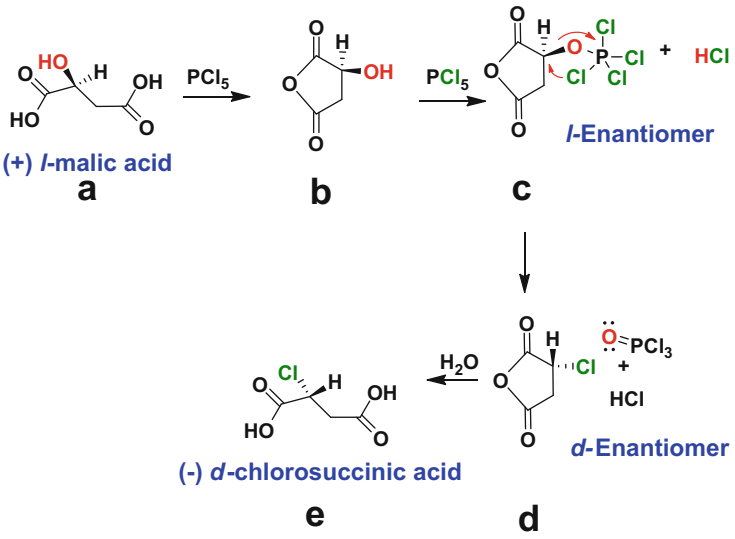


**Scheme 2.42** Inversion of configuration by $S_N2$ displacement by $PCl_5$ chloride ion converting malic acid into (−) R-chlorosuccinic acid

His hypothesis is correct for the reaction of silver hydroxide with R-chlorosuccinic as the second reaction, converting it back to S-malic acid. Remember, S-malic acid was the starting reagent for the synthesis of R-chlorosuccinic acid as the first reaction/intermediate. However, not all reactions proceed with inversion of configuration; one such example is the reaction of S-malic acid with thionyl chloride that proceeds with retention of configuration, as illustrated in Scheme 2.43.

Again, assuming complete conversion of malic acid into its cyclic anhydride form as the first step (Scheme 2.43-panel b). The alcohol of malic anhydride attacks thionyl chloride to form the protonated chlorosulfite intermediate (panel c). Electronic rearrangement ensues to release hydrogen chloride (panel d). There is some debate as to the intermediate formed proceeding from panel d to panel f.

Some assert that a formal charge is formed on the chlorosulfite moiety as depicted in panel e, to form an "intimate ion pair" with the carbon cation malic intermediate. Others assert that a concerted reaction ensues in which that as the carbocation is forming on the malic intermediate, while simultaneously the chloride anion is forming a bond with this cation center, resulting in an exchange reaction of oxygen for chloride in only one step. In either case, the observed product is S-chlorosuccinic acid (Scheme 2.43-panel g).

In summary, three reactions have been discussed to illustrate the capability of various reactions to retain or invert configuration of chlorosuccinic acid. These compounds are usually intermediates for further reactions, requiring a high degree of stereospecificity.

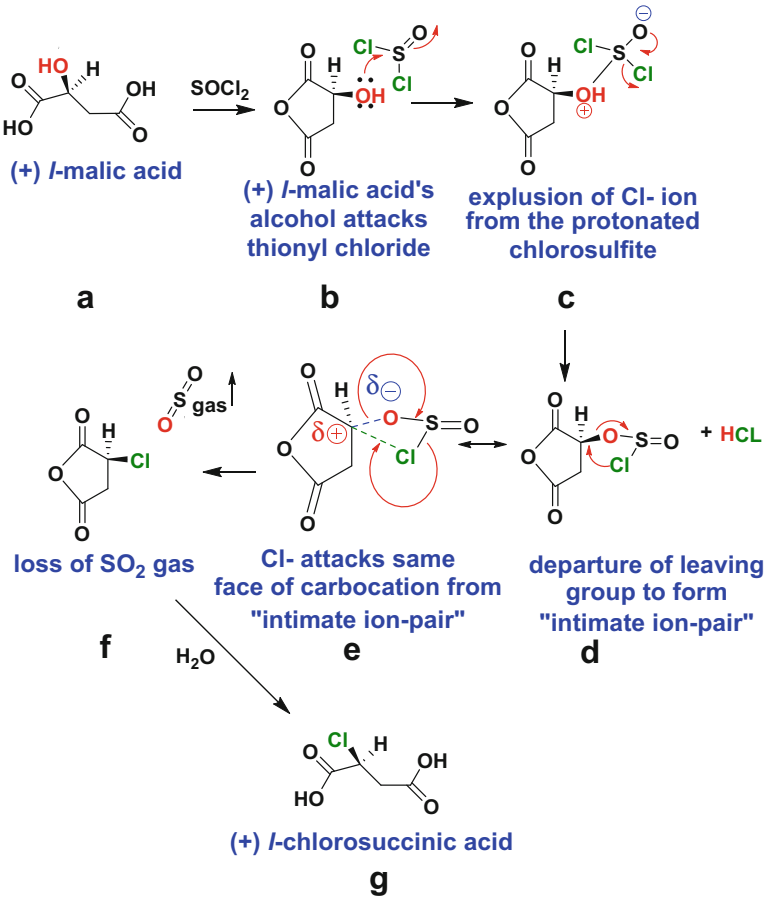


**Scheme 2.43** Retention of configuration by $S_N1$ reaction mechanism using thionyl chloride converting malic acid into (+)*l*−chlorosuccinic acid

### 2.5.4 *Addition of Halogens for Conversion of Maleic into Dihalosuccinate Compounds*

The addition of halogens directly to maleic anhydride forming dihalosuccinic anhydrides is another important chemical reaction. Chlorination of molten maleic anhydride yields α,β-dichlorosuccinic anhydride that can be subsequently hydrolyzed in water to form the dichlorosuccinic acid molecule, as outlined in Scheme 2.44 [119].

When maleic anhydride in water or its corresponding diacid is used, then a pair of diastereomers is produced, (*d*,*d*) and (*l*,*l*)-dichlorosuccinic acid (Scheme 2.44-panel a). Fumaric acid can be chlorinated but generates only one diastereomer, specifically (*d*,l)-dichlorosuccinic acid (panel b). The reaction is an anti-addition for both fumaric and maleate. The *trans*-configuration of fumarate along with *trans*-

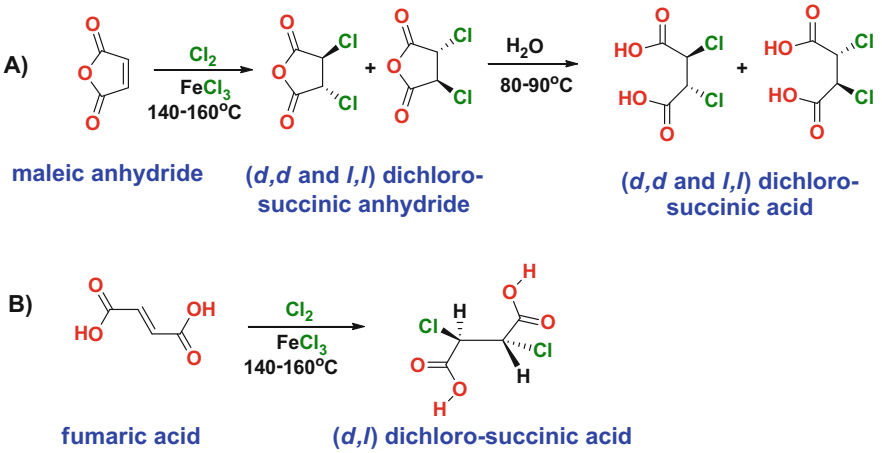


**Scheme 2.44** (**a**) Chlorination of maleic anhydride to form (*dd* and *l*,*l*)-dichloro-succinic anhydride or its diacid form, (**b**) while chlorination of fumaric acid generates (*d*,*l*)-dichloro-succinic acid

addition gives the net result of a syn-addition product, more properly named as the *meso*-isomer, as depicted in Scheme 2.44-panel b.

Maleic and fumarate can be brominated as well. Both maleic and fumarate preferentially form the *meso*-isomer as the major product at lower temperature ≈ −5 °C. In contrast, at 65 °C, only 46 % of the maleic product is in its *meso*-form [119]. The *meso*-isomer is the thermodynamically more stable form of this dibromo-derivative.

Mechanistically, the *trans*-addition of bromine to the fumarate electron-deficient double bond is straightforward, like that of chlorination of fumarate in Scheme 2.45-panel b. Unexpectedly, bromination of maleic generates the same product too, especially, given the results from the chlorination of maleic depicted in Scheme 2.45-panel a.

Isomerization of the double bond for maleic acid must occur during the bromine addition reaction onto maleic acid. It has been observed that increasing the level of bromide anion in the medium from 0.2 M to 4.0 M results in an increase in *meso*-isomer from 32 % to 73 %, respectively. Bromide and bromine, at lower temperatures, are known to isomerize double bonds. But the real driving force for this result is the large van der Waals radius of the bromine atom. In the meso-configuration(*d*, *l*), the bromine atoms are farther apart, residing on opposite faces of the molecule. In contrast, the (*d*,*d*)- and (*l*,*l*)-isomers can only assume a gauche orientation to prevent overlap of functional groups present. Therefore, these isomers have their bromine atoms in close spatial proximity to each other, thereby increasing the overall energy of the molecule due to electronic repulsion of the electron cloud surrounding both bromine atoms.

Molecular modeling results support this conclusion, that the meso-isomer is more thermodynamically stable. In this configuration, the two bromine atoms

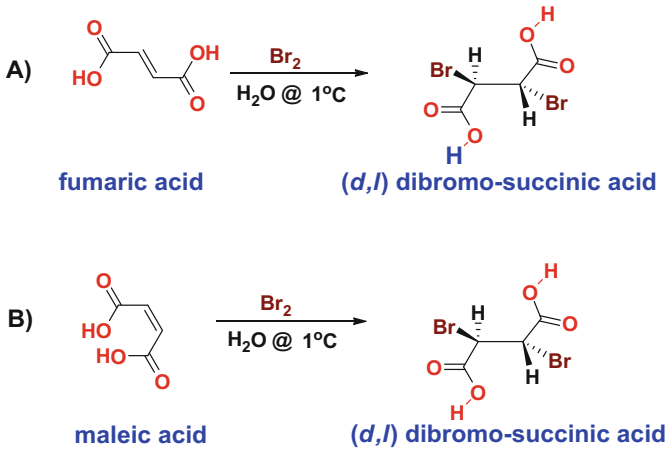


**Scheme 2.45** (**a**) Bromination of fumaric acid *to meso*-(*d*,*l*)-dibromo-succinic diacid, (**b**) while bromination of maleic acid mainly generates *meso*-(*d*,*l*)-dibromo-succinic diacid too

(brown) can adopt an anti-configuration (Fig. 2.15a), while the (*d*,*d or l*,*l*)-dibromo-succinic acid isomers can only adopt a gauche orientation as their lowest energy state (Fig. 2.15c).

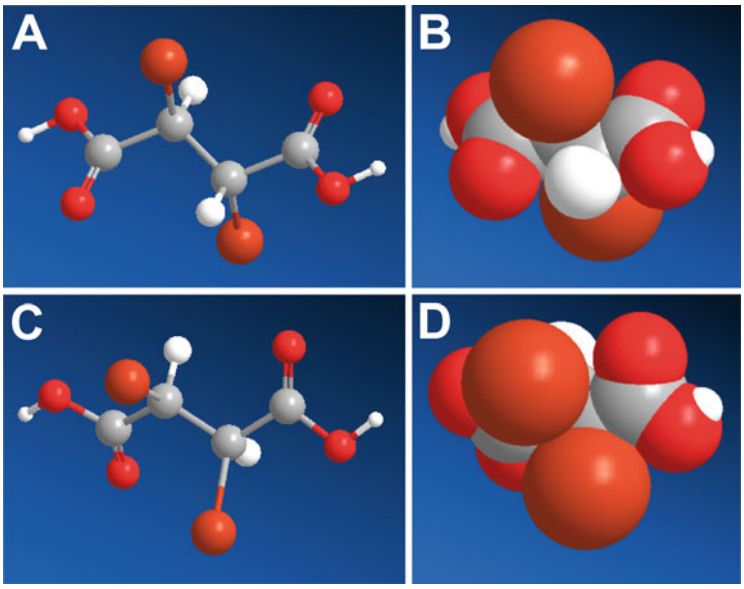


**Fig. 2.15** (**a**) *meso*-(*d*,*l*)-dibromo-succinic acid in anti-configuration, (**b**) space-filling model of meso-isomer versus (**c**) (*d*,*d or l*,*l*)-dibromo-succinic acid in gauche configuration, (**d**) space-filling model of (*d*,*d*)-isomer

This is even more apparent in the space-filling models, where the (*d*,*d*)-isomer exhibits more steric clutter between the bromine atoms in the gauche conformation (Fig. 2.15d), compared to the meso-isomer in the anti-orientation (Fig. 2.15b). The energy difference between these two conformers are 12 Kcal/Mole versus 15 Kcal/Mole for the *meso*-(*d*,*l*)-dibromo-succinic acid versus the (*d*,*d or l*,*l*)-dibromo-succinic acid isomers, respectively.

### 2.5.5 *Michael Additions to the Electron-Deficient Double Bond*

Dialkyl maleates and fumarates, as well as their monoalkyl salts, or any nonacidic form of maleates and fumarates can participate in Michael addition reactions due to the electrophilic character of the conjugated double bond. Resonance structures can be drawn that tacitly indicate the *beta*-carbon exhibits partial positive character, meaning that the *beta*-carbon also has the potential to be an electrophilic target (Scheme 2.46-panels a and c).

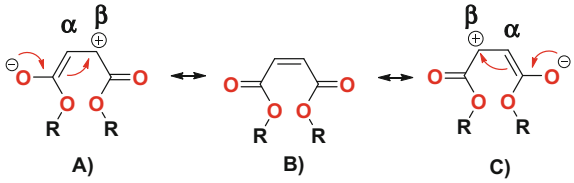


**Scheme 2.46** Maleate behaves as a Michael acceptor due to electrophilic character at the β-position

It was demonstrated that the structure of the activated *ene* such as the maleic double bond is crucial to the degree of activation [120, 121]. Inorganic catalysts have also been used to further activate the *ene* in this reaction. For example, Lewis acids such as $ZnCl_2$, $ZnI_2$, and $AlCl_3$ have been used as catalysts in Michael additions [122].

Nucleophilic (Nu) attack at the *beta*-carbon of the activated *ene* results in formation of an enol or enolate intermediate (Scheme 2.47-panels a or c). Usually, this intermediate collapses and the alpha-carbon is protonated (Scheme 2.46-panel d). This type of reaction is known as a "conjugate addition" or a "Michael addition."

Maleic and fumaric are well-known Michael acceptors and react with a variety of nucleophilic Michael donors, or inorganic nucleophiles. Regardless if the nucleophile is a Michael donor or not, the addition reaction is stabilized through an enolate-transition state, and protonation by solvent or directly with acid completes the reaction, as outlined in Scheme 2.47.

The reverse of a Michael addition can occur and is called a *beta-e*limination. This is often referred to as an "E1cb" mechanism. The E stands for "elimination"; the numeral 1 refers to the fact that, like the $S_N1$ mechanism, it is a stepwise

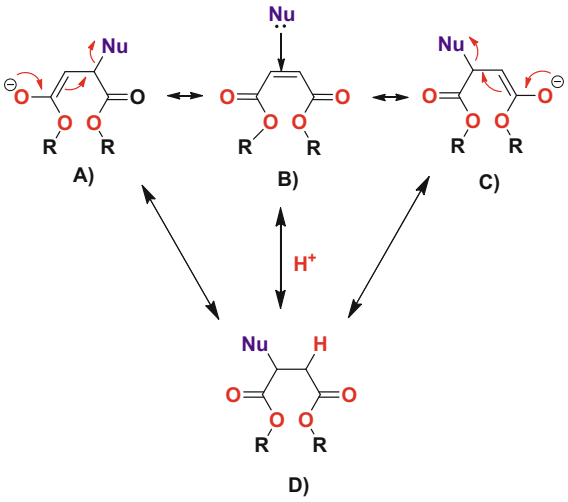


**Scheme 2.47** Michael addition of nucleophile (Nu) with dialkyl maleate, salt

reaction with first-order kinetics. The "cb" designation refers to the intermediate, which is the *c*onjugate *b*ase of the starting compound, as depicted in Scheme 2.48.

Because both Michael additions and *beta*-elimination or E1cb reactions proceed through a resonance-stabilized carbanion intermediate, it is essential that a carbonyl group be located in an appropriate position. This requirement is evident in the *beta*-elimination below to stabilize the carbanion intermediate (Scheme 2.48b–c).

Both Michael additions and *beta*-elimination are intimately related to one another. The reaction product is really dictated by the reaction conditions employed. Generally, Michael additions are performed at lower temperature in neutral to mildly basic conditions. *Beta*-eliminations are usually performed at higher temperature under highly basic conditions. Case in point, in 1948 Kloetzel reported that the nature of the reaction product of 2-nitropropane with diethyl fumarate depends on the level of diethylamine employed [123].

In particular, when using a catalytic amount of 0.2 mole of diethylamine, the simple Michael addition product is obtained in 90 % yield (Scheme 2.49 pathway A). However, when 1.25 equivalent of diethylamine is used, then a *beta*-elimination of the nitro-group occurs with 83 % yield (Scheme 2.49 pathway B). This reaction has been revisited by Ballini and coworkers in 2002 using dimethyl maleate to generate (E)-3-alkylidene succinic anhydrides and 3-alkyl succinic anhydrides [124].

Not all *beta*-elimination reactions generate a retro-Michael addition product of the starting reagents. It is possible that a Michael addition followed by a b*eta*-elimination can generate a whole new entity, as outlined in Scheme 2.49 pathway B.

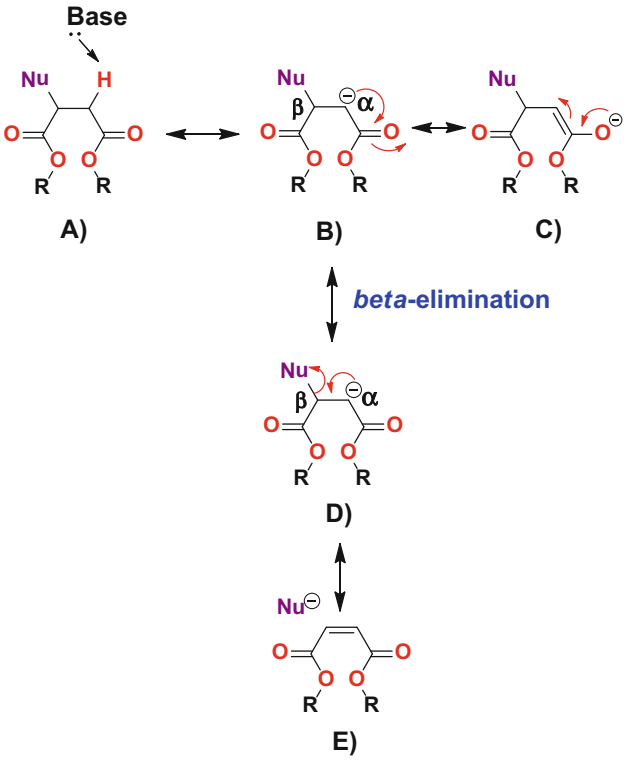


**Scheme 2.48** *Beta*-elimination or E1cb of nucleophile (Nu) with dialkyl maleate salt

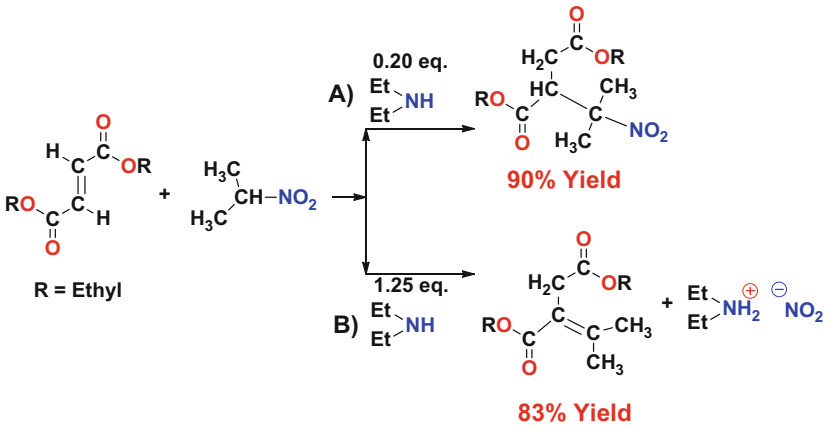


**Scheme 2.49** Michael addition of diethyl fumarate with 2-nitropropane using (**a**) 0.20 eq diethyl amine versus (**b**) using 1.25 eq diethyl amine followed by *beta*-elimination reaction

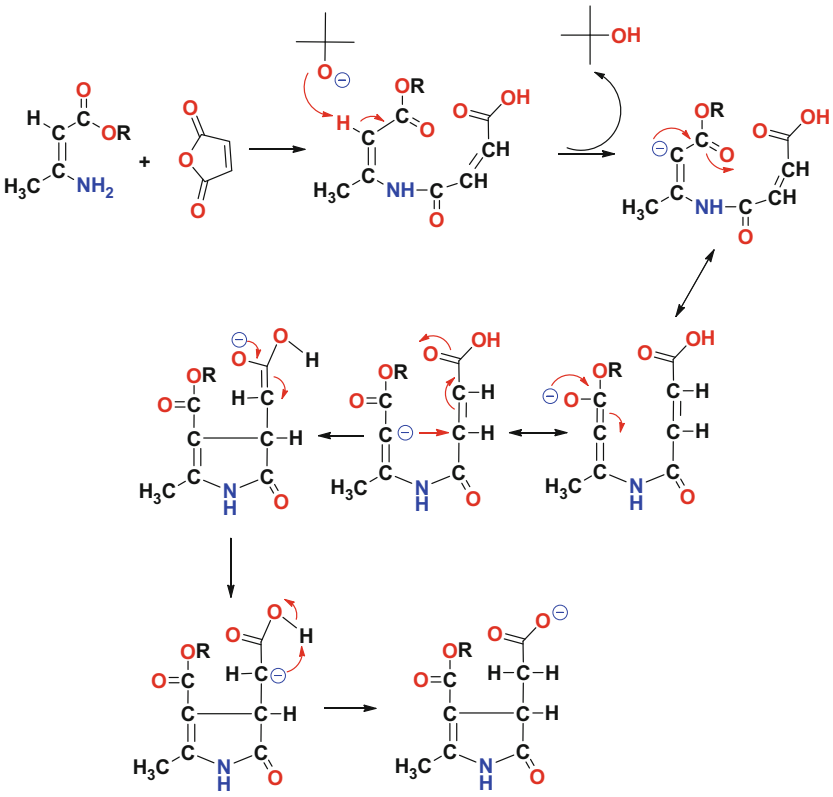

**Scheme 2.50** Cyclization of β-aminocrotonic ester with maleic anhydride

In some cases, an internal Michael reaction can occur and cause ring closure similar to the Robinson annulation. For instance, Szilagyi and Wamhoff reported the cyclization of β-aminocrotonic ester with maleic anhydride to form a highly substituted unsaturated pyrrolidone derivative, as depicted in Scheme 2.50 [125].

Another interesting reaction is the oligomerization of maleates and fumarates to form polycarboxylic esters using malonic or acetoacetate enolates as the polymerization initiator. Hence, the first step of the reaction is the Michael addition to maleate/fumarate, followed by anionic homopolymerization of maleate and/or fumarate diesters [126]. The resultant structures for these homopolymers are depicted in Scheme 2.51.

The remainder of this chapter will focus on the addition reactions to the activated and electron-deficient double bond of maleate and fumarate. But one should keep in mind that retro-reactions and *beta*-elimination reactions are also possible.

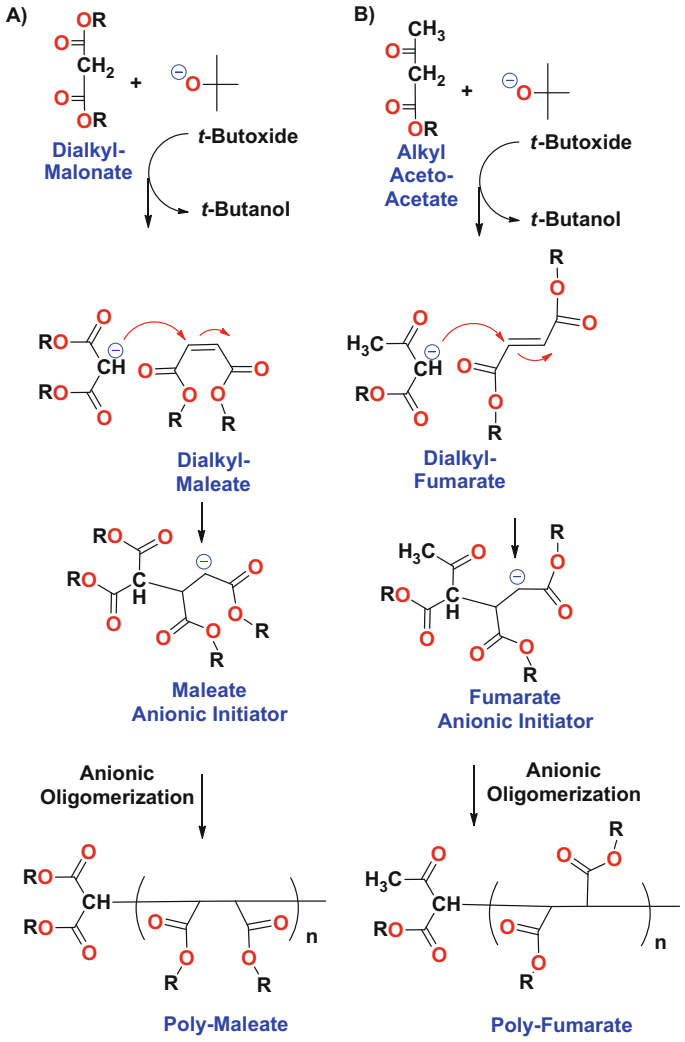


**Scheme 2.51** Poly-maleate or poly-fumarate initiated by malonic or acetoacetate enolates

## *2.5.6 Sulfonation and Thiol Additions*

The base-catalyzed thiol addition to the polarized double bond of maleic anhydride has been well known since the early 1960s [54, 127]. These processes are known as thiol–ene reactions. Thiol–ene reactions proceed through a thiolate anion addition mechanism, where the dielectric of the solvent indirectly plays a role in thiol dissociation, followed by a Michael addition of the thiolate anion onto maleic anhydride. These mechanisms are presented in Scheme 2.52.

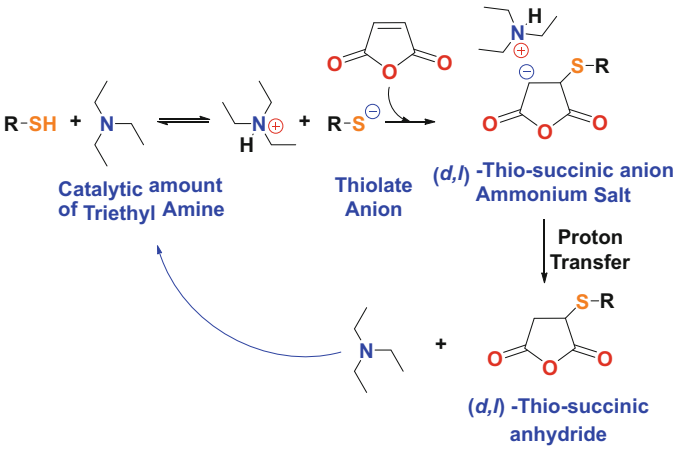


**Scheme 2.52** The thiol–ene reaction with maleic anhydride

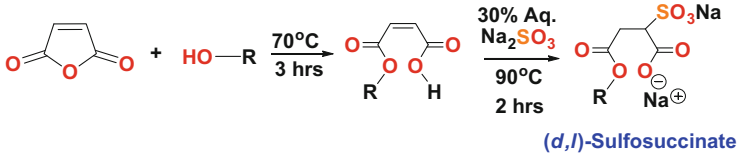


**Scheme 2.53** Formation of sulfo-succinates with maleic anhydride

Both alkyl and aryl thiols participate in this reaction in a straightforward manner. The greater the acid strength of the thiol, the quicker addition occurs, primarily due to a higher population of thiol present in its anionic form. The reaction proceeds readily under anhydrous conditions. Under aqueous conditions, the reaction becomes quite complicated, due to hydrolysis of maleic anhydride into maleic acid, enabling a number of side reactions.

Sulfonation of maleic anhydride proceeds in a similar fashion to thiol additions, where the nucleophilic alkali metal sulfonate moiety adds to the electron-deficient double bond, as illustrated in Scheme 2.53. The typical reaction is a two-step process, where the maleic anhydride is first reacted with an alcohol, usually a fatty alcohol, to form the monoester, and then the alkali metal salt of sulfite is added to form the well-known surfactant class of sulfo-succinates [128, 129].

### *2.5.7 Alkoxylation Reactions to the Double Bond*

As seen in the previous section on thiols, base-catalyzed alkoxy addition to the polarized double bond of dialkyl maleates can occur to generate a racemic mixture of alkoxy-succinates, as depicted in Scheme 2.54. This reaction readily proceeds at

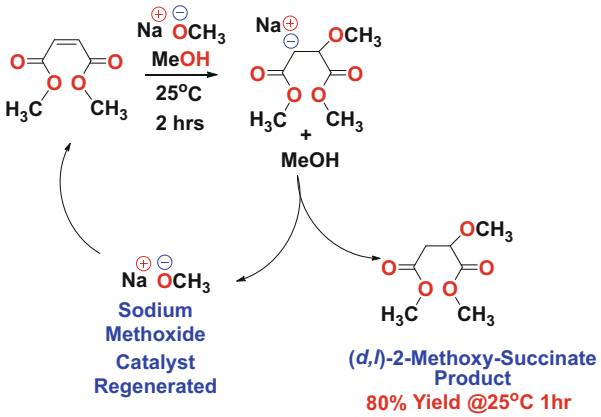


**Scheme 2.54** Formation of alkoxy-succinates from catalytic amount of sodium methoxide in methanol and dimethyl maleate

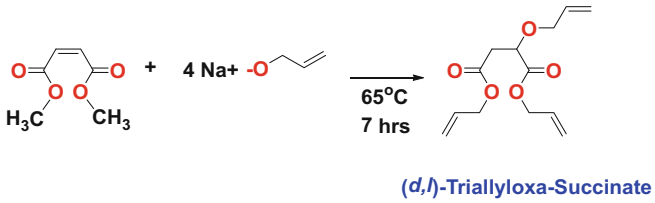


**Scheme 2.55** Formation of alkoxy-succinates from sodium allyloxide and dimethyl maleate (Adapted from [131])

room temperature with a reported yield of 80 % in 1 h [130]. Typically this reaction is carried out with an alkoxy anion identical in structure to the ester functionality, minimizing the complexity of the product that is formed by transesterification side reactions that cannot be completely controlled under the typical reaction conditions employed.

It must be recognized that not only does the alkoxy anion participate in a Michael addition reaction, it also reacts with the ester functionality and can transesterify. This is evidenced by the tri-allyloxa-succinate cross-linker structure depicted in Scheme 2.55 [131]. In particular, addition of the alkoxy anion of allyl alcohol to dimethyl maleate not only results in the addition across the double bond, but the methyl esters also participate in an exchange reaction to replace the methyl ester with the diallyl ester too.

### 2.5.8 *Amination, Amino-Acid Formation, and Biopolymer Synthesis*

Michael additions of ammonia, alkyl, and aryl amines to maleate salts and esters generate racemic amino-acid products. In fact, two out of the 20 naturally occurring amino acids found in proteins can be manufactured from maleic anhydride. These compounds are aspartic acid and asparagine. For example, addition of ammonium hydroxide to maleic or fumaric acid forms a racemic mixture of (*d*,*l*)-aspartic acid ammonium salt, while addition of ammonia in methanol to maleic anhydride generates the racemic amino-acid asparagine ammonium salt, as depicted in Scheme 2.56 [132].

Biodegradable polymers based on aspartic acid or asparagines have significance in the marketplace. For instance, poly-aspartic acids can be used as anti-scaling agents for heating and cooling water systems and corrosion inhibition [133–135], super-swelling hydrogels in diapers and feminine hygiene products [136], a builder in detergents, and as a dispersant [137]. As a polyelectrolyte, it has replaced poly-acrylic acid in many applications due to its benign nature and potential biodegradability as a more ecologically friendly alternative and *greener* product.

Synthetically, it is manufactured much like that of aspartic acid in Scheme 2.57, but requires much higher temperatures for condensation to occur [139]. The thermal polymerization is actually a condensation reaction instead for aspartic acid, or precursors of aspartic acid, and proceeds through a polyimide intermediate followed by mild alkaline hydrolysis to produce the polyamide poly-aspartate.

As NMR techniques were applied to characterize the intermediates and products, a mixture of the α, β nature of the residues became well known, and a preference for

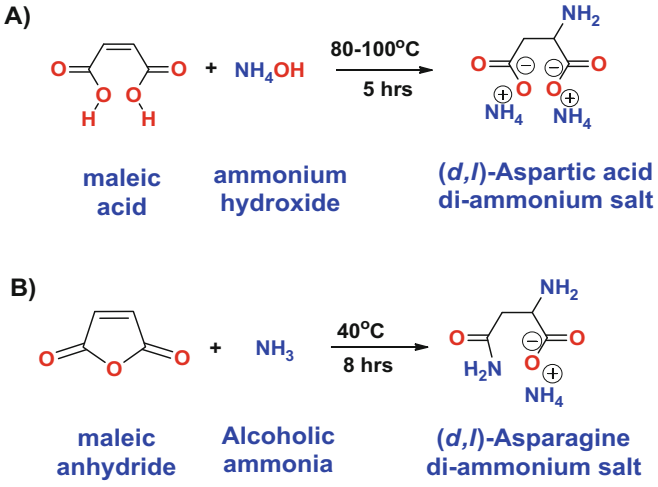


**Scheme 2.56** Formation of racemic amino acids; (**a**) aspartic and (**b**) asparagine from maleic anhydride

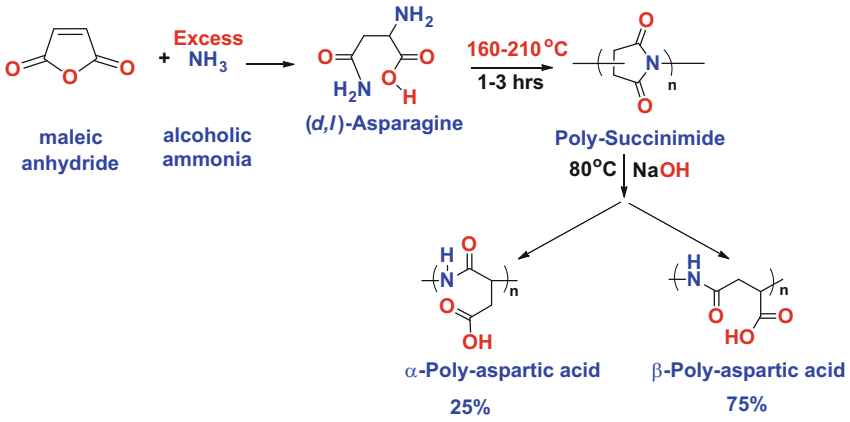


**Scheme 2.57** Formation of biopolymers poly-(*d*,*l*)-aspartate/asparagine from maleic anhydride (Adapted from [138])

the more flexible β-linkage was observed over the α-linkage by a 3:1 margin [140]. These configurational and structural isomers are related to isomeric structures generated along the polymer backbone, two related to the ring opening of the α, or β-carboxyl group, and two related to the *d*, or *l*-stereocenter.

Fox and Harada (1962) further demonstrated that the copolymerization of aspartic acid, or its precursors to aspartic acid, with other amino acids by heating admixtures at 160–210 °C for 1–3 h or a time sufficient to form a polyimide, resulted in branched poly-aspartates. If $H_3PO_4$ was added in an equimolar or lesser amount relative to the amounts of amino acids used, linear products with higher molecular weights were achieved at lower reaction temperatures. The polyimide was then decomposed by mild alkaline at 80 °C for 10 min, as outlined in Scheme 2.57 [138].

## 2.6 Cycloaddition (Diels–Alder) Reactions of Maleic Anhydride

Maleic anhydride is a potent dienophile in cycloadditions. These reactions are better known as Diels–Alder reactions. In fact, this type of reaction was discovered in the late 1920s by Otto Diels and Kurt Alder using maleic anhydride with dienes and trienes [141]. This reaction can synthesize complex chiral compounds related to natural products such as terpenes, sesquiterpenes, and alkaloids.

Diels and Alder reaction is extremely useful in forming cyclic rings in high yield and high stereospecificity. Diels–Alder reactions are also known to be reversible under certain conditions. The reverse reaction is known as the retro-Diels–Alder reaction. Most Diels–Alder adducts are aromatic, which is an additional driving force within this type of reaction.

The Diels–Alder reaction has been extensively used in the synthesis of complex natural molecules due to the formation of numerous chiral centers in one reaction, which are governed by the Woodward–Hoffmann rules. These theoretical rules involve the correlation of orbital symmetry to the outcome of a Diels–Alder reaction, as well as other electrocyclic reactions [142–144].

This reaction is neither polar nor ionic or radical-based either. It is known as a concerted pericyclic reaction, a reaction in which several bonds in the cyclic transition state are formed and severed simultaneously. A pericyclic reaction is a type of reaction wherein the transition state of the molecule(s) has a cyclic geometry, and the reaction proceeds in concerted fashion. Pericyclic reactions are usually rearrangement reactions. Some other major classes of pericyclic reactions include electrocyclizations (Nazarov) and sigmatropic rearrangements (Cope, Claisen) and group transfer.

When a diene and dienophile react with each other, sometimes more than one stereoisomer can be produced. The isomer that predominates is the one which involves maximum overlap of the pi-electrons in the cyclic transition state [144]. This reaction runs quickly when the diene bears an electron-donating group (EDG), while the dienophile contains an electron-withdrawing group (EWG), as summarized in Scheme 2.58. In general, the dienophile must have an

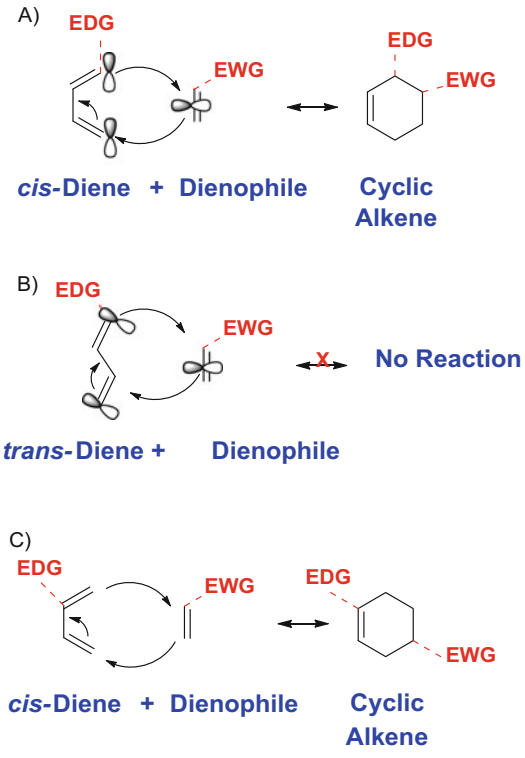


**Scheme 2.58** Diels–Alder reaction of a diene with a dienophile (Adapted from [145])

electron-withdrawing substituent for the reaction to readily proceed. Ethylene itself does not easily form Diels–Alder adducts. For ethylene to participate in a Diels–Alder reaction, extremes of pressure 1800 psi and temperature 185 °C are required [146]. Furthermore, the diene must be in the *s-cis*-conformation for proper alignment of the molecular orbitals to form the prerequisite bonds between the diene and dienophile, as shown in Scheme 2.58a.

Dienes in the *trans*-conformation do not form Diels–Alder adducts because of improper overlap of their molecular orbitals with the dienophile (Scheme 2.58b). Positioning of the electron-donating group (EDG) on the diene can also affect the alignment between the two reactants such that the terminal EDG will be vicinally attached to the carbon bearing the EWG in the dienophile (Scheme 2.58a). In contrast, internally positioned EDG will be positioned further apart from the EWG group, analogous to a *para*-orientation in the ring (Scheme 2.58c).

Dienes with bulky terminal substituents in the C1 and C4 positions decrease the rate of reaction, while bulky substituents at the C2 or C3 position of the diene actually increase reaction rate by presumably destabilizing the *trans*-conformation and forcing the diene into the more reactive *cis*-conformation [145].

The Diels–Alder cycloaddition reaction involves the 1,4-addition of a conjugated diene to a *cis*-alkene, resulting in two new sigma bonds, formed from two *pi* bonds. The resultant adduct thereby forms a six-membered ring. This reaction is quickest when the diene has two conjugated bonds locked within a ring system, such as cyclopentadiene or cyclohexadiene, enabling a fixed alignment of the requisite molecular orbitals in space. The molecule can also be an acyclic diene that can assume a *cis*-conformation. These isomers tend to react slower, since it must achieve the correct conformation before the reaction can proceed, as outlined in Scheme 2.58a versus 2.58b.

Maleic anhydride is a potent dienophile because of the electron-withdrawing substituents of the anhydride carbonyls. These resonance structures of maleic anhydride are further stabilized by the presence of the neighboring lone-pair electrons on the carbonyl group's oxygen atoms denoted by a blue-δ as outlined in Scheme 2.59. Hence, maleic anhydride's pi bond is clearly electron deficient and behaves as an electrophile to electron-rich dienes.

Retention of configuration for the reactants in the products implies that both new sigma bonds are formed simultaneously [145]. The stereochemical information in

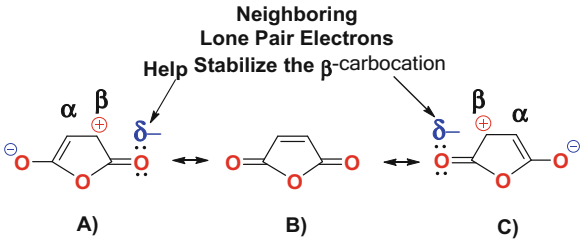


**Scheme 2.59** Resonance structures for maleic anhydride as a dienophile

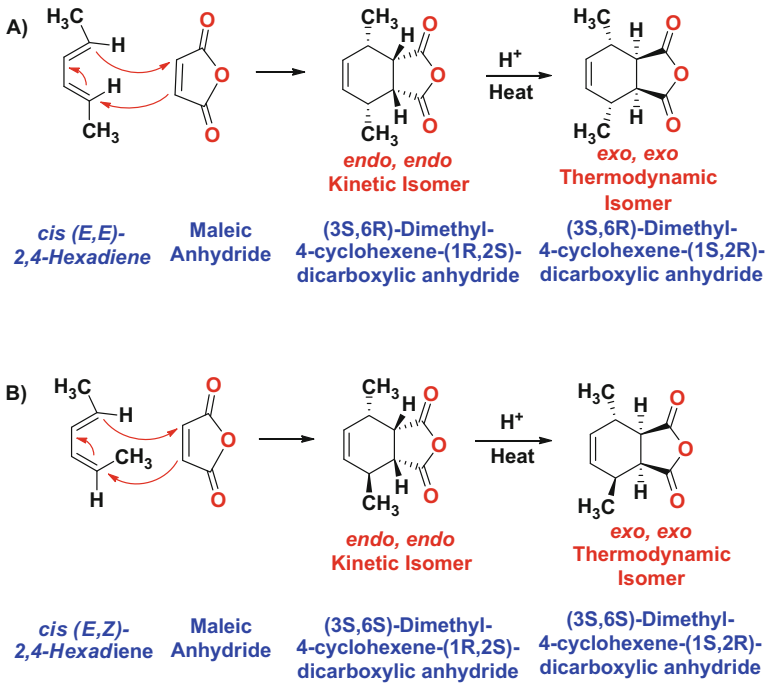


**Scheme 2.60** Retention of configuration between 2,4 hexadiene and maleic anhydride

the reactants is therefore retained within the products. For instance, (*E*)- and (*Z*)-dienes give rise to the adducts with corresponding *syn*- or a*nti*-stereochemistry, as presented in Scheme 2.60.

When the diene (*E*,*E*)-2,4-hexadiene reacts with maleic anhydride, the *pseudo-cis*-isomer for (3S,6R)-dimethyl-4-cyclohexene-1,2-dicarboxylic anhydride is formed (Scheme 2.60a); however, when (*E*,*Z*)-2,4-hexadiene is used, the pseudo-*trans*-isomer (3S, 6R)-dimethyl-4-cyclohexene-1,2-dicarboxylic anhydride is formed (Scheme 2.60b).

The kinetic *endo*,*endo*-isomer is formed first for both molecular entities (Scheme 2.60a, b). However, when application of an isomerization agent such as heat or acid is used, then the thermodynamically more stable *exo*,*exo*-isomer predominates [147]. The *exo*,*exo*-isomer has been found to be more reactive in ring-opening metathesis polymerization (ROMP), a topic that will be addressed in-depth in Chap. 6 [148].

The retention of configuration is also observed for the dienophile. Specifically, if the alkene is in the *trans*-configuration such as fumaroyl chloride (Scheme 2.61), then only the *endo*,*exo*-isomer (3S, 6R)-dimethyl-4-cyclohexene-(1R,2R)-diacyl chloride is formed due to symmetry factors within the molecule (Scheme 2.61a). In contrast, when maleoyl chloride is used, then the predisposed kinetic and thermodynamic isomers are again observed highlighting the retention of

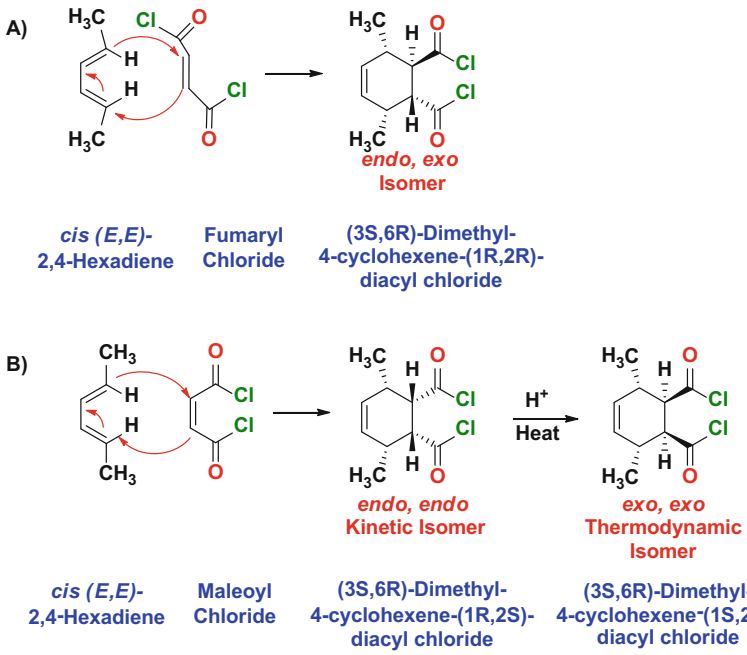


**Scheme 2.61** Retention of configuration between 2,4-hexadiene and fumaryl chloride or maleoyl chloride

configuration within the product (Scheme 2.61b). The reason for this can be explained by the mechanistic factors involved in the Diels–Alder reaction itself [148, 149].

For a pericyclic reaction to proceed, the p-orbitals for each reactant must overlap with each other and that the sign of the terminal orbitals in the HOMO of the diene and the LUMO of the dienophile must match. This happens naturally with the HOMO/LUMO overlap in the $[4\pi + 2\pi]$ Diels–Alder cycloaddition. In contrast, this fails with the HOMO/LUMO overlap in the analogous $[2\pi + 2\pi]$ cycloaddition reaction. Mechanistically, the cyclic transition state for the formation of the *endo*-isomer in this reaction involves a sandwich with the diene directly above the dienophile (Scheme 2.62) [150].

In such an arrangement, the electron-withdrawing group on the dienophile is geometrically placed under the diene. Furthermore, the electrons of the *pi* bonds are on the same face to each other and are called suprafacial. For instance, in the Diels–Alder addition of cyclopentadiene with maleic anhydride, the two molecules approach each other in the orientation depicted in Scheme 2.62b, as this orientation provides maximal overlap of pi bonds between the two reactants and favors formation of an initial *pi*-complex resulting in the final *endo*-product.

Illustrated in Fig. 2.16 is the endo- and exo-molecular orbital interactions between cyclopentadiene and maleic anhydride. The endo-product is favored

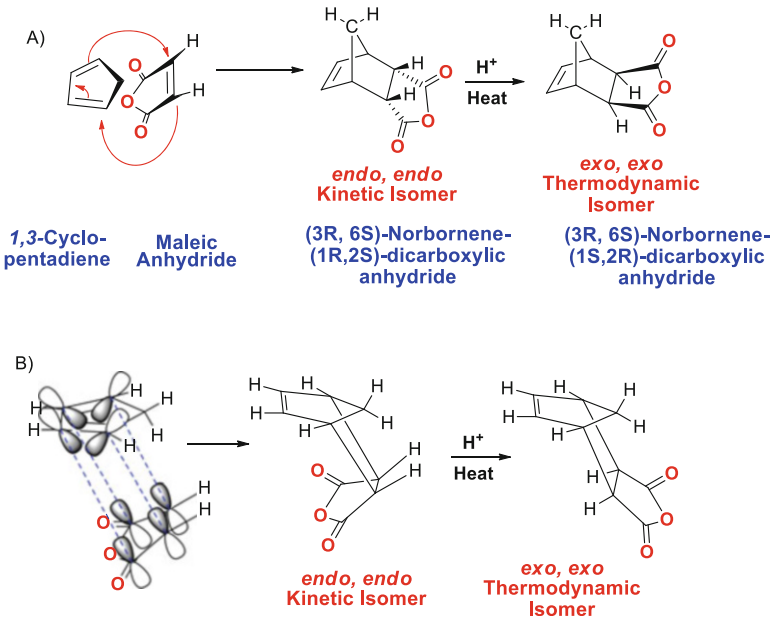


**Scheme 2.62** Diels–Alder reaction between cyclopentadiene and maleic anhydride (Adapted from [150])

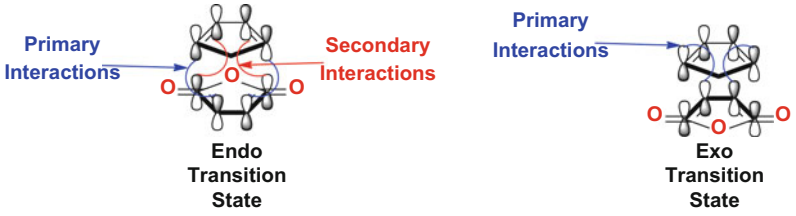


**Fig. 2.16** Diels–Alder molecular orbital interactions between the endo- and exo-orientations for cyclopentadiene and maleic anhydride (Adapted from [150])

because of secondary interactions highlighted in red that are absent in the exo-orientation. Therefore, this lowers the activation energy, and kinetically this isomer is favored over the more thermodynamically stable exo-isomer.

A consideration of the reactants' frontier molecular orbitals (FMO) makes it clearer why this occurs, as portrayed in Scheme 2.63. This reaction proceeds quickest when the HOMO and LUMO orbitals are energetically similar. Since the antibonding LUMO orbital is always higher in energy than the bonding HOMO orbital, anything to raise the energy of the HOMO orbital and/or lower the energy of the LUMO orbital can make Diels–Alder reactions even more facile. This can be achieved by adding electron-donating groups (EDGs) to the diene and/or electron-withdrawing groups (EWGs) to the dienophile [151].

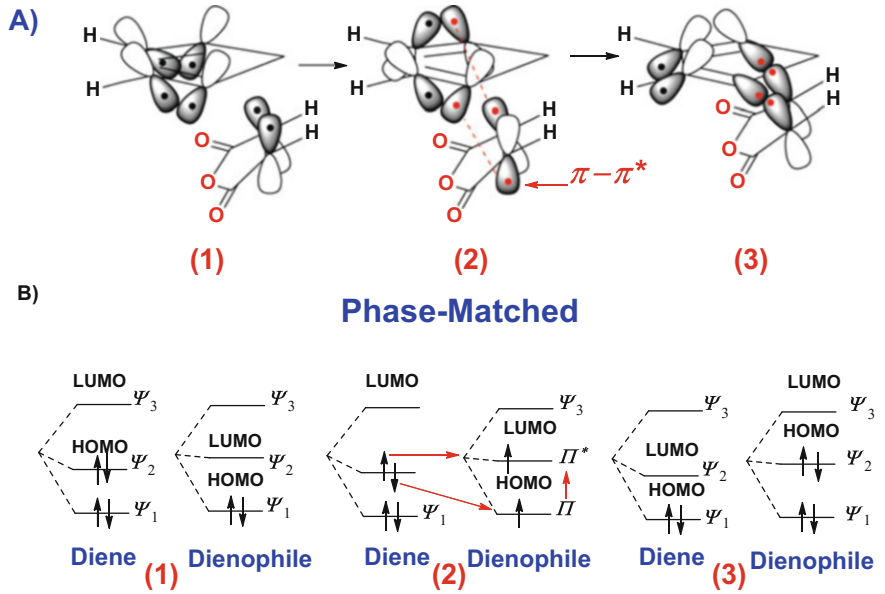


**Scheme 2.63** Frontier molecular orbital theory of Diels–Alder reaction between cyclopentadiene and maleic anhydride

Scheme 2.63 summarizes some of the reaction's major features involved. Panels 63 A1–A3 correspond to the approach of the diene and dienophile. Scheme 2.63-a1 illustrates the orientation of the diene's ether and the dienophile's anhydride group that are facing each other. The dienophile is partially under the diene so that their orbitals overlap. The electronic rearrangement between the two entities as a consequence of thermal energy (Scheme 2.63-a2) and the bond formation between the HOMO orbital of the diene to the LUMO orbital of the dienophile are phase matched so electrons can flow from HOMO to LUMO during bond formation (Scheme 2.63-a3). The corresponding energy diagram for each partner is directly under their respective figure panel, such as the b1 energy diagrams are directly under a1 orbital profiles, while b2 corresponds to a2, and b3 corresponds to a3.

Complexation between the diene and dienophile occurs with the diene aligning its orbitals over the dienophile in Scheme 2.63-a1 and b1. Upon thermal activation, a $\Pi \rightarrow \Pi^*$ transition occurs in the dienophile, denoted by the red electrons in Scheme 2.63-a2, while the diene's pi-electrons assume an antiparallel arrangement, corresponding to Scheme 2.63-b2. Note that in this transition state, the diene's C1 and C4 electrons and their corresponding orbitals are in phase with the dienophile orbitals, so that upon decay in Scheme 2.63-b2–3, the new sigma bonds may form.

The electrons flow from the HOMO orbitals to the LUMO orbitals to form the two new sigma bonds between the two reactants converting it to the Diels–Alder adduct product (Scheme 2.63-a3). Because the HOMO and LUMO of the two components are in phase, a bonding interaction occurs as depicted in Scheme 2.63-

a2–a3. Since the reactants are also in their ground state, the reaction is initiated thermally and does not require activation by UV light [152]. Using frontier molecular orbital theory, one can also predict which centers with the largest frontier-orbital coefficients will react more quickly, thereby enabling one to predict the major regioisomer that will result from a given diene–dienophile pair [153, 154].

Lewis acids such as zinc chloride, boron trifluoride, tin tetrachloride, and aluminum chloride among others can act as catalysts for Diels–Alder reactions by coordination to the dienophile. The complexed dienophile thereby becomes more electrophilic and more reactive toward the diene, increasing the reaction rate and often improving the regioselectivity and stereoselectivity. Lewis acid catalysis also enables Diels–Alder reactions to proceed at low temperatures [152–156].

Many other additives have been developed for influencing the stereoselectivity of the Diels–Alder reaction. These include chiral auxiliaries, chiral Lewis acids, Evans' oxazolidinones, oxazaborolidines, bis-oxazoline Cu chelates, and imidazoline catalysis, for affecting the diastereoselectivity and enantioselectivity of Diels–Alder reactions [157–163].

### 2.6.1 *Ring-Opening Metathesis Monomers from Maleic Anhydride*

Endo-selectivity is typically higher when employing maleic anhydride in the Diels–Alder reaction with cyclopentadiene or furan (Scheme 2.64). The most widely accepted explanation for this effect is due to a favorable interaction between the dienophile substituent's π electron system and the diene's (termed secondary orbital effects), though dipolar and van der Waals attractions [152, 164].

A number of new monomers are useful for ring-opening metathesis polymerization. These monomers can be made from many conjugated dienes, like cyclopentadiene, to form norbornene dicarboxylic anhydride (Scheme 2.62), or its esters from dialkyl maleates, amides, or maleimides, and 7-oxanorbornene derivatives from furan (Scheme 2.64). Other monomers include thiophene or

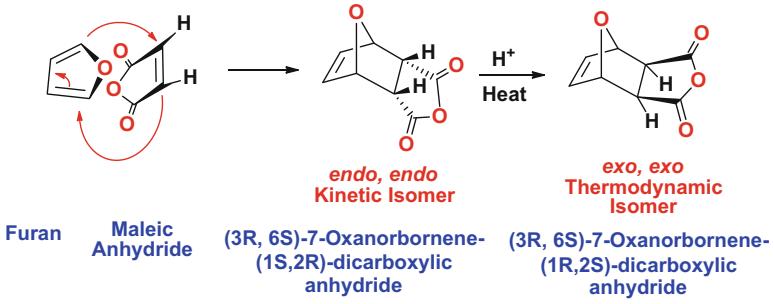


**Scheme 2.64** Diels–Alder reaction between furan and maleic anhydride

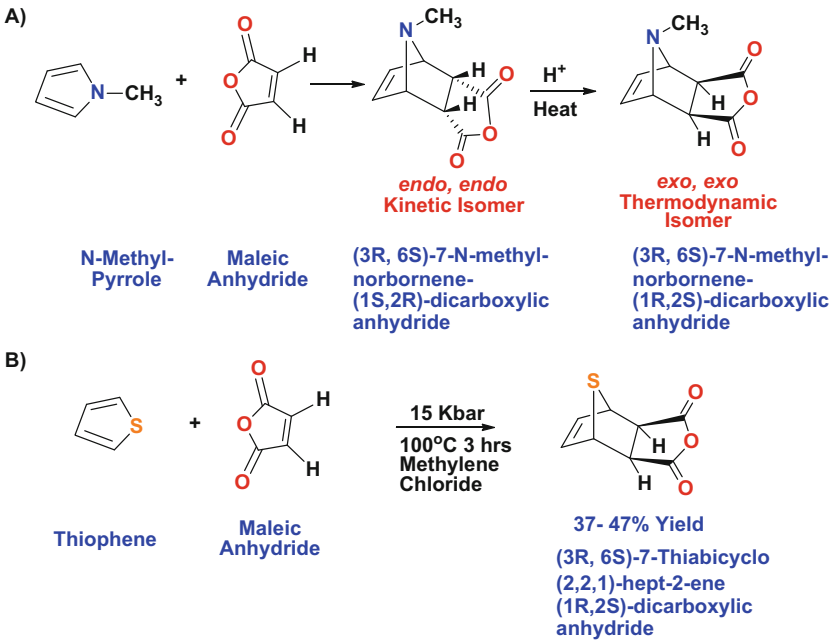


**Scheme 2.65** Diels–Alder reaction between *N*-methyl-pyrrole or thiophene with maleic anhydride

pyran-based derivatives (Scheme 2.65a, b). However, the thiophene adduct requires extreme temperature and pressure to obtain a moderate 37–47 % yield of Diels–Alder adduct [162]. These molecules can be further reacted to form a host of derivatives such as the diacid, mono- and di-alkali salts, esters, amides, imides, and more.

### *2.6.2 Maleated Fatty Acids and Vegetable Oils*

An especially useful transformation of the conjugated olefin system in fatty acids is the Diels–Alder reaction. Many conjugated fatty acids like sorbic acid can react with maleic anhydride to form Diels–Alder adducts. These adducts possess greater functional diversity due to the anhydride functionality, which can react further into a whole host of derivatives. An example of this transformation is presented in Scheme 2.66.

Normally, fatty acids derived from vegetable oils do not have conjugated double bonds. Three typical unsaturated fatty acids from triglycerides, namely, oleic acid, linoleic acid, and linolenic acid, are depicted in Fig. 2.17. These molecules do not participate in Diels–Alder reactions.

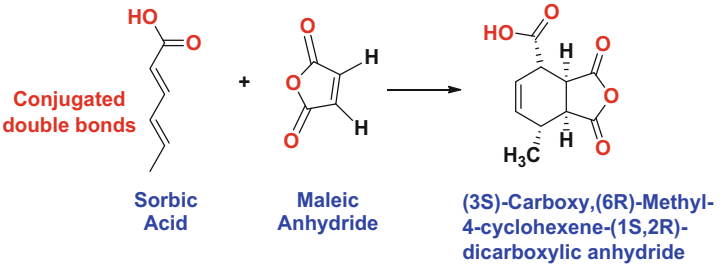


**Scheme 2.66** Diels–Alder reaction between sorbic acid with maleic anhydride

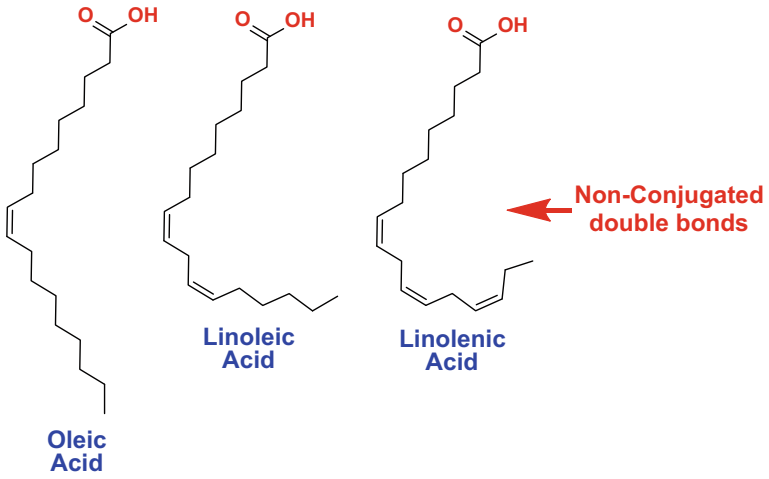


**Fig. 2.17** Chemical structures for typical non-conjugated fatty acids found in plants and animals

Linoleic and linolenic fatty esters can be isomerized from their non-conjugated state into a conjugated one by the treatment with alcoholic base, as depicted in Scheme 2.67 [165]. In doing so, the non-conjugated linoleic fatty ester is converted into conjugated linoleic fatty ester. Once formed, this conjugated linoleic fatty ester can now participate in a straightforward Diels–Alder reaction.

This reaction enables derivation and enhanced functionality of the fatty acids in several ways. For example, maleic anhydride will react with a conjugated fatty acid or ester to form the (3S)alkyl carboxy, (6R) alkyl-4-cyclohexene-(1S,2R)-dicarboxylic anhydride (Scheme 2.68). By this relatively simple reaction [166], which can be carried out at about 100 °C, one can obtain a trifunctional acid in near-quantitative yield.

Other dienophiles or activated monoolefins that have been transformed into Diels–Alder adducts with conjugated linoleic acids are listed below [167]. Not all of them react as readily as maleic anhydride. For example, acrolein gives a 97 % yield of the Diels–Alder adduct at 100 °C, as does maleic anhydride. Acrylonitrile

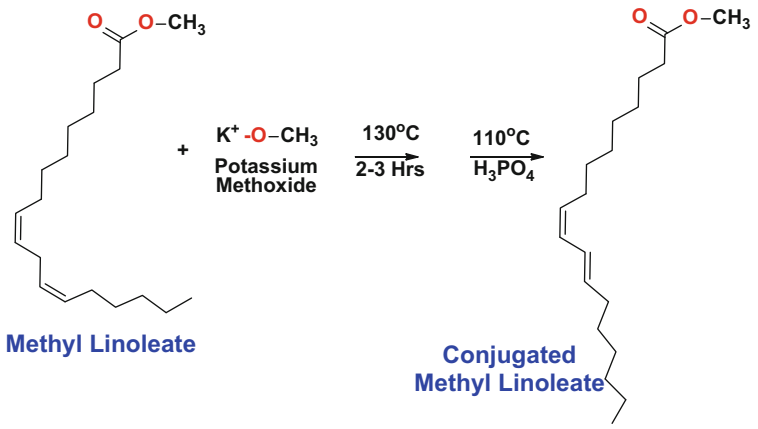


**Scheme 2.67** Isomerization of methyl linoleate into a conjugated methyl linoleate by base treatment followed by neutralization

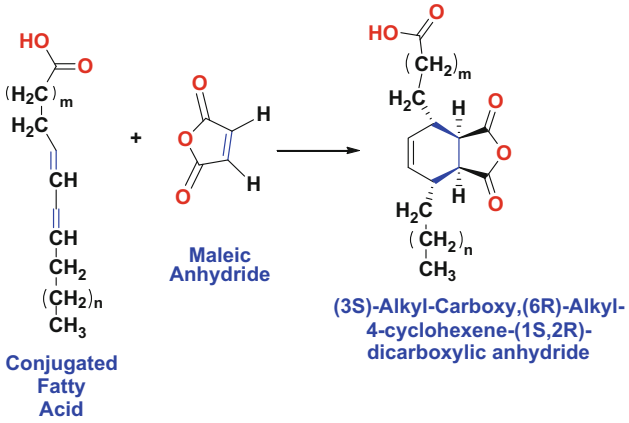


**Scheme 2.68** Diels–Alder reaction between conjugated fatty acid with maleic anhydride

and β-nitrostyrene give only a 27 % yield of adduct at 200 °C, while acrylic acid at this temperature gives a 96 % yield. Fumaric acid reacts to the same extent and under the same conditions as acrylic acid. Methyl vinyl sulfone gives an 80 % yield of adduct at 200 °C. Tetracyanoethylene, an extremely reactive dienophile, will react quantitatively with conjugated linoleic acids at about 50 °C [168].

Adduct reactions, such as those just mentioned, are generally carried out in chloroform or benzene solution in a closed reactor in the presence of a small amount of a polymerization inhibitor, such as hydroquinone. Acetic acid, or even water, in catalytic amounts has been reported to increase the rate of adduct formation with conjugated linoleic acids [169]. Use of a polar solvent such as acetonitrile, with no added water or acid, facilitates adduct formation.

The preferred isomer for the Diels–Alder reaction has the *trans–trans* configuration. It has been reported that the use of small amounts of sodium or potassium

bisulfites [170], sulfur [171], selenium, iodine, or noble metals will isomerize the *cis–trans*-isomer to the *trans–trans* form. Accordingly, optimum utilization of the conjugated system in the feedstock of fatty acids for adduct formation under mild conditions is obtained by the use of one of these isomerization catalysts. The addition of the dienophile itself can be promoted with a little acid, as mentioned earlier. The multifunctional Diels–Alder reaction product illustrated in Scheme 2.68 is characterized by a substituted cyclohexene ring in a long-chain fatty acid.

The polyfunctional Diels–Alder adducts of these fatty acids can serve as intermediates for further derivation. For example, the adduct with maleic anhydride can be reacted with primary amines or ammonia to give imides that may be water dispersible. The aldehyde group of the acrolein adduct can be reduced to an alcohol group. A derivative such as this has the complete functionality for a polyester in one molecule, yet the hydroxyl and carboxyl groups are separated enough to avoid lactone formation.

Ethylene, propylene, and even-numbered *alpha*-olefins from $C_4$ to $C_{20}$ have been adducted to the diene system of conjugated linoleic acid. These reactions are carried out at 260 °C under pressure and result in branched-chain, high molecular weight fatty acids [172].

## 2.7 "Ene" Reactions of Maleic Anhydride: "Ene" Reaction

A reaction closely related to the Diels–Alder reaction, and one that can be used to increase the functionality of unsaturated fatty acids, is the "ene" reaction. This reaction is also known as the "Alder-ene" reaction. This reaction is not as facile as Diels–Alder because much higher reaction temperatures are needed, usually 200–230 °C without solvent, and it requires a more highly reactive enophile, such as maleic anhydride. The ene reaction typically requires higher temperatures due to the stereo-electronic requirement of breaking the allylic C–H σ-bond.

The enophile can be an alkene or alkyne that couples to the "ene" to form a new sigma bond between the two molecules, along with a migration of the "ene" double bond and a concomitant 1,5 hydride shift from the ene to the enophile. This reaction is best summarized by Scheme 2.69.

Enes are π-bonded molecules that contain at least one active hydrogen atom at the allylic, or α-position. Possible ene components include olefinic, acetylenic,

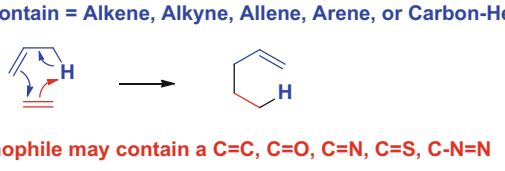


**Scheme 2.69** The "ene" or Alder-ene reaction between an "ene" with an enophile (Adapted from [173])

allenic, aromatic, cyclopropyl, and carbon-hetero bonds [173]. Typically the allylic hydrogen of an allenic component will participate in the ene reaction.

Enophiles are also π-bonded molecules, which have electron-withdrawing substituents that significantly lower the LUMO orbital of the π bond. Possible enophiles contain carbon–carbon multiple bonds (olefins, acetylenes, benzynes), carbon-hetero multiple bonds (C=O in the case of carbonyl-ene reactions, C=N, C=S, C≡P), hetero–hetero multiple bonds (N=N, O=O, Si=Si, N=O, S=O), cumulene systems (N=S=O, N=S=N, C=C=O, C=C=S, $SO_2$), and charged π systems (C=N+, C=S+, C≡O+, C≡N+). The enophile may also be an aldehyde, ketone, or imine, in which case β-hydroxy or β-aminoolefins are obtained. These compounds may be unstable under the reaction conditions, so that at elevated temperature (>400 °C), the reverse reaction takes place—the retro-ene reaction.

Lewis acids catalyze the ene reaction and can produce high yields and superior selectivities at much lower temperatures. The main frontier-orbital interaction occurring in an ene reaction is between the HOMO of the ene and the LUMO of the enophile (Scheme 2.70) [171]. The HOMO of the ene results from the combination of the π-bonding orbital in the vinyl moiety and the C–H bonding orbital for the allylic hydrogen and proceeds in a concerted fashion [174].

If the enophile becomes more polar, as in the presence of heteroatoms, its LUMO orbital has a larger influence on the carbon atom of the enophile, yielding a better C–C overlap and a poorer H–X one. This translates into a lowering of the activation barrier. The concerted nature of the ene process has been supported experimentally [175, 176], and the reaction can be designated as [σ2s + π2s + π2s] in the Woodward–Hoffmann notation [132–144]. For example, the ene reaction of cyclopentene and cyclohexene with diethyl azodicarboxylate can be catalyzed by free-radical initiators. As seen in Scheme 2.71, the stepwise nature of the process is favored by the stability of the cyclopentenyl or cyclohexenyl radicals [177, 178].

The success of any ene reaction is largely influenced by the steric accessibility to the ene's allylic hydrogen. In general, methyl and methylene H atoms are abstracted more easily than methine hydrogens. In thermal ene reactions, the order of reactivity for the abstracted H atom is primary > secondary > tertiary, irrespective of the thermodynamic stability of the internal olefin product. In Lewis-acid-promoted reactions, the enophile–Lewis acid pair employed determines largely the relative

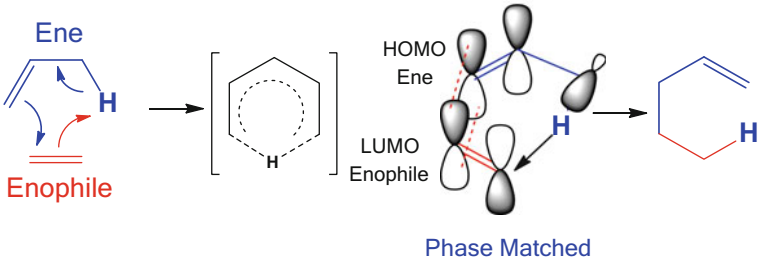


**Scheme 2.70** Concerted mechanism for the ene reaction (Adapted from [173])

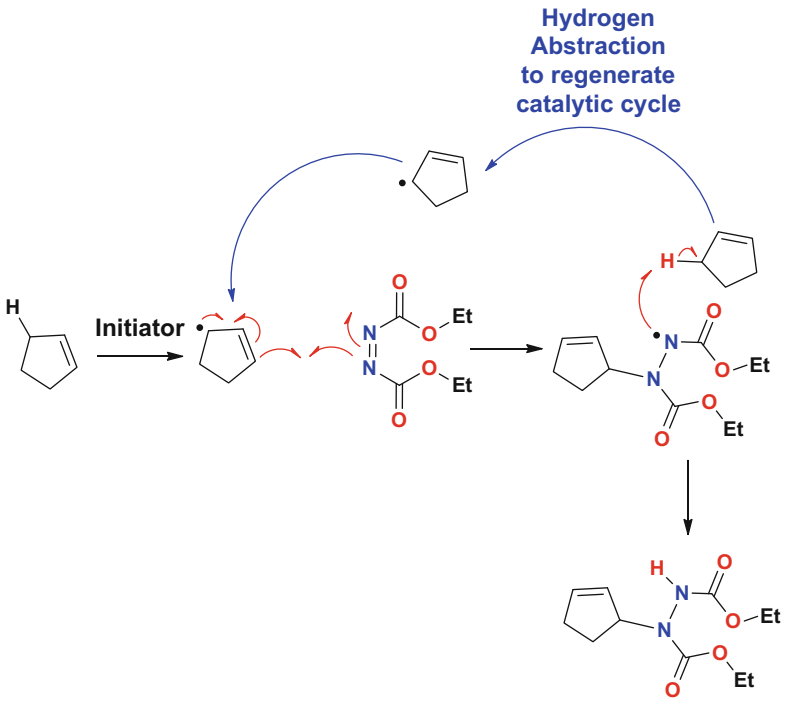


**Scheme 2.71** Stepwise, free-radical pathway for the ene reaction (Adapted from [177])

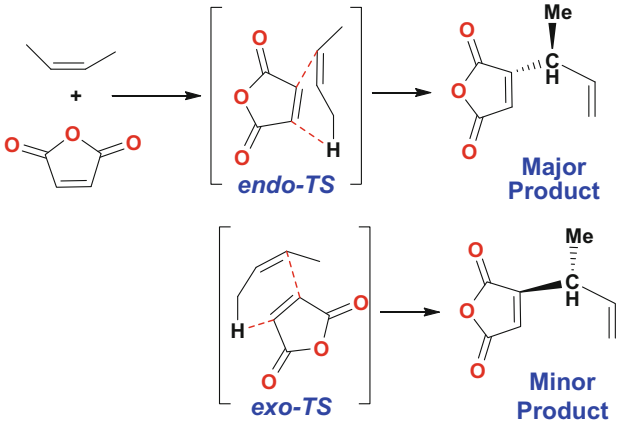


**Scheme 2.72** Endo-preference for the ene reaction (Adapted from [180])

ease for abstraction of methyl versus methylene hydrogens [179, 180]. In terms of the diastereoselection with respect to the newly created chiral centers, an *endo*-preference has been qualitatively observed, but steric effects can easily modify this preference, as depicted in Scheme 2.72.

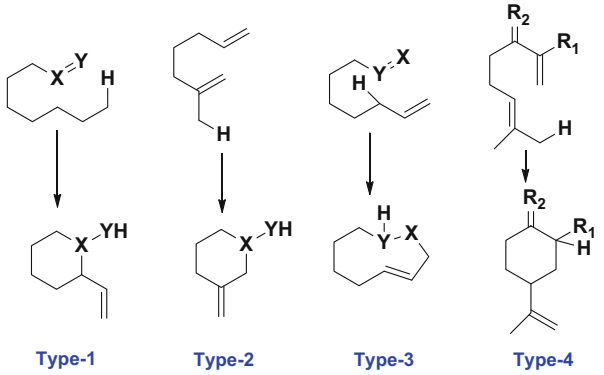


**Scheme 2.73** Types of intramolecular ene reactions (Adapted from [180])

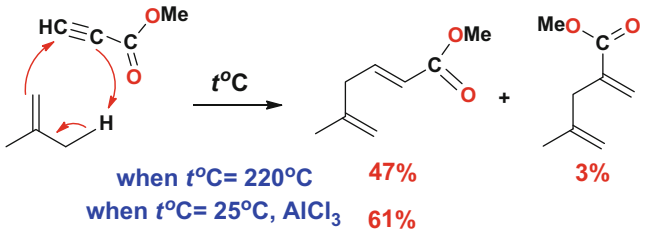


**Scheme 2.74** Improvements brought to the ene reaction by Lewis acid catalysis

In the position of attachment between the ene and enophile, Oppolzer [180] has classified both thermal and Lewis-acid-catalyzed intramolecular ene reactions as types I, II, and III, and Snider [181] has added a type IV reaction (Scheme 2.73) [173].

Thermal ene reactions have several shortcomings, such as the need for very high temperatures and the possibility of side reactions, like proton-catalyzed olefin polymerization or isomerization reactions. Since enophiles are electron deficient, it was rationalized that their complexation with Lewis acids should accelerate the ene reaction, as observed for the reaction shown in Scheme 2.74.

As seen in Scheme 2.75, Lewis-acid-catalyzed ene reactions can proceed either through a concerted mechanism that has a polar transition state or through a stepwise mechanism with a zwitterionic intermediate. The ene, enophile, and choice of catalyst can all influence which pathway is the lower energy process. In broad terms, the more reactive the ene or enophile-Lewis acid complex is, the more likely the reaction is to be stepwise [181].

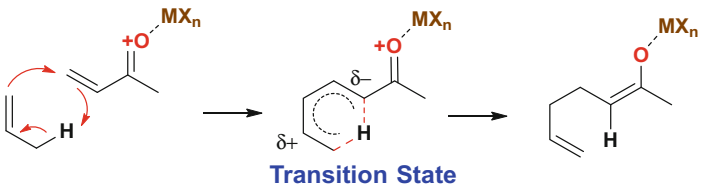


**Scheme 2.75** Mechanisms of Lewis-acid-catalyzed ene reactions (Adapted from [181])

### 2.7.1 *Ene Reactions of Fatty Acids and Oils with Maleic Anhydride*

The use of the ene reaction has been exploited to add functionality and polarity to simple olefins like unsaturated fatty acids or vegetable oils especially when using maleic anhydride. Maleic anhydride reacts with one mole of non-conjugated linoleic acid to form the ene adduct as depicted in Fig. 2.18a. This reaction provides

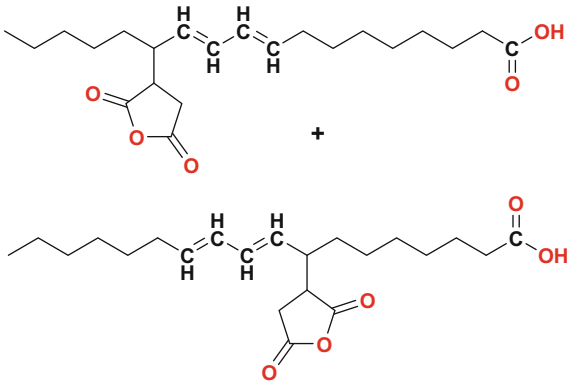


A) Reaction Product of Linoleic Acid with Maleic Anhydride thereby forming conjugated double-bonds

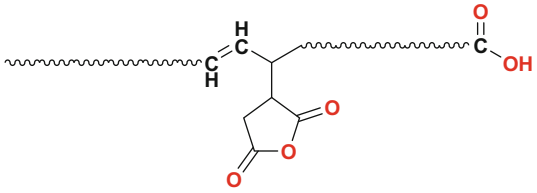


B) Reaction Product of Oleic Acid with Maleic Anhydride

**Fig. 2.18** Chemical structures for ene adduct of (**a**) maleic anhydride with non-conjugated linoleic acid (**b**) and that with oleic acid

a conjugated diene that can be further functionalized through the Diels–Alder reaction, as depicted in Fig. 2.18a.

By use of the "ene" reaction, it is possible to attach more than one mole of maleic anhydride onto the fatty acid chain. If the reaction is stopped after addition of one mole of maleic anhydride, a polycarboxylic alkyd intermediate can be obtained whose conjugated site provides good "built-in" air-drying properties. With the addition of more than one mole of maleic anhydride to linoleic acid, one can obtain a highly acidic material capable of further reaction with a primary amine or ammonia to yield imides that could be water dispersible.

In contrast, when oleic acid is used as the ene component, there is still one double bond in the product after one mole of maleic anhydride has been added, as depicted in Fig. 2.18b. However, this double bond is sterically hindered by the maleic anhydride group. Thus, addition of a second mole of maleic anhydride is unfavorable.

### 2.7.2 *Grafted Polyethylene or Polypropylene with Maleic Anhydride*

Similarly, polymers like polyethylene or polypropylene can be grafted with maleic anhydride via the ene reaction, instead of free-radical process that tends to lower the molecular weight due to chain scission reactions, as illustrated in Scheme 2.76.

Polypropylene is a very large volume product (8,013,000 metric tons in the USA in 2003). One of the major problems with its use is that there are no polar functional groups in the polymer to provide reactive sites. A typical way to solve this problem is to add in a small amount of material which contains polar groups attached to a low molecular weight polypropylene backbone. The polypropylene backbone bonds to the bulk polypropylene and the polar groups allow reactivity with external materials.

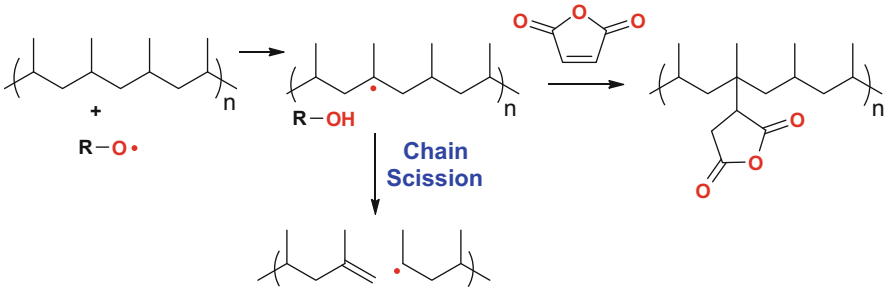


**Scheme 2.76** Free-radical addition of maleic anhydride onto polypropylene also results in chain scission

The most common polar group that is incorporated is maleic anhydride. Typical of this approach is Eastman® E43, Eastman® AP550, or Arkema Orevac® grafted polypropylenes. A major problem with these materials is that they contain relatively low amounts of functional groups. The amount of maleic anhydride is determined by its acid number or SAP number. This is defined as the number of milligrams of KOH required to neutralize 1 g of the polymer. The polymers mentioned above have acid numbers of about 40–45. This corresponds to approximately 4 wt% of the polymer being from maleic anhydride.

It is difficult to increase the amount of maleic anhydride. The maleic anhydride is typically attached by grafting initiated by a radical chain process. It has been found that polypropylene undergoes chain scission via radical processes [182, 183]. This chain scission results in significant loss of physical properties due to decreases in the molecular weight of the polypropylene and consequent decreases in viscosity.

This method employs succinic-terminated polypropylene formed via the ene reaction onto vinylidene-terminated polypropylene. This polypropylene is often, but not exclusively, prepared by metallocene catalysis. It has been discovered that grafting maleic anhydride onto this polymer does not result in significant chain scission or polymerization (Scheme 2.76).

The process involves heating maleic anhydride in the presence of a polypropylene that has been formed using a metallocene catalyst in such a way that a single terminal vinylidene group results on each molecule. The subsequent ene addition of maleic anhydride onto this polymer chain end affords the desired product, as shown in Scheme 2.77 [182].

Polymerization of this maleic anhydride/polypropylene ene adduct would then yield a highly maleated polypropylene polymer, as summarized in Scheme 2.78.

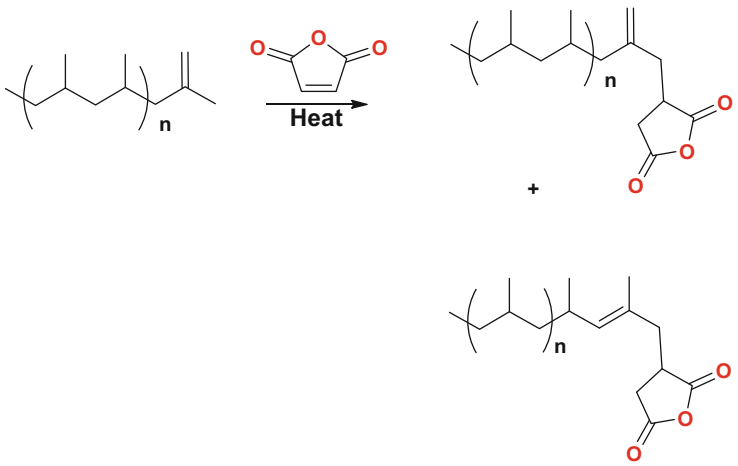


**Scheme 2.77** Ene addition of maleic anhydride onto polypropylene (Adapted from [182])

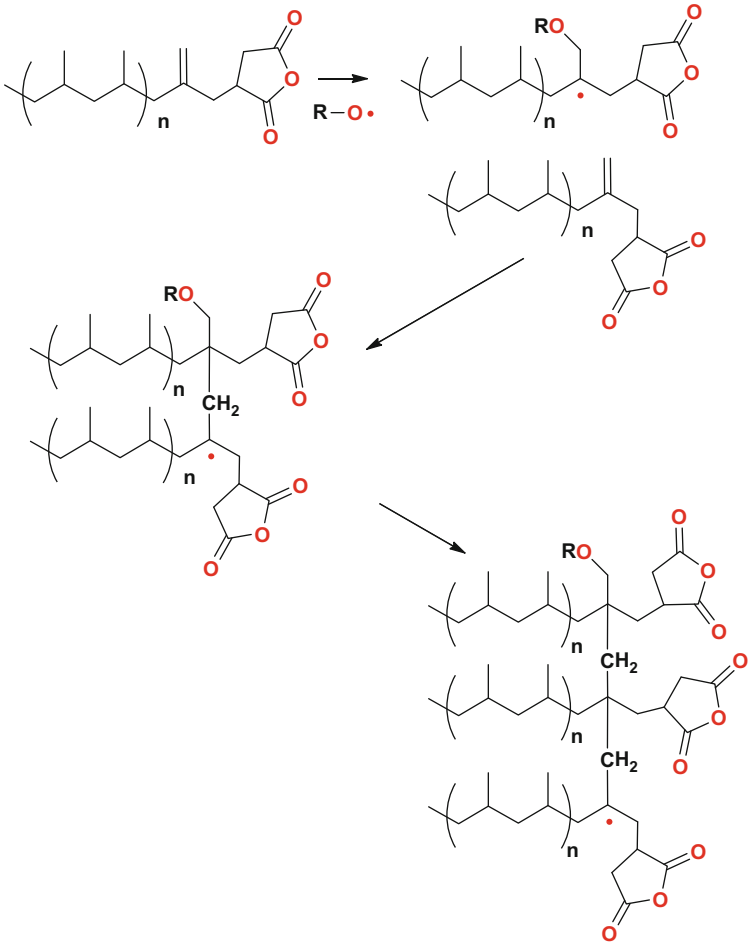


**Scheme 2.78** Oligomerization of maleic anhydride/polypropylene ene adduct (Adapted from [182])

It is also known that olefins will form alternating polymers with maleic anhydride in the presence of radicals [1, 3]. This has been shown to happen for polypropylenes prepared via metallocene catalysts. This happens because metallocene catalysts produce polypropylenes that have a single vinylidene group on the end of each molecule. Such polymerization is schematically shown in Scheme 2.79.

As can be seen from the end result shown above where polypropylene chains are joined by succinic anhydride moieties, the molecular weight greatly increases as does the viscosity of the material. Likewise, a number of structural isomers of oligomeric-maleated-polypropylene can be generated, Schemes 2.77–2.79.

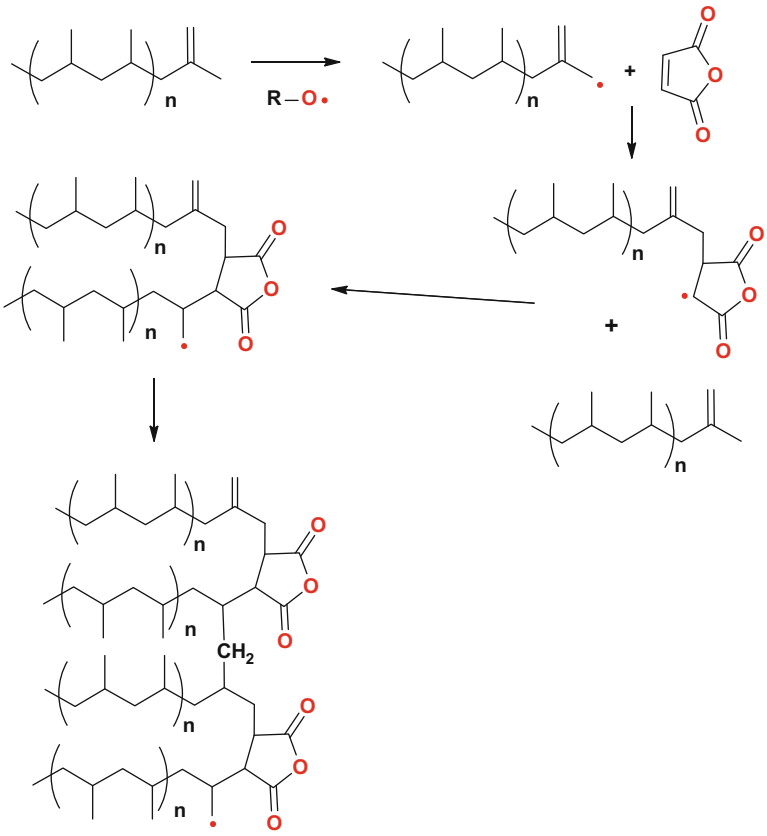


**Scheme 2.79** Oligomerization of in situ formed maleic anhydride/polypropylene graft (Adapted from [182])

## 2.8 Photochemistry of Maleic Anhydride

The photochemistry of maleic anhydride is diverse and highly complex. One of the simplest examples is the photoaddition of maleic anhydride to ethylene. In the first step of the reaction, a $(2\pi + 2\pi)$ photoaddition occurs (Scheme 2.80). According to Woodward–Hoffmann rules, this addition is thermally disallowed, but it is photochemically allowed.

The frontier molecular orbital argument is that the LUMO and the HOMO of ethylene are phase mismatched to maleic anhydride and cycloaddition is symmetry forbidden. But a photon promotes one of the electrons into the LUMO making a transient diradical species. The excited state HOMO is now phase matched to combine with the LUMO, and cycloaddition is symmetry allowed.

Maleic anhydride is also known to form two different classes of adducts with benzene versus alkylbenzenes, depending on the conditions of excitation. At reflux temperatures, in the presence of catalytic amounts of peroxides, adducts of Type-I

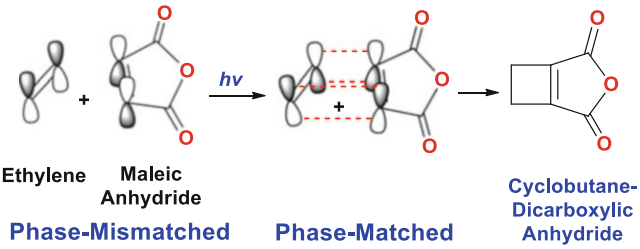


**Scheme 2.80** Photo-cycloaddition of ethylene with maleic anhydride

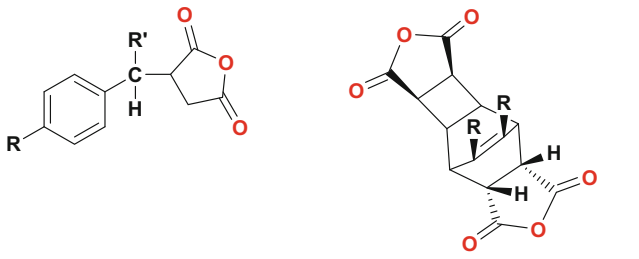


**Fig. 2.19** Photochemical reactions yielding Type-I and Type-II structures

are formed (Fig. 2.19) [183, 184]. A free-radical chain reaction is thought to be involved via abstraction of the benzylic hydrogen, and then a oligomerization/polymerization ensues. The oligomeric chain-length based on the ratio of product to peroxide varied from 20 to 100.

In contrast, at 25–35 °C and in the presence of UV radiation, Type-II adducts are formed instead (Fig. 2.19) [185–190]. Excited aromatic molecules or charge-transfer complexes are thought to be involved as the reaction intermediates. This addition reaction is sensitized by addition of benzophenone, which accelerates the rate of reaction, but not required for the reaction to proceed. It appears that benzophenone is essential if only sunlight is used as the source of radiation [191].

Interestingly, benzene adducts of maleic anhydride form readily, while alkyl-substituted-benzene adducts are sluggish and only partially react as poly-maleic anhydride oligomers are formed as the major reaction product under Type-II reaction conditions. Type-II adducts were also formed under gamma radiation but only 4 % incorporation of maleic anhydride occurred [192]. The main product was a mixture of poly-maleic anhydride oligomers.

The photoaddition of maleic anhydride to benzene generates a very stable 2:1 adduct (II) formed in a formal sense by an exo-1,2- and endo-1,4-additions (Scheme 2.81) [190]. Note that it is also aromatic too.

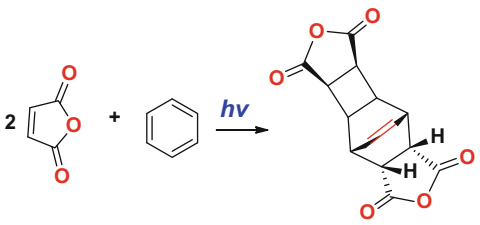


**Scheme 2.81** Photochemistry of maleic anhydride in benzene

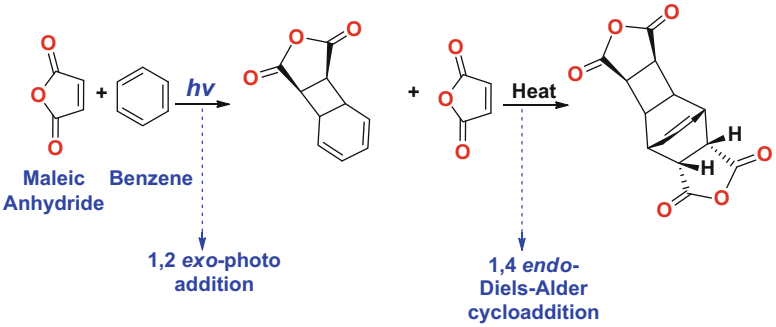


**Scheme 2.82** Reaction sequence of photochemical/Diels–Alder reactions for maleic anhydride in benzene

The reaction sequence is believed to follow a (2+2)-1,2-photochemical exo-cycloaddition, followed by a (4+2)-1,4-Diels–Alder endo-cycloaddition reaction, as summarized in Scheme 2.82. The finding of a 1,2-exo-photocycloaddition is surprising rather than the exo-2,3-addition which would be expected on purely steric grounds. It is both the stereospecific orientation of the donor–acceptor charge-transfer complex that is formed, along with the steric factors involved that account for this result.

Reactions of this type have been shown to involve charge-transfer excitation within a weak complex formed between the reactants in the first step of this photoaddition reaction [183, 192]. Relatively electrophilic benzene derivatives such as benzonitrile or nitrobenzene show no such excitation with maleic anhydride and do not photoadd to these types of molecules [193]. It is readily apparent that in the maleic anhydride-benzene versus alkyl-benzene reactions, two types of reactions are prevalent, one by free-radical processes yielding oligomeric compounds. The other involves excited molecules or charge-transfer complexes forming monomeric Type-II adducts.

### *2.8.1 Photodimerization of Maleic Anhydride*

Photodimerization of maleic anhydride has been well known since the early 1960s. The process for the preparation of the di-anhydride by dimerizing maleic anhydride

by subjecting a solid-state layer of maleic anhydride directly to light having a wave length between about 175 and 400 nm, and can be photosensitized with benzophenone [194]. Like the photo-adduct of maleic anhydride with benzene, the (2+2) exo-photocycloaddition was obtained. The maleic rings are in the *trans*-orientation to the cyclobutane ring, as presented in Scheme 2.83.

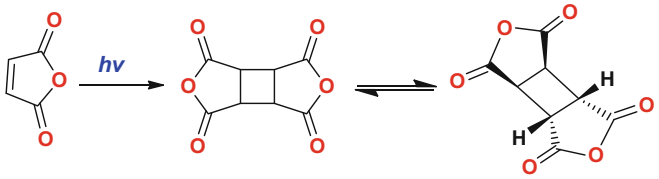


**Scheme 2.83** Photodimerization of maleic anhydride in the solid state

## 2.8.2 *Photochemistry of Maleimide*

Maleimide behaves similarly to maleic anhydride with respect to photocycloadditions with itself and with benzene (Schemes 2.84 and 2.85, respectively) [195]. But unlike maleic anhydride, maleimides readily photopolymerize. Bis-maleimides are also useful photo-cross-linkers. In fact, photopolymerizations can be carried out in both the liquid and the solid state [196].

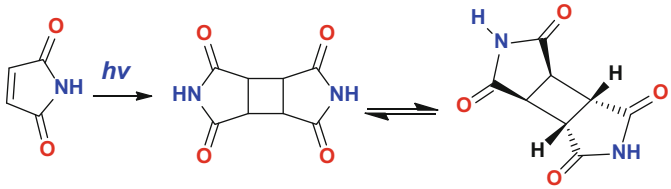


**Scheme 2.84** Photodimerization of maleimide in the solid state

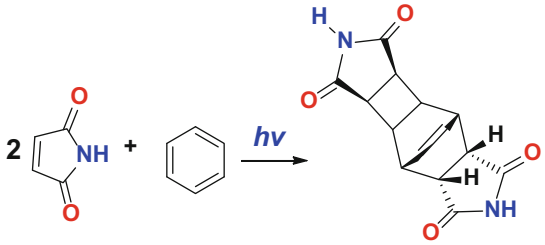


**Scheme 2.85** Photochemistry of maleimide in benzene

### 2.8.3 *Photoinitiation and Photopolymerization of Maleimide*

Photo-induced free-radical polymerization of N-substituted maleimides with vinyl ethers has been extensively studied [197–199]. These UV curable systems do not require any external photoinitiator and are not susceptible to oxygen inhibition enabling polymerization in air. The mechanism of initiation in the case of maleimide/vinyl ether system involves an electron transfer followed by a proton transfer. It was found that the rate of polymerization and degree of conversion are highly dependent on presence of labile hydrogens [197]. Mechanistically this can be summarized by Scheme 2.86.

The first step involves excitation of maleimide by 308 nm laser, since maleimide has two lambda maxima at 260 nm and 320 nm. This results in the formation of a diradical species as depicted in Scheme 2.86 structure-A. Resonance stabilizes this

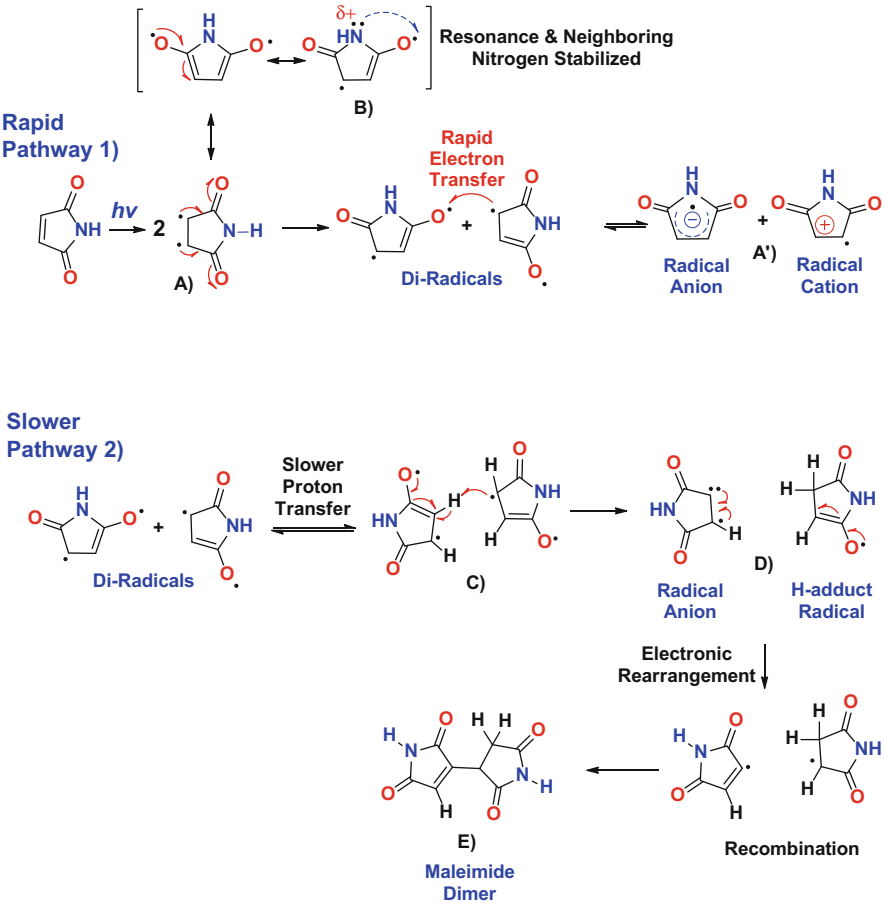


**Scheme 2.86** Photoinitiation by maleimide in water or monomer

diradical across six atoms onto the carbonyl-oxygen atoms, shown in Scheme 2.86 structure-B, thereby lowering the activation energy needed to achieve this transient intermediate. The combination of the nitrogen's lone-pair electrons and nitrogen's electronegativity allows these electrons to stabilize the oxygen diradical illustrated in Scheme 2.86 structure-B.

Once the diradical is formed, there are two potential directions for the cyclic pathway to proceed. The most rapid pathway is an electron-transfer event with maleimide itself, forming a radical anion and radical cation pair (Scheme 2.86 structure-A′). Chain-transfer solvents or other monomers that may be present can also have an effect. The radical anion was definitively observed in this reaction as observed by electron-spin resonance (ESR) results [200]. The radical cation rapidly isomerizes to generate a neutral radical and a proton (Scheme 2.86 structure-A′).

Meanwhile, the oxygen diradical can proceed along the slower pathway to generate the H-adduct radical by hydrogen abstraction from another oxygen diradical as shown in Scheme 2.86 structure-C, or from other chain-transfer agents that may be present. The H-adduct radical was also definitively observed in this reaction as observed by ESR experiments [200]. Note that formation of this H-adduct radical is accompanied by the formation of another molecule of radical anion too.

This anion can further propagate the radical polymerization, or it can recombine with the proton released from the radical cation to generate another molecule of neutral radical. The lack of observable neutral radicals in this study may suggest rapid dimerization to generate maleimide dimers (Scheme 2.86 structure-E). There are multiple radical species that can easily be formed from maleimide for free-radical polymerization to occur by this photoinitiator-free system.

Similarly, the photocyclodimerization of bis-maleimides can be carried out under the influence of ultraviolet radiation. These reactions can be activated by adding to the solution sensitizing agents, such as carbonyl-containing aromatic compounds, (e.g., benzophenone or Michler's ketone). The concentration of the bis-maleimides in the solvent may vary widely. However, the best results are obtained with approximately 5-to-10 moles of bis-maleimide per liter of solvent used. ln this case, the concentration of the sensitizing agent averages 50 moles per liter. While irradiation of the bis-maleimides may be carried out with a high-pressure mercury vapor lamp or any other light source emitting in the range of 300–400 nm [201–205], their usefulness will extend well into the future.

## References

1. Trivedi BC, Culbertson BM (1982) Maleic anhydride. Plenum, New York
2. Marsh RE, Ubell E, Wilcox HE (1962) Acta Crystallogr 15:35
3. Felthouse TR, Burnett JC, Horell B, Mummey M, Kuo Y (2001) Kirk Online. Wiley Interscience, New York, pp 1–58
4. Considine G (ed) (2006) Van Nostrand's scientific encyclopedia. Wiley, New York

5. Pohanish RP (ed) (2012) Sittig's handbook of toxic and hazardous chemicals and carcinogens, 6th edn. Elsevier, Oxford, UK
6. Acton QA (ed) (2013) Anhydrides-advances in research and application. Scholarly Editions, Atlanta, GA
7. Bednowitz AL, Post B (1966) Acta Crystallogr 21:566
8. Bodewig C (1881) Z Kristallogr 5:559–560
9. Yardley K (1925) J Chem Soc Trans 1:2207–2219
10. Lonsdale K (1939) Proc R Soc Lond Ser A 171:541–568
11. Shahat M (1952) Acta Crystallogr 5:763–768
12. Williams JGB (1974) Acta Crystallogr B Struct Crystallogr Cryst Chem 30:1249–1257
13. Day GM, Trask AV, Motherwell WDS, Jones W (2006) Chem Commun 1:54
14. Back RA, Parsons JM (2011) Can J Chem 59(9):1342
15. Swern D (1957) In: Adams R (ed) Organic reactions, vol 7. Wiley, New York, p 378
16. White RW, Emmons WD (1962) Tetrahedron 17:31
17. Saotome M, Itoh Y, Terashi M (1973) Japan Kokai 73:38435
18. Saotome M, Itoh Y, Terashi M (1973) Japan Kokai 73:39436
19. White RW, Emmons WD (1965) UK Patent No. GB-986,058
20. Pechmann HV (1882) Ber Dtsch Chem Ges 15:881
21. Pets AG (1964) In: Olah G (ed) Friedel-Crafts and related reactions, vol 3. Wiley, New York
22. Aslan T, Ozarslan AE, Ridvanoglu N, Sahbaz F, Yurdakul A (2005) EP Patent 1513868
23. Li H, Chen H, Shen Z, Lin S (2002) Polymer 43:5455
24. Cutter LA, Nunn RE (1979) US Patent 4,145,375A
25. Winey DA (1979) US Patent 4,148,987A
26. Okudan A, Baktir S, Sagdic A (2013) Adv Polym Technol 32:E451
27. Relles HM (1974) US Patent 3,810,913
28. Brotherton TK (1967) US Patent 3,337,662
29. Dean JA (ed) (1992) Langes handbook of chemistry, 14th edn. McGraw-Hill Book, New York
30. Roedig A, Bernemann P (1956) Liebigs Ann Chem 600:1
31. Maahs G (1964) Angew Chem Int Ed Engl 3:316
32. O'Niel MJ (ed) (2013) Merck Index, 15th edn. RSC Publishing, Cambridge, UK
33. Temple J (1929) J Am Chem Soc 51(6):1754
34. Pomogailo AD, Dzhardimalieva GI, Kestelman VN (eds) (2010) Macromolecular metal carboxylates and their nanocomposites, Chap 4.2.1, Springer series in material science, vol 138. Springer, Berlin
35. Prasad R, Kumar S, Kumar A (2005) J Therm Anal Calorim 81:441
36. (2005) Kirk-Othmer encyclopedia of chemical technology, vol 15, 5th edn. Wiley, Hoboken, NJ, pp 1–49
37. (2012) Ullmann's encyclopedia of industrial chemistry, vol 22. Wiley-VCH, Weinheim, pp 145–155
38. Lange N, Sinks M (1930) J Am Chem Soc 1:2602–2604
39. Burnop VC (1963) UK Patent No. GB-933,102
40. Harrison IT, Harrison S (1971) Compendium of organic synthetic methods, vol 1. Wiley-Interscience, New York
41. Harrison IT, Harrison S (1974) Compendium of organic synthetic methods, vol 2. Wiley-Interscience, New York
42. Hegedus LS, Wade L (1977) Compendium of organic synthetic methods, vol 3. Wiley-Interscience, New York
43. Nakashima S et al (1989) US Patent 4,833,267
44. Bhagade SS, Nageshwar GD (1978) Chem Petro-Chem J 9(7):3
45. Pietrzyk DJ (1990) Chromatogr Sci 47:585

46. Bartoli G, Bosco M, Carlone A, Dalpozzo R, Marcantoni E, Melchiorre P, Sambri L (2007) Synthesis 22:3489
47. Robert C, de Montigny F, Thomas CM (2011) Nat Commun 2:586
48. DiCiccio AM, Coates GW (2011) J Am Chem Soc 133:10724
49. Gomzi Z, Zrncevic S (1980) Croat Chem Acta 53(1):25
50. (1989) Chem Abstr 110:137443f
51. Wilmott M et al (1990) World Patent WO-9,008,121
52. Vera-Castaneda E et al (1987) US Patent 4,740,272-A
53. Sogah DY et al (1987) Macromolecules 20:1473
54. Horsley LH (1973) In: Gould RF (ed) Azeotropic data-III. American Chemical Society, Washington, DC
55. Konen JC, Clocker ET, Cox RP (1945) Oil Soap 22:57
56. Thielpape E, Flude A (1454) Chem Ber B66:1454
57. Dmuchovsky B, Vineyard BD, Zienty FB (1964) J Am Chem Soc 86:2874
58. Sanders GC, Duchateau R, Lin CY, Coote MI (2012) Macromolecules 45:5923
59. Kosmin M, Butler JM (1952) US Patent 2,610,202
60. Coleman LE, Bork JF, Dunn H (1959) J Org Chem 24:135
61. Mizzoni RH, Spoerri PE (1951) J Am Chem Soc 73:1873
62. Tawney PO, Snyder RH, Bryan CE, Congr RP, Dovell FS, Kelly RJ, Stitler CH (1960) J Org Chem 25:56
63. Deshpande SR, Maybhate SP, Likhite AP, Chaudhary PM (2010) Indian J Chem 49B:487
64. Doi S, Takayanagi Y (1989) US Patent 4,812,579
65. Parsons CF (1989) US Patent 5,115,061A
66. Musa OM (2008) US Patent 7,456,280
67. Dershem S (2011) US Patent 8,043,534 B2
68. Synder RH (1955) US Patent 2,717,908
69. Synder RH (1957) US Patent 2,788,349
70. Swartz DA (2008) US Patent 7,462,689 B2
71. Allen BB, Wyatt B, Henze HR (1939) J Am Chem Soc 61:843
72. Freudenberger D, Wunder F, Fernoltz H (1978) (Hoechest) US Patent 4,096,156
73. Schwenk E, Papa D, Witman B, Ginsberg HF (1944) J Org Chem 9:175
74. Gao S, Tian W, Shi L (2012) Trans Met Chem 37:757
75. Li J, Tian WP, Shi L (2011) Catal Lett 141:565
76. Brownstein AM (1991) Chem Tech 21:506
77. Castiglioni GL, Ferrari M, Guercio A, Vaccari A, Lancia R, Furnagalli C (1996) Catal Today 27:181
78. Lancia R, Vaccari A, Fumagalli C, Armbruster E (1977) US Patent 5,698,713
79. Thomas WD, Taylor PD, Tomfohrde HF (1992) US Patent 5,149, 836
80. Thakur DS, Roberts BR, Sullivan TJ, Vichek AL (1992) US Patent 5,155,086
81. Wegman RW, Bryant DR (1993) US Patent 5,191,091
82. Bjornson G, Sturk J (1992) US Patent 5,086,030
83. Hara Y, Kusaka H, Inagaki H, Takahashi K, Wada K (2000) J Catal 194:188
84. Liu P, Liu Y, Yin YQ (1999) J Mol Catal A 138:129
85. Yuan HJ, Zhang C, Huo W, Ning C, Tang Y, Yi Z, Cong D, Zhang W, Luo J, Li S, Wang Z (2014) J Chem Sci 1:141
86. Pillai UR, Demessie ES, Young D (2003) Appl Catal B Environ 43:131
87. Li J, Tian WP, Wang X, Shi L (2011) Chem Eng J 175:417
88. Zhang RC, Yin HB, Zhang DZ, Qi L, Lu HH (2008) Chem Eng J 140:488
89. Yu Y, Guo YL, Zhan WC, Guo Y, Wang YQ (2011) J Mol Catal A Chem 337:77
90. Herrmann U, Emig G (1998) Ind Eng Chem Res 37:759
91. Lu WJ, Lu GZ, Guo Y, Guo YL, Wang YS (2003) Catal Commun 4:177
92. Wang Q, Cheng HY, Liu RX, Hao JM, Yu YC, Zhao FY (2009) Catal Today 148:368
93. Liu P, Liu Y, Yin Y (1999) J Mol Catal A Chem 138:129

94. Feng YH, Yin HB, Wang AL, Xie T, Jiang TS (2012) Appl Catal A Gen 425:205
95. Meyer CI, Marchi AJ, Monzon A, Garetto TF (2009) Appl Catal A Gen 367:122
96. Bond GC, Phillipson JJ, Wells PB, Winterbottom JM (1966) Trans Faraday Soc 62:443
97. Takahashi R, Elving PJ (1967) Electrochim Acta 12:213
98. Gao Y (2013) US Patent Application 20130134047 A1
99. Brieger G, Neslrick TJ (1974) Chem Rev 74(5):567
100. Vaclavik J, Sot P, Vilhanova B, Pechacek J, Kuzma M, Kacer P (2013) Molecules 18:6804
101. Wu X, Wang C, Xiao J (2010) Platinum Met Rev 54(1):3
102. Kuhn R, Ebel F (1925) Ber Dtsch Chem Ges 58B:919
103. Backvall JE (ed) (2010) Modern oxidation methods, 2nd edn. Weinheim, Wiley-VCH
104. Payne G, Williams P (1959) J Org Chem 24:54
105. Venturello C, Alneri E, Ricci M (1983) J Org Chem 48:3831
106. Sato K, Aoki M, Ogawa M, Hashimoto T, Noyori R (1983) J Org Chem 61:8310
107. Yoshida A, Yoshimura M, Uehara K, Hikichi S, Mizuno N (2006) Angew Chem Int Ed 45:1956
108. Anelli PL, Banfi S, Montanari F, Quici S (1989) J Chem Soc Chem Commun 779
109. Patil AO, Zushma S (2013) US Patent 8,519,057-B2
110. Adkins H, Krsek G (1948) J Am Chem Soc 70:383
111. Umemura S, Ikada Y (1975) Japan Patent 50-101320
112. Dennis AJ, Harrison GE, Wyber JP (1985) European Patent EP0096987 B1
113. Ramsey SH, Schultz RG (1993) US Patent 5,210,295 A
114. Kitahara K (1961) US Patent 2,972,565
115. McKenzie B (1911) J Chem Soc 99:1923
116. Gawron O, Glaid AJ, Fondy TP, Bechtold MM (1962) J Am Chem Soc 84:3877
117. Katakis D, Vrachnou-Astra E, Konstantatos J (1986) J Chem Soc Dalton Trans Inorg Chem 1:1491
118. Johnson CR, Bade TR (1982) J Org Chem 47:1205
119. Clifford AM, Long JR (1947) US Patent 2,425,509
120. Weiss H (1977) J Am Chem Soc 99:1670
121. Chan JW, Hoyle CE, Lowe AB, Bowman M (2010) Macromolecules 43(15):6381
122. Baik W, Yoon CH, Koo S, Kim H, Kim J, Kim J, Hong S (2004) Bull Korean Chem Soc 25 (4):491
123. Kloetzel MC (1948) J Am Chem Soc 70:3571
124. Ballini R, Bosica G, Fiorini D, Righi P (2002) Synthesis 5:681
125. Szilagyi G, Wamhoff H (1974) Acta Chim Acad Sci Hung 82:375
126. Bergmann ED, Ginsburg D, Pappo R (1959) The Michael reaction. In: Adams R (ed) Organic reactions, vol 10. Wiley, New York, p 179
127. Zienty FB, Schleppnik BD, Vineyard (1962) J Org Chem 27:3140
128. Nguyen VG, Alexander M (2012) EP Patent EP2480070 A2
129. Patil HV, Kulkarni RD, Mishra S (2013) Int J Chem Chem Eng 3:69
130. Gusmeroli M, Mormile SM, Gironda R, Mirenna L, Osti S (2004) World Patent WO 2004/103041 A1
131. Rothrock HS (1944) US Patent 2,346,612
132. Mazo GY, Mazo J, Vallino B, Ross RJ (1999) US Patent 5,872,285
133. Hirbrunner P, Berthlet R (1976) US Patent 3,979,449
134. Hasson D, Shemer H, Sher A (2011) Ind Eng Chem Res 50:7601
135. Zahuriaan-Mehr MJ, Pourjavadi A, Salimi H (2009) Poly Avd Technol 20:655
136. Thombre SM, Sarwade BD (2005) J Macromol Sci A 42:1299
137. Boehmke G, Schmitz G (1995) US Patent 5,468,838
138. Fox S, Harada WK (1962) US Patent 3,052,655 A1
139. Saudek V, Drobnik J (1981) Polym Bull 9:473
140. Wolk SK, Swift G, Paik YH, Yocom KM, Smith RL, Simon ES (1994) Macromolecules 27:7613

141. Diels O, Alder K (1929) Chemische Berichte 62(8):2081
142. Woodward RB, Hoffmann R (1965) J Am Chem Soc 87(2):395
143. Hoffmann R, Woodward RB (1965) J Am Chem Soc 87(9):2046
144. Woodward RB, Hoffmann R (1969) Angew Chem Int Ed 8(11):781
145. Craig D, Shipman JJ, Fowler RB (1961) J Am Chem Soc 83(13):2885
146. Houk KN, Lin YT, Brown FK (1986) J Am Chem Soc 108(3):554
147. Gajewski JJ, Peterson KB, Kagel JR (1987) J Am Chem Soc 109(18):5545
148. Bailey ME (1960) US Patent 2,959,599
149. Benedicto A, Novack BM, Grubbs RH (1992) Macromolecules 25:5893
150. Kloetzel MC (1948) Org React 4:1
151. Holmes HL (1948) Org React 4:60
152. Carey FA, Sundberg RJ (2007) Advanced organic chemistry: Part B: Reactions and synthesis, 5th edn. Springer, New York
153. Hyung Woo S (1994) Tetrahedron Lett 35(23):3957
154. Schrock RR, Lewis JJ (1973) J Am Chem Soc 95:4102
155. Houk KN, Luskus LJ (1971) J Am Chem Soc 93(18):4606
156. Fernandez I, Bickelhaupt FM (2014) J Comput Chem 35(5):371
157. Williamson KL, Hsu YFL (1970) J Am Chem Soc 92(25):7385
158. Evans DA, Chapman KT, Bisaha J (1988) J Am Chem Soc 110(4):1238
159. Corey EJ, Loh TP (1991) J Am Chem Soc 113(23):8966
160. Corey EJ, Shibata T, Lee TW (2002) J Am Chem Soc 124(15):3808
161. Ryu DH, Corey EJ (2003) J Am Chem Soc 125(21):6388
162. Johnson JS, Evans DA (2000) Acc Chem Res 33(6):325
163. Ahrendt KA, Borths CJ, MacMillan DWC (2000) J Am Chem Soc 122(17):4243
164. Kobuke Y, Sugimoto T, Furukawa J, Fueno T (1972) J Am Chem Soc 94(10):3633
165. Midland MM, Tramontano A (1978) J Org Chem 43(7):1471
166. Danzig MJ, O'Donnell JL, Bell EW, Cowan JC, Teeter HM (1957) J Am Oil Chem Soc 34:136
167. Teeter HM, O'Donnell JL, Schneider WJ, Gast LE, Danzig MJ (1957) J Org Chem 22:512
168. Miller WR, Cowan JC (1962) J Am Oil Chem Soc 39:380
169. Gast LE, Bell EW, Teeter HM (1956) J Am Oil Chem Soc 33:278
170. Silverstone GA (1968) GB Patent 1,141,690
171. Toseland P, Ord AJL (1967) GB Patent 1,046,207
172. Friedrich JP, Bell EW, Beal RE (1962) J Am Oil Chem Soc 39:420
173. Paderes GD, Jorgensen WL (1992) J Org Chem 57(6):1904
174. Inagaki S, Fujimoto H, Fukui KJ (1976) J Am Chem Soc 41(16):4693
175. Fernandez I, Bickelhaupt FM (2012) J Comput Chem 33(5):509
176. Stephenson LM, Mattern DL (1976) J Org Chem 41(22):3614
177. Thaler WA, Franzus BJ (1964) J Org Chem 29(8):2226
178. Hoffmann HMR (1969) Angew Chem Int Ed 8(8):556
179. Mikami K, Shimizu M (1992) Chem Rev 92(5):1021
180. Oppolzer W, Snieckus V (1978) Angew Chem Int Ed Engl 17(7):476
181. Snider BB (1980) Acc Chem Res 13(11):426
182. Hanna PK, Truong (2009) European Patent EP1805238 A4
183. Biokford WC, Fisher GS, Dollear F, Swift CE (1948) J Oil Chem Soc 25:251
184. Beavers EM (1954) US Patent 2,692,270
185. Bryce-Smith D, Gilbert A (1965) J Chem Soc 1:918
186. Hammond GS, Hardham WH (1963) Proc Chem Soc 1:63
187. Bryce-Smith D, Lodge JE (1962) J Chem Soc 1:2675
188. Groveinstein R, Rao DV, Taylor JW (1961) J Am Chem Soc 83:1705
189. Schenk GO, Steinmetz R (1960) Tetrahedron Lett 21:1
190. Angus HJF, Bryce-Smith D (1960) J Chem Soc 1:4791
191. Vickery B, Gilbert A, Bryce-Smith D (1965) GB Patent 986,348

192. Raciszewski Z (1966) Chem Ind (Lond) 1:418
193. Hardham WH, Hammond GS (1967) J Am Chem Soc 89(13):3200
194. Walter GG (1964) US Patent 3,203,886 A1
195. Shim SC, Pill-Hoon B (1982) Bull Kor Chem Soc 3(3):115
196. Yamada M, Takase I, Koutou N (1968) J Polym Sci B Polym Lett 6(12):883
197. Andersson H, Hult A (1997) J Coat Technol 69(885):91
198. Lee CW, Kim JM, Han DK, Ahn KD (1999) J Macromol Sci A Pure Appl Chem 36(10):1387
199. De Schurijver FC, Smets GJ (1971) US Patent 3,622,321 A1
200. Von Sonntag J, Beckert D, Knolle W, Mehnert R (1999) Radiat Phys Chem 55:609
201. Kohli P, Scranton AB, Blanchard GJ (1998) Macromolecules 31(17):5681
202. Jonsson S, Viswanathan K, Lindgren K, Swami SN, Ng LT (2003) Polym Preprint 44(1):7
203. Kyrides LP (1940) Org Synth 40:51
204. Liwschitz Y, Zilkha A (1955) J Am Chem Soc 77:1265
205. Feuer H, White EH, Wyman JE (1958) J Am Chem Soc 80:3790
206. Tzoganakis C, Vlachopoulos J, Hamielec AE (1988) Chem Eng Prog 1:47
207. Suwanda D, Lew R, Balke ST (1988) J Appl Polym Sci B 35(4):1033